National Library of Canada

Acquisitions and Bibliographic Services Branch

395 Wellington Street
Ottawa, Ontario
K1A 0N4

Bibliothèque nationale du Canada

Direction des acquisitions et des services bibliographiques

395, rue Wellington
Ottawa (Ontario)
K1A 0N4

Your file Votre référence

Our file Notre référence

NOTICE

The quality of this microform is heavily dependent upon the quality of the original thesis submitted for microfilming. Every effort has been made to ensure the highest quality of reproduction possible.

If pages are missing, contact the university which granted the degree.

Some pages may have indistinct print especially if the original pages were typed with a poor typewriter ribbon or if the university sent us an inferior photocopy.

Reproduction in full or in part of this microform is governed by the Canadian Copyright Act, R.S.C. 1970, c. C-30, and subsequent amendments.

AVIS

La qualité de cette microforme dépend grandement de la qualité de la thèse soumise au microfilmage. Nous avons tout fait pour assurer une qualité supérieure de reproduction.

S'il manque des pages, veuillez communiquer avec l'université qui a conféré le grade.

La qualité d'impression de certaines pages peut laisser à désirer, surtout si les pages originales ont été dactylographiées à l'aide d'un ruban usé ou si l'université nous a fait parvenir une photocopie de qualité inférieure.

La reproduction, même partielle, de cette microforme est soumise à la Loi canadienne sur le droit d'auteur, SRC 1970, c. C-30, et ses amendements subséquents.

Canada

UNIVERSITY OF ALBERTA

Stratigraphic and Diagenetic Controls on Aquitard Integrity and Hydrocarbon Entrapment, Bashaw Reef Complex, Alberta, Canada.

by

Mark Rowland Hearn

A thesis submitted to the Faculty of Graduate Studies and Research in partial fulfillment of the requirements for the degree of Master of Science.

DEPARTMENT OF EARTH AND ATMOSPHERIC SCIENCES

Edmonton, Alberta
Spring 1996

National Library of Canada

Acquisitions and Bibliographic Services Branch

395 Wellington Street
Ottawa, Ontario
K1A 0N4

Bibliothèque nationale du Canada

Direction des acquisitions et des services bibliographiques

395, rue Wellington
Ottawa (Ontario)
K1A 0N4

Your file Votre référence

Our file Notre référence

The author has granted an irrevocable non-exclusive licence allowing the National Library of Canada to reproduce, loan, distribute or sell copies of his/her thesis by any means and in any form or format, making this thesis available to interested persons.

L'auteur a accordé une licence irrévocable et non exclusive permettant à la Bibliothèque nationale du Canada de reproduire, prêter, distribuer ou vendre des copies de sa thèse de quelque manière et sous quelque forme que ce soit pour mettre des exemplaires de cette thèse à la disposition des personnes intéressées.

The author retains ownership of the copyright in his/her thesis. Neither the thesis nor substantial extracts from it may be printed or otherwise reproduced without his/her permission.

L'auteur conserve la propriété du droit d'auteur qui protège sa thèse. Ni la thèse ni des extraits substantiels de celle-ci ne doivent être imprimés ou autrement reproduits sans son autorisation.

ISBN 0-612-10717-5

Canada

UNIVERSITY OF ALBERTA

Library Release Form

Name of Author: **Mark Rowland Hearn**

Title of Thesis: **Stratigraphic and Diagenetic Controls on Aquitard Integrity and Hydrocarbon Entrapment, Bashaw Reef Complex, Alberta, Canada.**

Degree: **Master of Science**

Year this Degree Granted: **1996**

Permission is hereby granted to the University of Alberta Library to reproduce single copies of this thesis and to lend or sell such copies for private, scholarly, or scientific research purposes only.

The author reserves all other publication and other rights in association with the copyright in the thesis, and except as hereinbefore provided, neither the thesis nor any substantial portion thereof may be printed or otherwise reproduced in any material form whatever without the author's prior written permission.

Mark R. Hearn

Mark R. Hearn
7, Berners Way
Faringdon,
OXON
England
SN7 7BG

Date: 19th April, 1996

UNIVERSITY OF ALBERTA

Faculty of Graduate Studies and Research

The undersigned certify that they have read, and recommend to the Faculty of Graduate Studies and Research for acceptance, a thesis entitled "**Stratigraphic and Diagenetic Controls on Aquitard Integrity and Hydrocarbon Entrapment, Bashaw Reef Complex, Alberta, Canada**" by **Mark Rowland Hearn**, in partial fulfillment of the requirements for the degree of **Master of Science**.

Dr. H.G. Machel (Supervisor)

Dr. B. Jones

Dr. M.E. Evans

Date: 3rd April 1996

ABSTRACT

This study is an investigation of aquitard characterization and hydrocarbon entrapment in the area of the Bashaw Reef Complex, east-central Alberta. Hydrocarbon pool distribution in the Upper Devonian (Frasnian) dolostone reservoirs of the Leduc Formation and in the overlying Nisku Formation and Camrose Member is controlled by the effectiveness of a relatively thin aquitard in the Ireton Formation that separates the two reservoir intervals. Over the Bashaw Reef Complex, the Ireton aquitard commonly is ≤25 metres thick and <1 metre in some places. These "thins" of <1 metre are interpreted to have been deposited over paleotopographic highs. Subsequently, the effects of differential compaction on the reef complex has led to a thicker Ireton aquitard drape being present over the present-day highs of the reef complex.

Facies variations in the Ireton aquitard are characterized by an increase in carbonate content from 50% in off-reef areas to >80% over the paleotopographic highs. Early replacement dolomitization of all formations (by a proposed reflux model) generated intercrystalline porosity in the order of 3-4% in the carbonate-rich (>80%) Ireton aquitard facies.

Subsequent petroleum entrapment within the Bashaw Reef Complex mostly occurred within the present-day highs that are draped by >10 m of Ireton aquitard. Where the Ireton aquitard drape is <10 m, breaching and re-migration from Leduc traps to Nisku Formation/Camrose Member traps can be suspected. A critical control on breaching, however, appears to be the influence of facies and carbonate content on dolomite crystal growth and the development of intercrystalline porosity. Generally, breaching has occurred where there is an average of >80% carbonate in the aquitard drape, and invariably where the aquitard is <4 metres thick. Many of the Nisku Formation/Camrose Member pools are situated either directly above or up-dip from these breaches.

ACKNOWLEDGEMENTS

Wow, at last, *fini*..... I can place this thesis on the shelf and allow the dust to settle. I only say this because, as is so often the case of other theses, the pages of this thesis may not see the light of day again.....but who knows!

As is customary at this point, I shall now say thank you to all those people who have contributed to this thesis and to my life here in Edmonton.

To begin, I must acknowledge Dr. Hans Machel for accepting me under his supervision and for providing me with a thesis topic to get my fingers stuck into (not to mention my brain). Equally, thanks must also go to Ben Rostron for laying the foundations for this thesis project and providing motivational words of wisdom (whether he knew it or not) that kept me on the path to completion.

Financial support was provided by an NSERC (Strategic) grant to Drs. H. Machel and E. Mountjoy; Andre Chow arranged partial funding from Chevron for core logging fees; and the University of Alberta provided Teaching and Research Assistantships.

Editorially, this thesis was passed through a number of hands whose red pens all greatly enhanced the final version. Thanks go to Hans for wading through the "rough" drafts and the slightly better ones, Dr. Brian Jones and Dr. Ted Evans (Committee Members), Frank Stoakes (Chapter 2), and Dr. Paul "Smelly" (....can I really say libelous things like that in a thesis!?) Blanchon who brought me to a different, presumably better, level of thinking (but who knows for how long). I am also extremely indebted to Frank Stoakes for his permission to utilize a number of diagrams from the SCG (1989) consultancy report (*i.e.*, Figures 2.1, 2.2, and 2.3), without which my interpretations may have floundered, or at the very least, forced me to make them myself!

During the course of the thesis I was assisted both intellectually and technically, and to varying degrees, by numerous people and establishments. I am grateful to the staff of the ERCB Core laboratories (Calgary) for their help during my summer of core logging. For MICPM data I thank Jerry Shaw and Rosemary French of the Petroleum Recovery Institute (Calgary), and for Rock-Eval Pyrolysis analyses Martin Fowler of the ISPG (Calgary). Thin sections were admirably made by Don Resultay of the University of Alberta, and often at short notice. In addition, I had the opportunity to converse with a number of "learned" geologists, all of which gave me useful insights into my thesis.

These include: Andre Chow, Tony Cadrin, Tony Geier, Bill May, Al Clark, Gord Tebutt, Mark Caplan, Ian Hunter, and many, many more. Last but not least, I very much appreciate the guidance that Dr. Pat Cavell gave throughout this thesis.

At last I have the opportunity to acknowledge all those friends and colleagues for being a part of my life as a graduate student.... where shall I start????

First of all I would like to thank my adopted "mother", Jen Vézina, for listening to my babblings (or a least looking like she was listening!). Next, the terrible trio, Steven "Trivia Boy" Grant, Kent "Tiger" Wilkinson, and Joanne Jensen for, among other things, partaking with me in the quaffing of the odd one or two...hmm...coffees, what else! To the Machel clan, thanks go to Mat Grobe, Kim Manzano, Erinn Horrigan, and Harald Huebscher. Finally, thanks to all the rest of you folks, Da(y)ve Hills, Paul Blanchon, Brent Wignall, Leo Piccoli, Howard Brekke, Betsy "Cheesecake" Willson, Jason (Tex) Montpetit, István Almási, Karen Fallas, Sheri Gilmour, Roberto Batalas, and numerous others.

I conclude by giving my warmest thank you to my parents and family for their support and kindness (monetary kindness too!) from afar.

TABLE OF CONTENTS

CHAPTER 1 1

INTRODUCTION 1

1.1 Introduction 1
1.2 Objectives 4
1.3 Study Area and Core Control 5
1.4 General Stratigraphy and Geologic History 5

CHAPTER 2 9

SEDIMENTOLOGY 9

2.1 Leduc Formation 9
2.2 Camrose Member and Nisku Formation 11
2.3 Paleotopographic "Lows" in the Bashaw Reef Complex? 19
2.4 Differential Relief of Reef-Complex Margins 20
2.5 Synopsis 24

CHAPTER 3 26

DIAGENESIS 26

3.1 Petrographic and Geochemical Characteristics 26
3.1.1. Limestones 26
3.1.2. Matrix replacement dolomites 28
3.1.3. Pore-lining dolomite cements 34
3.1.4. Anhydrite phases and calcite cements 37
3.1.5. Fracturing and dissolution 40
3.1.6. Other diagenetic products 40
3.2 Discussion. 41
3.2.1. Early diagenesis 41
3.2.2. Replacement dolomitization 42
3.2.3. Cement phases 50
3.2.4. Pore generation 51
3.2.5. Compaction 53
3.3 Synopsis 54

CHAPTER 4 55

HYDROCARBON RESERVOIR DATA 55

4.1 Pool Distribution, Structure, and Hydrocarbon Column Heights 55
4.2 Reservoir Characteristics 62
4.2.1. Leduc Formation 62
4.2.2. Nisku Formation and Camrose Member 62
4.3 Trapping Styles 65
4.3.1. Leduc Formation (D-3) pools 65

4.3.2. Nisku Formation/Camrose Member (D-2) pools 66
4.4 Reservoir Production Data 67
4.5 Hydrocarbon Data 71

CHAPTER 5 73

THE IRETON AQUITARD 73
5.1 Sedimentology 73
5.1.1. Thickness and composition 74
5.1.2. Facies and facies distribution 78
5.1.3. Discussion 84
5.2 Petrologic and Petrophysical Data 84
5.2.1. Hand sample and thin section analysis 86
5.2.2. Rock-Eval Pyrolysis 90
5.2.3. MICPM data 94
5.2.4. Stable isotope analysis 99
5.2.5. Magnetic anomalies 102

CHAPTER 6 104

SYNTHESIS AND DISCUSSION 104
6.1 Determination of Ireton Aquitard Breaching Locales 104
6.2 Breaching Characteristics 104
6.3 Control of Breaching Locales on Pool Distribution 109
6.3.1. Leduc Formation (D-3) reservoirs 109
6.3.2. Nisku Formation/Camrose Member (D-2) reservoirs 110
6.4 Hydrocarbon Migration and Entrapment 112
6.4.1. Oil migration 112
6.4.2. Hydrocarbon gas migration 115
6.4.3. H_2S gas migration 116
6.5 Implications for Exploration 116

CHAPTER 7 118

CONCLUSIONS 118

REFERENCES 121

APPENDIX I 127

APPENDIX II 132

List of Tables

Table 1.1: Details of core examined 6

Table 3.1: Isotopic data and dolomite types 30

Table 4.1: Hydrocarbon column thicknesses 61

Table 5.1: Percentage carbonate content values of the Ireton aquitard 76

Table 5.2: Thin section data on presence or absence of oil/bitumen 89

Table 5.3: Rock-Eval Pyrolysis data 91

Table 5.4: MICPM data 96

Table 5.5: Hydrocarbon column heights required to breach MICPM plugs 98

Table 6.1: Leaky versus sealing Ireton aquitard cores, and breaching dataset 105

List of Figures

Chapter 1 1

Figure 1.1: Location map of the study area in east-central Alberta 2
Figure 1.2: Detailed map of the study area 3
Figure 1.3: Schematic lithostratigraphy of the Upper Devonian 7

Chapter 2 9

Figure 2.1: Isopach map of the Leduc Formation 10
Figure 2.2: Facies distribution map of the Camrose Member 12
Figure 2.3: Facies distribution map of the lower Nisku Formation 13
Figure 2.4: Typical facies of the Camrose Member and Nisku Fm. 15
Figure 2.5: Comparison of shallow ramp facies models 16
Figure 2.6: Ireton aquitard thickness over Bashaw Reef paleotopography 18
Figure 2.7: Cross section of the raised interior to the reef complex 21
Figure 2.8: A schematic of reef accretion and later compaction 25

Chapter 3 26

Figure 3.1: Paragenetic sequence and burial history 27
Figure 3.2: Plot of $\delta^{13}C$ versus $\delta^{18}O$ isotopes of replacement dolomites 29
Figure 3.3: Dolomite textures in the Bashaw area 31
Figure 3.4: Photomicrographs of matrix replacement dolomite types 33
Figure 3.5: Photomicrographs of pore-lining dolomite cement types 36
Figure 3.6: Photographs of other diagenetic phases 39
Figure 3.7: Dolomitization models and their application to the Bashaw area 43
Figure 3.8: Schematic of dolostone distribution and reflux dolomitization 44
Figure 3.9: Comparison of replacement dolomite isotopes to other areas 46
Figure 3.10: $\delta^{13}C$ versus elevation from the top of the Calmar Formation 49

Chapter 4 55

Figure 4.1: Detailed outline of Leduc Fm. (D-3) pools and H_2S content 56
Figure 4.2: Detailed outline of Nisku/Camrose (D-2) pools and H_2S content 57
Figure 4.3: Structural cross section A-A′ 58
Figure 4.4: Structural cross section B-B′ 59
Figure 4.5: Structural cross section C-C′ 60
Figure 4.6: Characteristic reservoir rocks of D-3 and D-2 pay zones 64
Figure 4.7: Production pressure-decline curves for the Bashaw area 68
Figure 4.8: Pressure elevation plot for the Clive area 70
Figure 4.9: Pressure-depth plot for well 6-22-38-24W4 70

CHAPTER 5 **73**
Figure 5.1: Detailed isopach map of the Ireton aquitard 75
Figure 5.2: Distribution of the average Ireton aquitard carbonate content 77
Figure 5.3: Depositional environments and facies of the Ireton aquitard 79
Figure 5.4: Typical facies of the Ireton aquitard 82
Figure 5.5: Distribution map of the Ireton aquitard environments 83
Figure 5.6: Schematic of Ireton aquitard deposition over the Bashaw reef 85
Figure 5.7: Recognition of hydrocarbon breaches in the Ireton aquitard 88
Figure 5.8: Pseudo-Van Krevelen diagram of lower Nisku Fm. samples 93
Figure 5.9: Ireton aquitard MICPM curves 95
Figure 5.10: Cross section schematic of $\delta^{13}C$ values in the wells analyzed 101
Figure 5.11: Graph of magnetic susceptibility versus carbonate content 103

CHAPTER 6 **104**
Figure 6.1: Flow chart for the determination of aquitard integrity 106
Figure 6.2: Ireton aquitard isopach, breaching locales, carbonate content 108
Figure 6.3: D-2 pool distribution and relationship to Leduc compaction 111
Figure 6.4: Suspected migration pathways through the Bashaw Reef 114

CHAPTER 1

INTRODUCTION

1.1 Introduction.

In the early 1950's a series of oil and gas plays was discovered within the area of the Upper Devonian Bashaw Reef Complex in east-central Alberta, Canada (Figures 1.1 and 1.2). Recent evaluations of oil and gas in place for the study area estimate reserves of 86 x $10^6 m^3$ and 50 x $10^9 m^3$, respectively (Energy Resources Conservation Board (ERCB), 1991). Exploration in the region is focused on relatively smaller, subtle traps (Geological Survey of Canada (GSC), 1988) in what is now considered a "mature" exploration area by the petroleum industry.

Oil and gas production is from dolostone reservoirs of the Leduc Formation, and from the overlying Camrose Member (Ireton Formation)/Nisku Formation. These reservoirs are separated by a relatively thin (<25 m) aquitard[1] of the Ireton Formation (hereinafter referred to as the "Ireton aquitard").

The close spatial association between the Camrose Member/Nisku Formation pools and the underlying Leduc Formation pools, as well as similar oil signatures, has led to speculation that either direct communication (no intervening Ireton aquitard), fractures, or a thinning of the Ireton aquitard allowed Camrose Member/Nisku Formation pools to be charged from the Leduc Formation (GSC, 1988; Stoakes Campbell Geoconsulting Ltd. (SCG), 1989; Creaney and Allan, 1990). Furthermore, strong hydrogeologic evidence (potentiometric surfaces, pressure-depth plots and formation-fluid chemistries) indicate that present-day formation waters are ascending from the Leduc Formation into the Camrose Member/Nisku Formation (Paul, 1994; Rostron, 1995), at a rate of 1.3 mm/day (Paul, 1994). These data led Rostron (1995) to suggest that formation waters and hydrocarbons breach(ed) the Ireton aquitard where it thins to < 6 metres.

---

[1] It should be noted that all rocks have an intrinsic permeability > zero (see Rostron, 1995, for discussion). The term "aquitard" is used within this thesis when no time frame is denoted. The term "seal" will only be used in the context of a particular time frame, whereby a rock can act as an effective seal for hydrocarbon trapping.

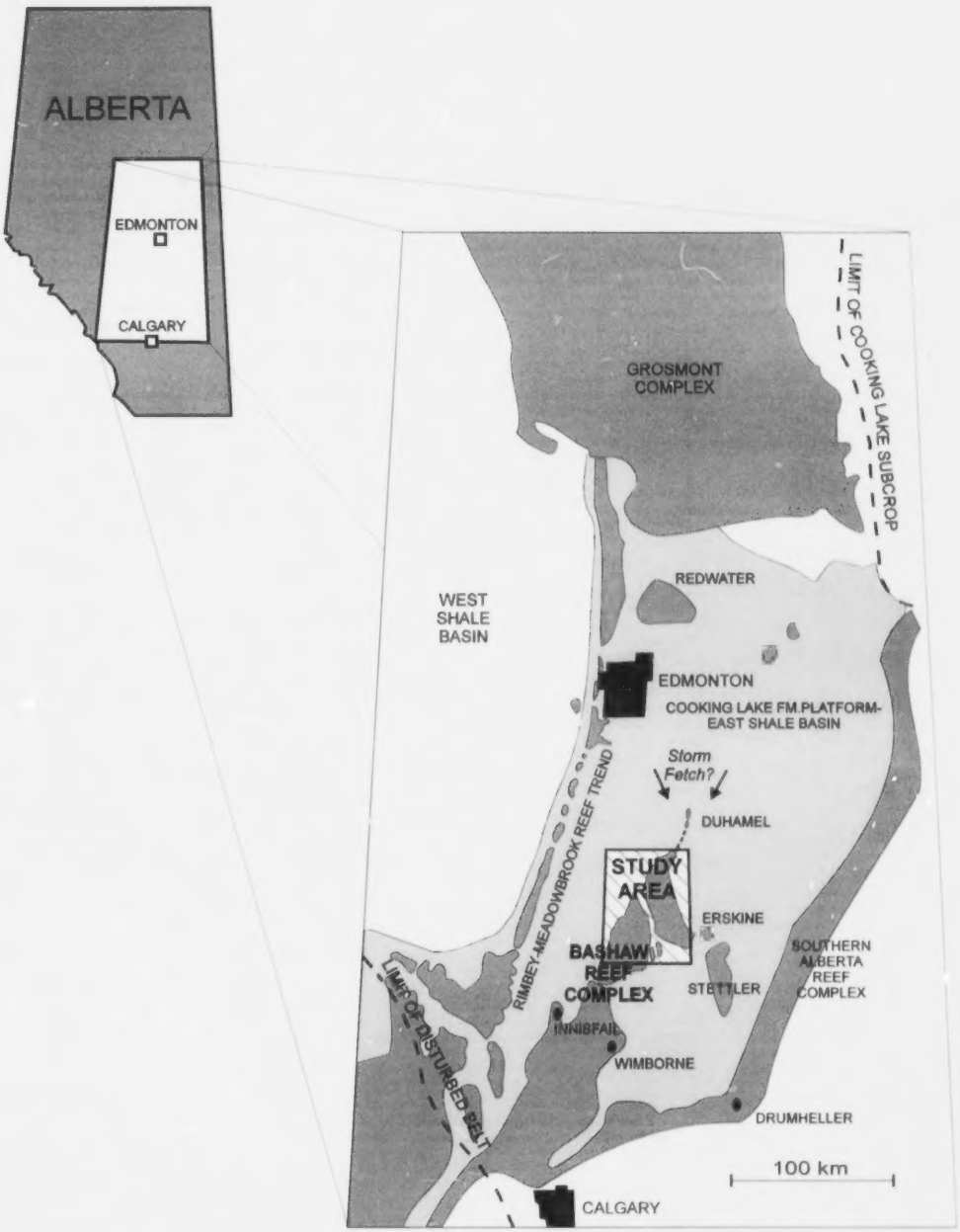

Figure 1.1: Location map of the study area in east-central Alberta. Dark-grey shading denotes the outline of the major Upper Devonian reef complexes within the area; light-grey shading denotes the extent of the Cooking Lake Formation platform upon which most of the reefs accreted.

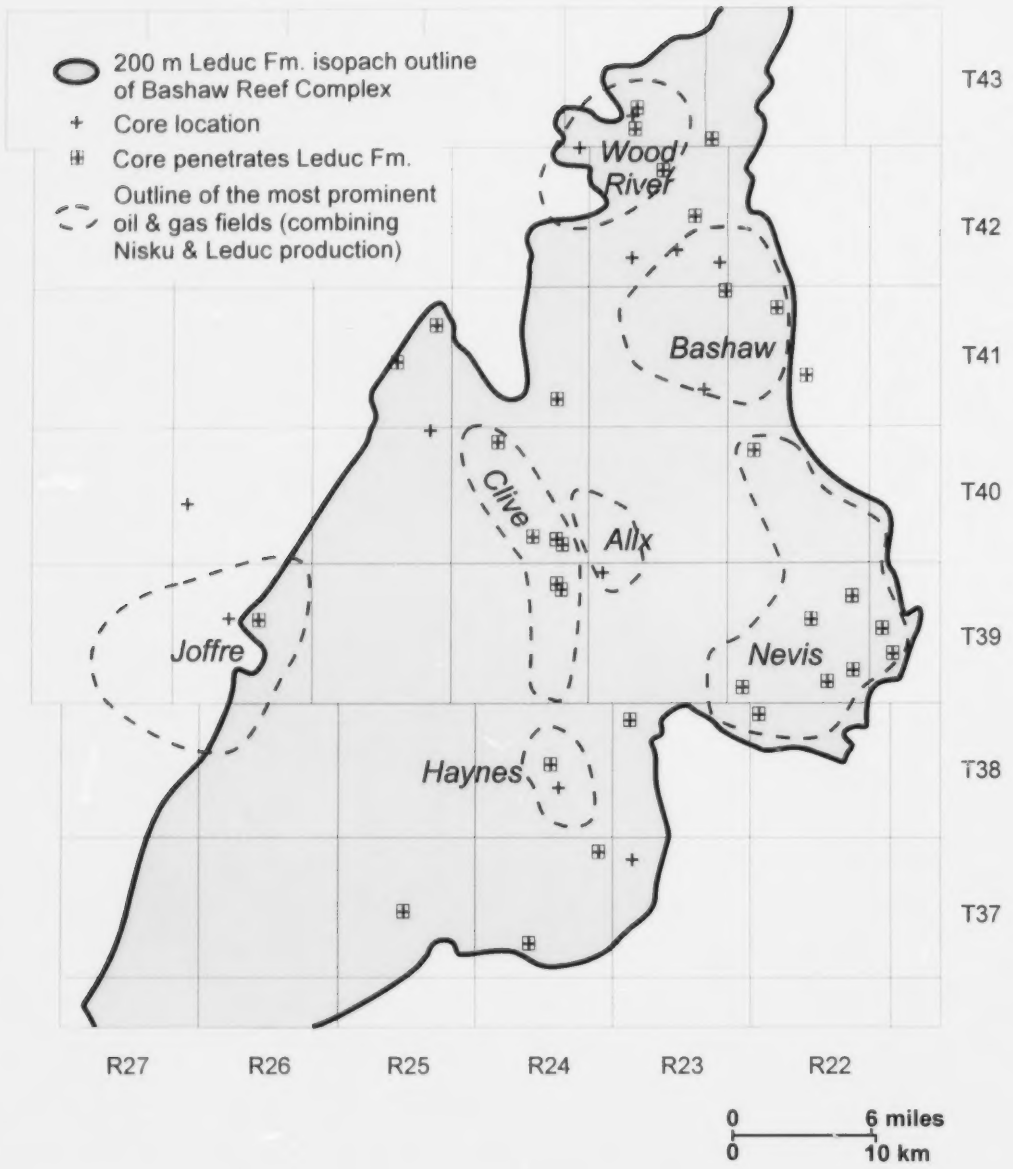

Figure 1.2: Detailed map of the study area indicating the position of the cores studied and the 200 m isopach outline of the Bashaw Reef Complex (SCG, 1989). Names of the most prominent oil and gas fields are also indicated.

To date, no physical study of the Ireton aquitard has been performed to determine the exact nature of the inferred hydrocarbon migration pathways between the two reservoir intervals. The evaluation of aquitard integrity is an important aspect of any hydrocarbon reservoir assessment and is commonly overlooked (Downey, 1984). Two scales of observation are required (micro and macro) in order to make a reasonable assessment of the sealing properties of an aquitard (Downey, 1984). This provides information concerning aquitard lithology, thickness, capillary properties, and lateral extent, and serves to give an understanding of the trap geometry, the hydrocarbon column sustainable by the "seal", and the areas of potential breaching.

1.2 Objectives.

The primary objective of this study is to provide physical evidence of the suspected breaching of the Ireton aquitard by hydrocarbons over the Bashaw Reef Complex, using petrographical, petrophysical, mineralogical, and geochemical techniques. In addition, an assessment will be made on the control these breaches have on the distribution of hydrocarbon pools in the area. The general approach includes:

1) an evaluation of the general sedimentology, diagenesis, present day structure, and reservoir characterization of the Bashaw area;
2) a macro- and micro-scale study of the Ireton aquitard; including lithology, diagenesis, distribution, thickness, and petrophysical properties, as well as visible evidence of breaching;
3) determining specific locations of breaching of the Ireton aquitard, including the application of stable oxygen and carbon isotope analysis and magnetic anomaly mapping to the identification of breaching locales; and
4) an evaluation of hydrocarbon migration and entrapment in the study area relating to the properties of the Ireton aquitard.

A further objective of this study is to demonstrate the significance of understanding aquitard integrity in the exploration of hydrocarbons, and to suggest that a more regional study of the Ireton Formation in the Western Canada Sedimentary Basin (WCSB) may yield new exploration prospects, *e.g.*, above the Rimbey-Meadowbrook reef trend (Rostron, 1995; Wilkinson, 1995).

1.3 Study Area and Core Control.

The study area is situated in the subsurface of east-central Alberta (Figures 1.1 and 1.2). The Bashaw Reef Complex covers an area of approximately 1960 km^2, within Townships 37-43 and Ranges 22-27W4. The Devonian strata of interest form a structural homocline, with present-day burial depths ranging from 1700 m to 2200 m, and a regional dip of approximately 1° to the south-west.

Over 1000 m of core from 45 wells (Figure 1.2, Table 1.1) were examined at the Calgary Core Research Center of the ERCB. Core selection primarily concentrated on those cores with continuous recovery from the Leduc Formation, through the Ireton aquitard, and into the Camrose Member/Nisku Formation. Regionally, the Ireton aquitard is rarely cored (a function of oil company desire to understand reservoir characteristics but not the confining medium). However, the Ireton aquitard is thin within the area and some coring has continued through the aquitard between the two reservoir intervals. Core control, as shown in Figure 1.2, clearly is sparse for such a large area.

1.4 General Stratigraphy and Geologic History.

The general stratigraphic nomenclature for the Upper Devonian strata of central Alberta was established by the Geological staff of Imperial Oil (1950). Since then, numerous papers have dealt with the stratigraphy of the area (*e.g.*, Belyea, 1955; Andrichuk, 1958a, 1958b; McCrossan, 1961; Stoakes, 1980).

This study concerns the Frasnian formations of the Woodbend and Winterburn groups, and in particular the Ireton aquitard of the Ireton Formation (Figure 1.3). Below is a summary of the stratigraphy and geologic history for this interval in east-central Alberta. A more comprehensive regional stratigraphic framework for the Upper Devonian of the WCSB is presented in Wendte *et al.* (1992).

The Frasnian Woodbend Group (Figure 1.3) was initiated by the deposition of a widespread carbonate platform — the Cooking Lake Formation. A relative rise in sea level followed which led to the local development of Leduc Formation reefs upon gentle topographic highs that probably existed on the Cooking Lake Formation platform. Vertical reef accretion then commenced together with inter-reef sedimentation of the Duvernay Formation, and later the Ireton Formation.

Well Location	No. of m / ft Logged	Core Interval Logged
01-31-37-23W4	40 ft	6034-6074ft
11-09-37-24W4	18.2 m	2023-2041m
06-36-37-24W4	32.6 m	1818-1850.6m
16-16-37-25W4	79 ft	6770-6849ft
06-31-38-22W4	56 ft	5560-5616ft
08-31-38-23W4	27 m	1788-1815m
02-15-38-24W4	104 ft	6116-6220ft
06-22-38-24W4	93 ft	3122-6215ft
04-17-39-21W4	291 ft	5419-5710ft
02-19-39-21W4	66 ft	5494-5560ft
14-02-39-22W4	72.5 ft	5370-5442.5ft
10-06-39-22W4	67 ft	5662-5729ft
06-12-39-22W4	105 ft	5399-5504ft
10-22-39-22W4	79 ft	5517-5596ft
11-25-39-22W4	67 ft	5503-5570ft
10-31-39-23W4	63 ft	5921-5949 / 5960-5995ft
16-26-39-24W4	35.5 m	1836-1871.5m
02-35-39-24W4	40 m	1812-1852m
11-21-39-26W4	81 ft	6910-6991ft
10-22-39-26W4	60.5 m	2110-2170.5m
13-29-40-22W4	82 ft	5455-5537ft
16-02-40-24W4	18.25 m	1915-1933.25m
02-10-40-24W4	44 ft	6163-6207ft
02-11-40-24W4	63 ft	6275-6338ft
05-33-40-24W4	36.5 m	1818-1836.5 / 1852-1870m
13-36-40-25W4	105 ft	6155-6260ft
10-18-40-26W4	49 ft	6814-6863ft
03-15-41-22W4	131 ft	5527-5650 / 5750-5770 / 5813-5901ft
04-33-41-22W4	37 ft	5710-5747ft
08-11-41-23W4	10.75 m	1753.5-1764.25m
16-36-41-23W4	16 m	1720-1736m
02-11-41-24W4	50 ft	5966-6046ft
16-15-41-25W4	12 m	1988-2000m
06-25-41-25W4	66 ft	6254-6420ft
08-08-42-23W4	14.15 m	1790.25-1804.4m
10-10-42-23W4	15 m	1724-1739m
02-12-42-23W4	80 ft	5584-5664ft
02-23-42-23W4	41 ft	5821-5862ft
04-34-42-23W4	79 ft	5756-5835ft
14-36-42-24W4	18 m	1776-1794m
06-06-43-22W4	35 ft	5489-5524ft
12-03-43-23W4	50 ft	5599-5649ft
08-09-43-23W4	18 m	1667-1685m
12-10-43-23W4	17.5 m	1664-1681.5m
11-9-44-24W4	45 ft	5790-5835ft
45 wells	approx. 1100m of core	

Table 1.1: Details of the cores examined in this study.

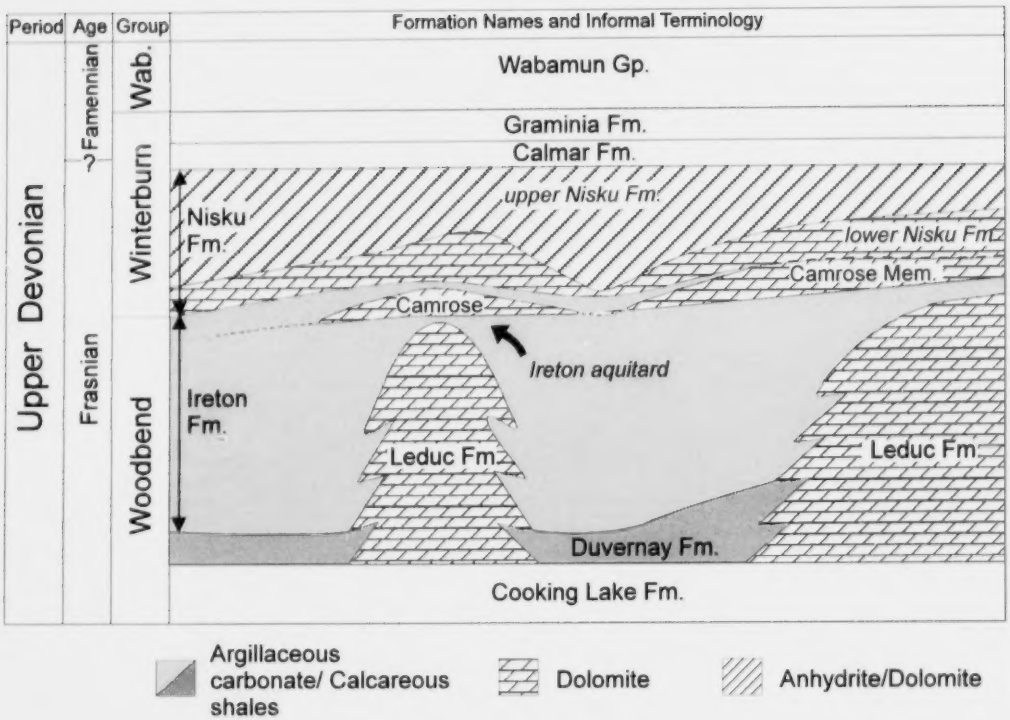

Figure 1.3: Schematic lithostratigraphy for the Upper Devonian of east-central Alberta, including the assignment of informal terminology (in italics).

The Ireton Formation is mainly composed of fine grained carbonates and siliciclastics, and was deposited as a series of progradational clinoforms in the East Shale Basin (Figure 1.1) from east to west (Oliver and Cowper, 1963), that eventually draped the Bashaw Reef Complex. Deposits on these clinoforms are characterized by a shallow-water fine-grained, carbonate-rich platform (≥50% carbonate), a silt/clay-rich slope (~25% carbonate), and a fine-grained, carbonate-rich basin (~75% carbonate) (Campbell and Oliver, 1968). In some parts of the basin, the platform portion of the clinoform is composed of a pure carbonate biostrome, the best documented example of which is in the Grosmont area to the north of the study area (Cutler, 1983). In east-central Alberta, a biostromal platform is present in the upper portion of the Ireton Formation, and is known as the Camrose Member (Figure 1.3), first described by Belyea (1958). This biostromal platform is best developed to the east of the study area over the Southern Alberta Reef Complex (Figure 1.1) (Stoakes, 1977). However, it is also present as a thin platform over the Bashaw Reef Complex, and is separated from the reef complex by a thin layer of the more fine-grained sediments of the Ireton Formation (the Ireton aquitard).

The Ireton Formation filled much of the basinal relief and draped the ~200 m thick Leduc Formation reefs bringing the period of Woodbend Group sedimentation to a close. This was followed by deposition of the Winterburn Group.

The Winterburn Group was initiated by the development of a biostromal platform that forms part of the Nisku Formation (Figure 1.3). This biostromal platform will be informally referred to as the "lower Nisku Formation" and is considered regionally conformable with the Ireton Formation (although hardgrounds are found in the Bashaw area). The lower Nisku Formation is commonly found to be contiguous with the Camrose Member over the Bashaw Reef Complex. This lower Nisku Formation platform sequence was initiated in response to a relative rise in sea-level. Gradually these platform carbonates built up to sea-level within the West Pembina area to the west of Bashaw, and the waters became more restricted. In the Bashaw area this led to a regressive hypersaline phase of evaporite deposition (informally referred to as the "upper Nisku Formation") and culminated in the progradation of the Calmar Formation silts and shales. The Winterburn Group ended in a marine transgression and the deposition of the Graminia Formation (Figure 1.3).

CHAPTER 2

SEDIMENTOLOGY

Since the Leduc Nº 1 oil field was discovered in 1947, numerous papers have dealt with the sedimentology of the Devonian in the WCSB. However, the Bashaw Reef Complex appeared to have been overlooked until the study of Gilhooly (1987). He described in detail the sedimentology of the Camrose Member and Nisku Formation in the Bashaw area (Gilhooly, 1987). Subsequently, a report by Stoakes Campbell Geoconsulting (SCG; 1989) provided further sedimentological and facies interpretations of the area. This chapter provides a brief synopsis of these two reports, and together with observations made in this study, is used as a background for observations and discussions in the subsequent chapters. A detailed discussion of the Ireton aquitard is presented separately in Chapter 5.

2.1 Leduc Formation.

To date no published facies analysis exists for the Bashaw Reef Complex. SCG (1989) provided an explanation for some of the sedimentological features of the reef complex from the construction of a detailed Leduc Formation isopach map (Figure 2.1), but did not provide any facies correlations. In this study, core was examined from a restricted interval, approximately the uppermost 30 m of the Leduc Formation, and in particular the production horizon that forms in the present-day highs of the reef complex.

The approximate paleotopography that existed at the end of Leduc Formation sediment deposition has been inferred from isopach mapping of the Leduc by SCG (1989; Figure 2.1). In particular, the highs that developed around the margins of the reef complex were inferred to represent a "raised rim" (Figure 2.1; SCG, 1989), however, as discussed in a later section (Section 2.3), this inference may not be accurate and the isopach maps may only portray the present-day relief of the complex.

Facies analysis of cores derived from the uppermost Leduc Formation (Figure 1.2) suggest that organic reef growth (*e.g.*, bulbous, hemispherical and tabular stromatoporoids,

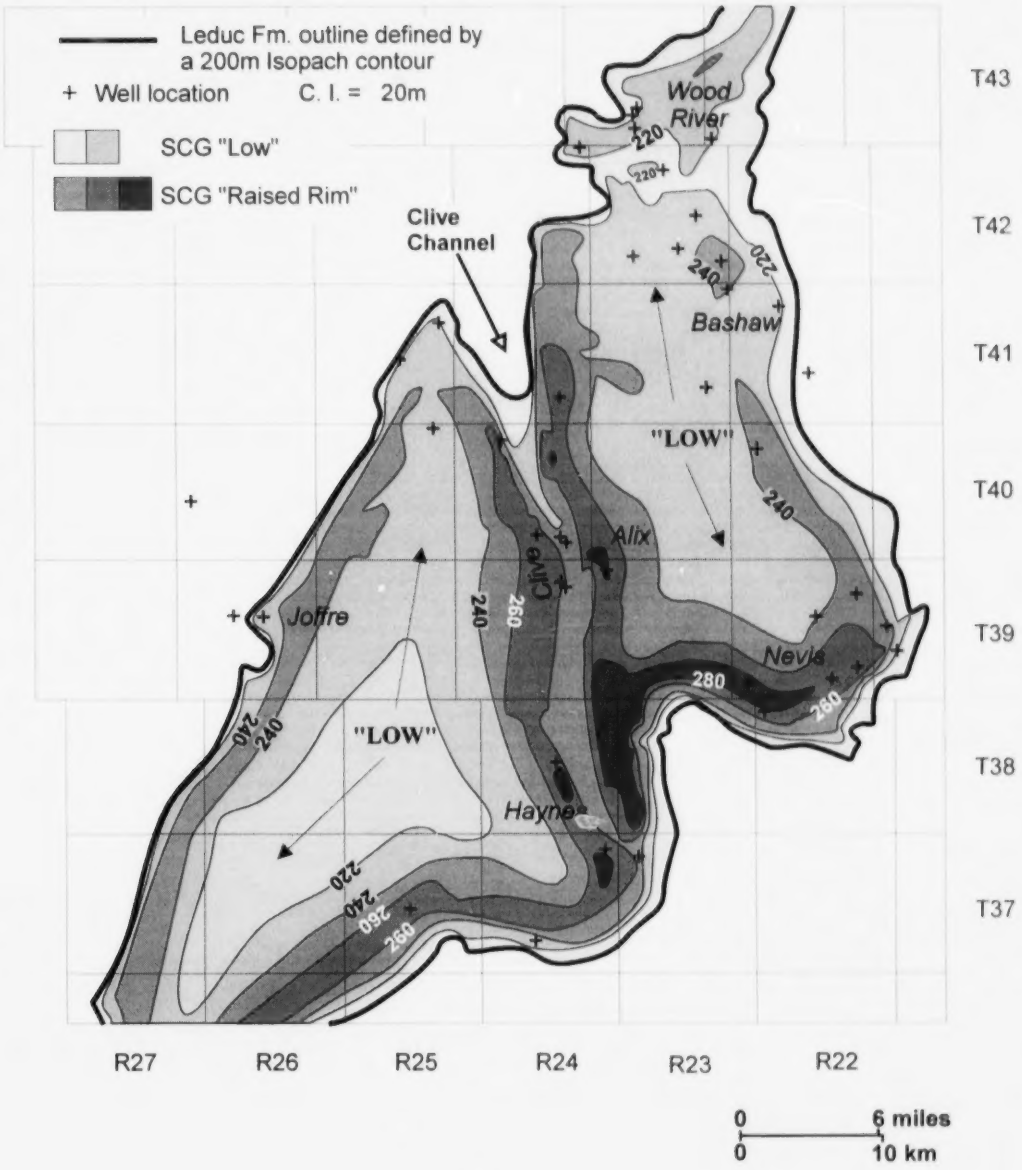

Figure 2.1: Isopach map of the Leduc Formation (modified from SCG, 1989).

and corals) is "patchy" or discontinuous and interfingers with interior *Amphipora* lagoonal facies. This discontinuous reefal development has also been noted in other reef complexes towards the end of sediment deposition of the Leduc Formation, *e.g.*, in the Redwater and Golden Spike reefs (Klovan, 1964; McGillivray and Mountjoy, 1975). In particular, the development of the reef margin in the Nevis and Haynes areas (Figure 1.2) is more like a "patch reef" and seems to be associated with sediments that suggest a less turbulent environment. Cores from the northern and western "raised rim" also display evidence of reefal organisms, although, non are considered part of an organic framework. Hence, in the area of the "raised rims", a continuous organic framework is not present in the uppermost Leduc Formation.

The contact between the Leduc Formation and the Ireton aquitard is rarely sharp and mostly forms a transitional boundary. This is the case particularly in the Nevis and Haynes areas where thin shale/silt interlayers are seen metres below the continuous, tight Ireton aquitard, which render contact picks rather speculative on gamma-ray logs. In the northern part of the complex there is limited evidence of sharper contacts, and in places erosive lags are seen.

Unfortunately, the restricted core intervals covering the transition between formations prevented facies correlations in this study.

2.2 Camrose Member and Nisku Formation.

The Camrose Member and lower Nisku Formation are composed of biostromal platform facies and their distributions shown in Figures 2.2 and 2.3. Good core control enabled Gilhooly (1987) to divide the Nisku and Calmar formations into 18 distinct facies (*e.g.*, Figure 2.4), whereas SCG (1989) preferred to use less detailed facies associations, *e.g.*, biostromal shelf, distal shelf.

Although many of Gilhooly's 18 facies fit into the shallow-ramp facies model of Machel and Hunter (1994; Figure 2.5), some do not. Instead, these facies typically developed under hypersaline conditions that were initiated during the deposition of sediments of the upper Nisku Formation. Sedimentary structures indicative of hypersalinity, such as nodular-mosaic to bedded massive anhydrite (Maiklem *et al.*, 1969) dominate the upper Nisku Formation (Gilhooly's facies 1 and 2; Figure 2.4a). Subtidal

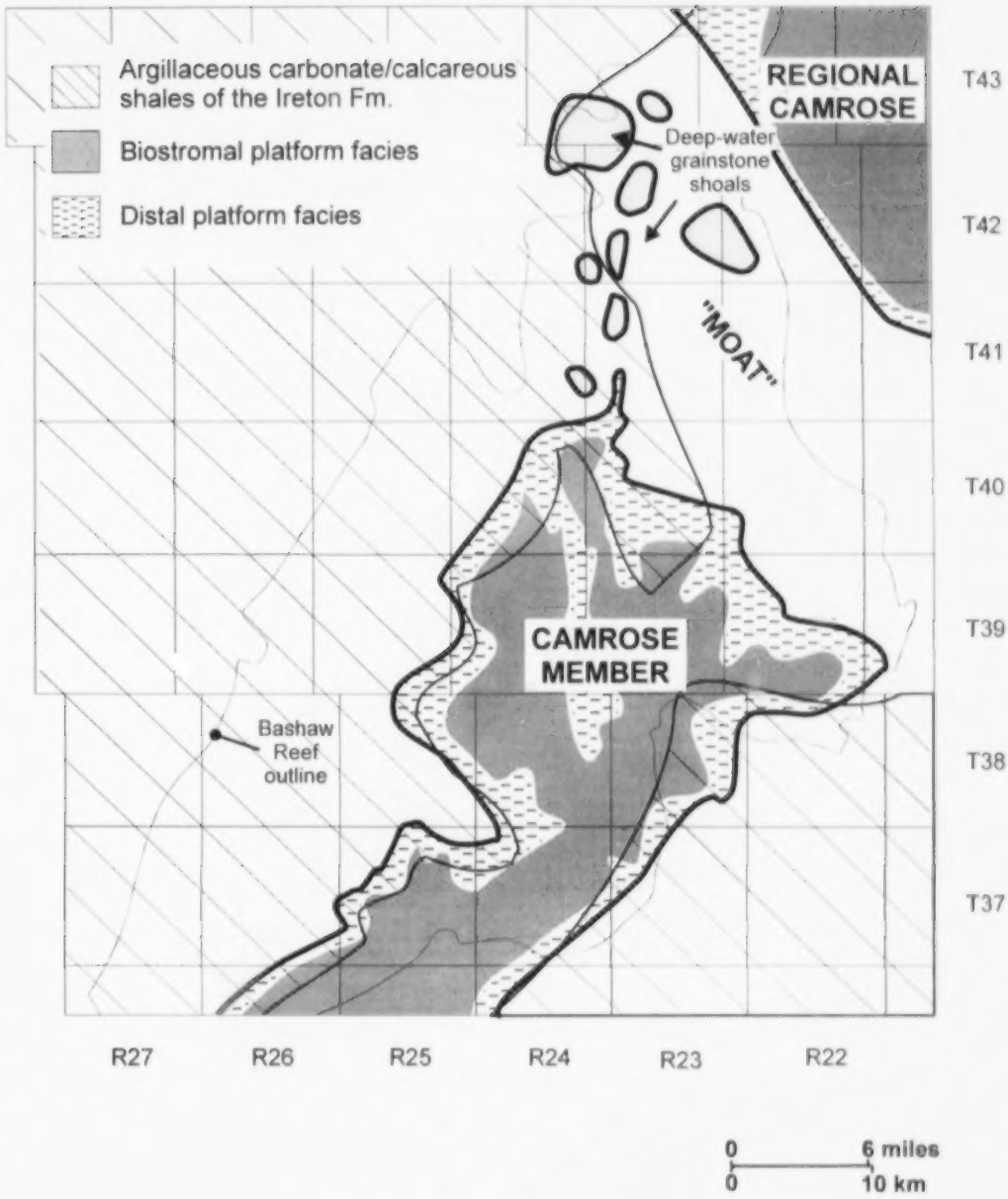

Figure 2.2: Facies distribution map of the Camrose Member over the Bashaw Reef Complex and the approximate extent of the argillaceous carbonate/calcareous shales of the Ireton Formation over the Camrose Member (modified from SCG, 1989).

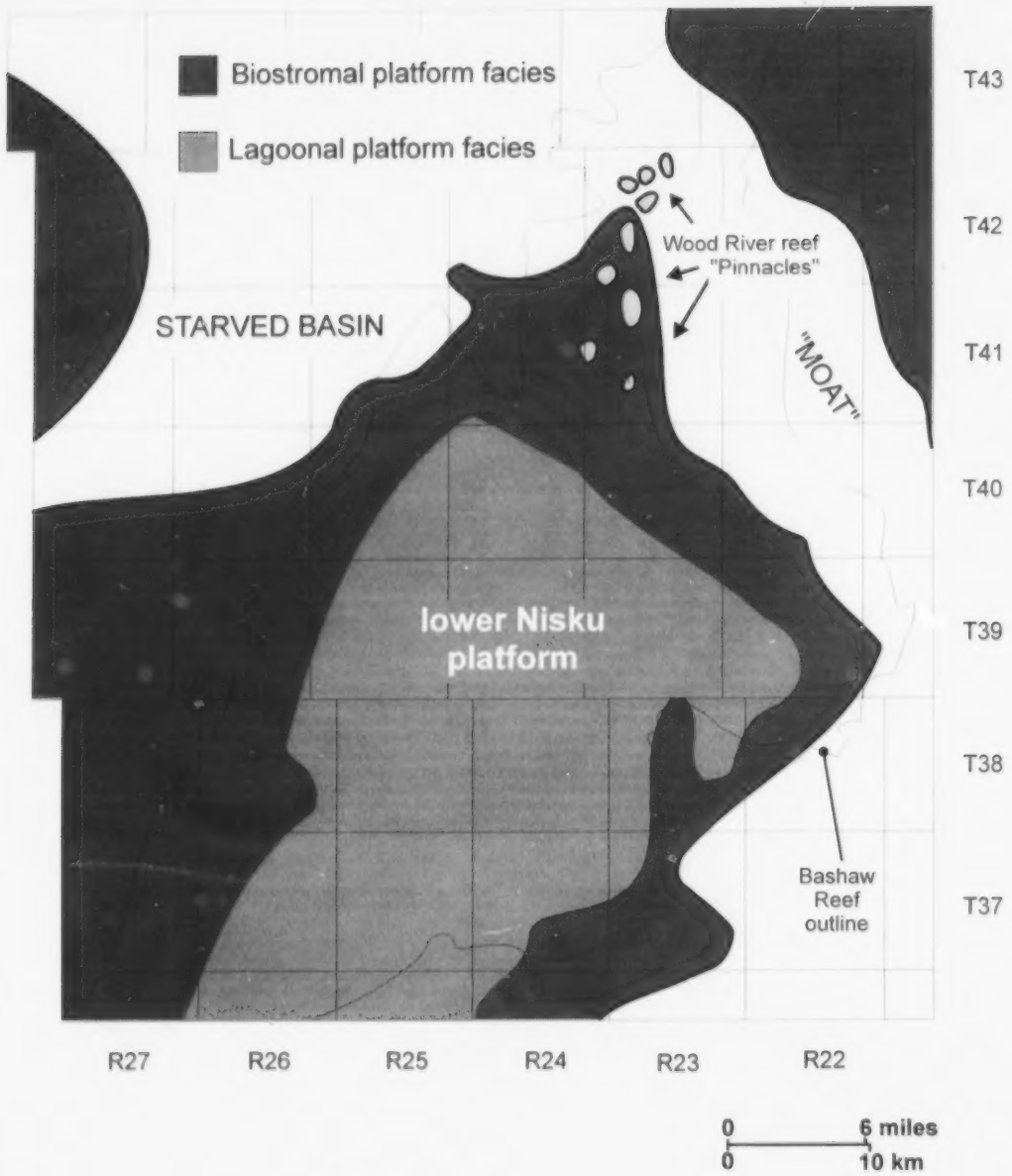

Figure 2.3: Facies distribution map of the lower Nisku Formation (modified from SCG, 1989).

FIGURE 2.4: Typical facies types of the Camrose Member and Nisku Formation.

a) Nodular mosaic anhydrite of the upper Nisku Formation. Facies 1 of Gilhooly (1987). 4-34-42-23W4, 5760 ft. Scale = dime coin (17 mm).

b) Banded fine and coarse crystalline dolostone associated with an evaporitic/peritidal environment in the Camrose Member/lower Nisku Formation. Facies 14 of Gilhooly (1987). 4-17-39-21W4, 5518 ft. Scale = dime coin (17 mm).

c) Algal laminite — a transitional facies between the platform facies of the lower Nisku Formation and the hypersaline conditions of the upper Nisku Formation. Facies 3 of Gilhooly (1987) and Facies f of Machel and Hunter (1994). 2-12-42-23W4, 5649 ft. Scale bar = 17 mm.

d) Floatstone/wackestone with a few replaced coral(?) fragments in the Camrose Member/lower Nisku Formation platform. Facies 5 and 6 of Gilhooly (1987) and facies e of Machel and Hunter (1994). 6-12-42-23W4, 5418 ft. Scale bar = 17 mm.

e) Skeletal floatstone comprised of corals (*Thamnopora*?), *Amphipora*, and some molds and vugs of possibly tabular to bulbous stromatoporoids — common in the shallow platform environment of the Camrose Member/lower Nisku Formation. Facies 9 of Gilhooly (1987) and Facies d Machel and Hunter (1994). 8-31-38-23W4, 1791.5 m. Scale = dime coin (17 mm).

f) Floatstone comprised of wafer-like stromatoporoids (*Euryamphipora*?) common in the deeper-water platform environment of the Camrose Member/lower Nisku Formation. Facies 12 of Gilhooly (1987) and Facies c Machel and Hunter (1994). 6-36-37-24W4, 1832.7 m. Scale bar = 17 mm.

Figure 2.4: Typical facies of the Camrose Member and Nisku Formation.

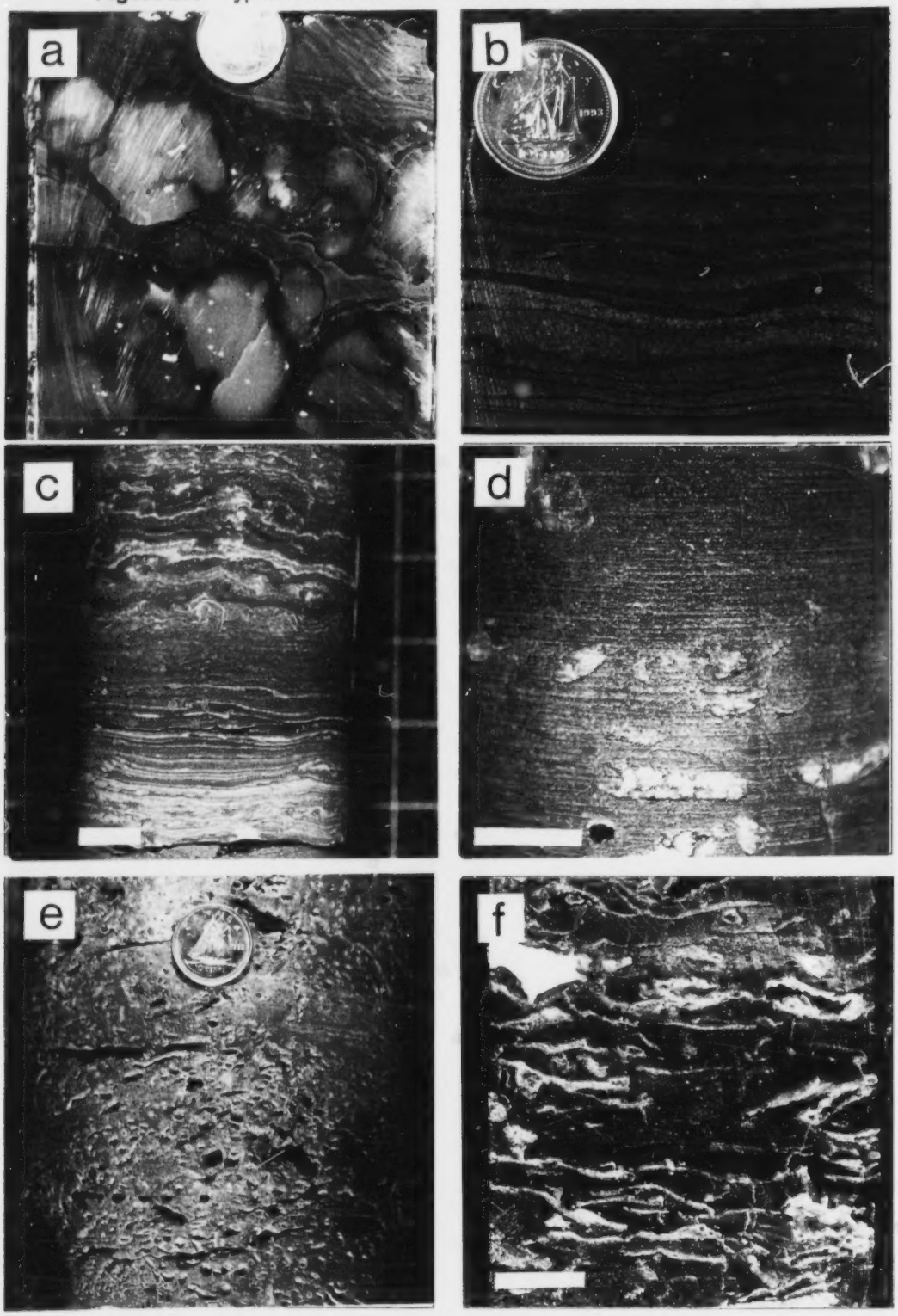

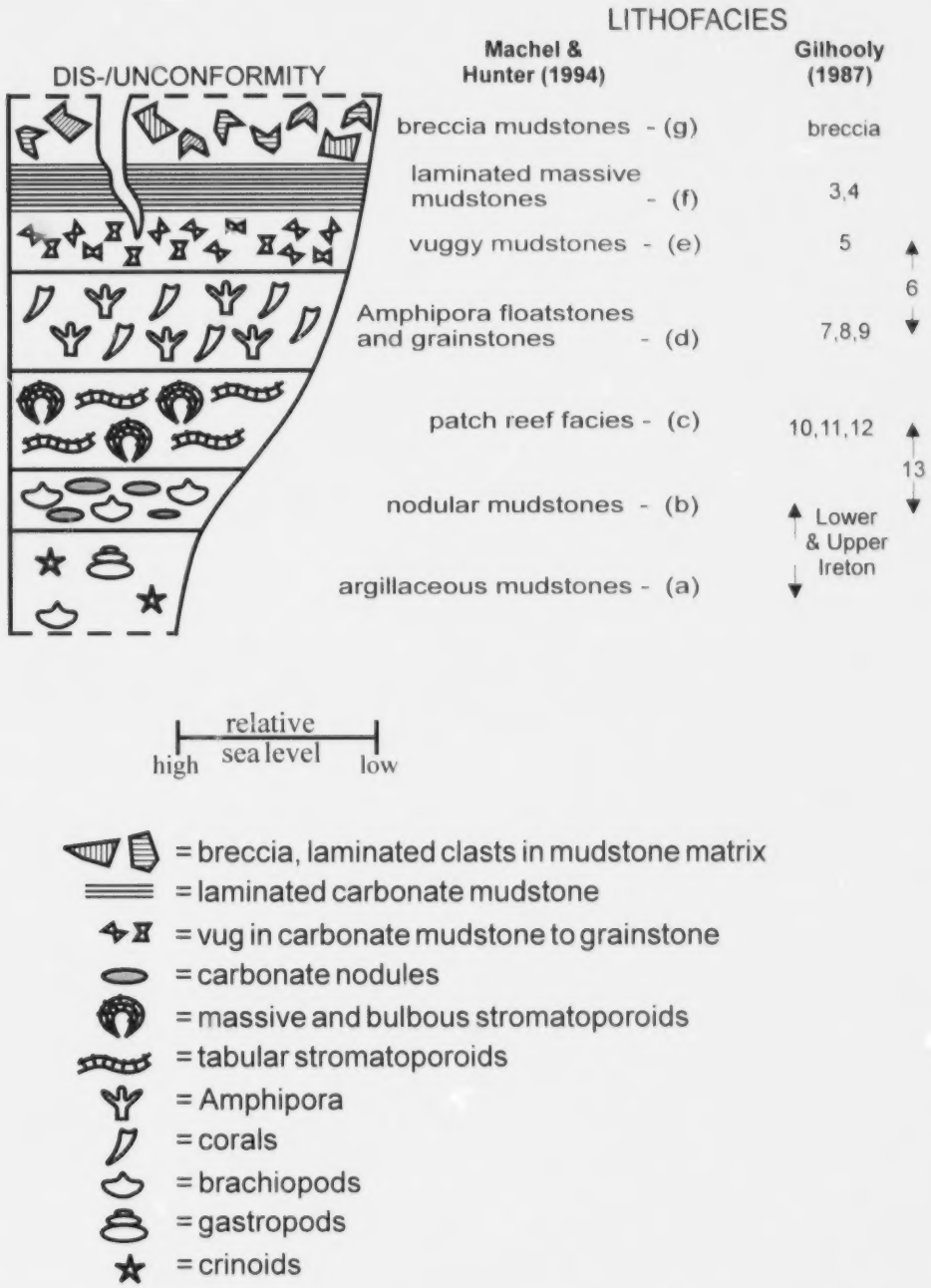

Figure 2.5: Comparison of the shallow ramp facies model (codes a - g) of Machel and Hunter (1994) and facies (numbered codes) defined by Gilhooly (1987).

facies types also occur locally (Gilhooly's facies 14 and 15) but are clearly associated with the evaporitic/peritidal facies. Facies 14, of Gilhooly (1987), is particularly well developed beneath an evaporitic basin, in an area informally known as the "Moat" (Dixon *et al.*, 1991; Figure 2.3) and is also present (in one core) in a starved basin to the northwest (Figure 2.3). This facies is a banded fine and coarse crystalline dolostone (possibly storm related) with a high organic content (Figure 2.4b). SCG (1989) suggested it to be a condensed sequence deposited in mesosaline conditions and ascribed it to the Camrose Member/lower Nisku Formation, forming a transition between the Ireton aquitard and the evaporites of the upper Nisku Formation. Two terrigenous clastic sediments are also present: green shale/silt interlayers of the Woodbend and Winterburn groups, which are probably related to storm events (Wendte and Stoakes, 1982), and silt/sandstones of the Calmar Formation.

Above the reef complex, the biostromes of the Camrose Member and lower Nisku Formation are usually in direct contact, with only minor incursions of argillaceous carbonates and calcareous shales of the Ireton Formation occurring over the Camrose Member (Figure 2.2). This direct contact has made them difficult to differentiate and has led to a wide disparity in the interpreted distributions of the two biostromes (presented by Gilhooly, 1987 and SCG, 1989). The distribution map of the Camrose Member and lower Nisku Formation produced by SCG (1989) is deemed the most accurate (Figures 2.2 and 2.3) and is in agreement with stratigraphic correlations made in this study (*e.g.*, Figure 4.4). A comparison of the distributions of these biostromes (Figures 2.2 and 2.3) with the inferred topographic highs that existed at the end of Leduc Formation sediment deposition (Figure 2.6) suggests there is some control exerted by the underlying reef complex. The Camrose Member is defined by Gilhooly (1987) and SCG (1989) to be a single shallowing-upward cycle.

Although the separation of the Camrose Member and lower Nisku Formation is important stratigraphically, the two biostromal units are effectively continuous in terms of hydrocarbon migration and trapping. Only within the Clive area do argillaceous carbonates and calcareous shales of the Ireton Formation split this reservoir (Figure 4.4).

The uppermost contacts of the Ireton aquitard with the Camrose Member and lower Nisku Formation are relatively sharp and are likely submarine hardgrounds (SCG,

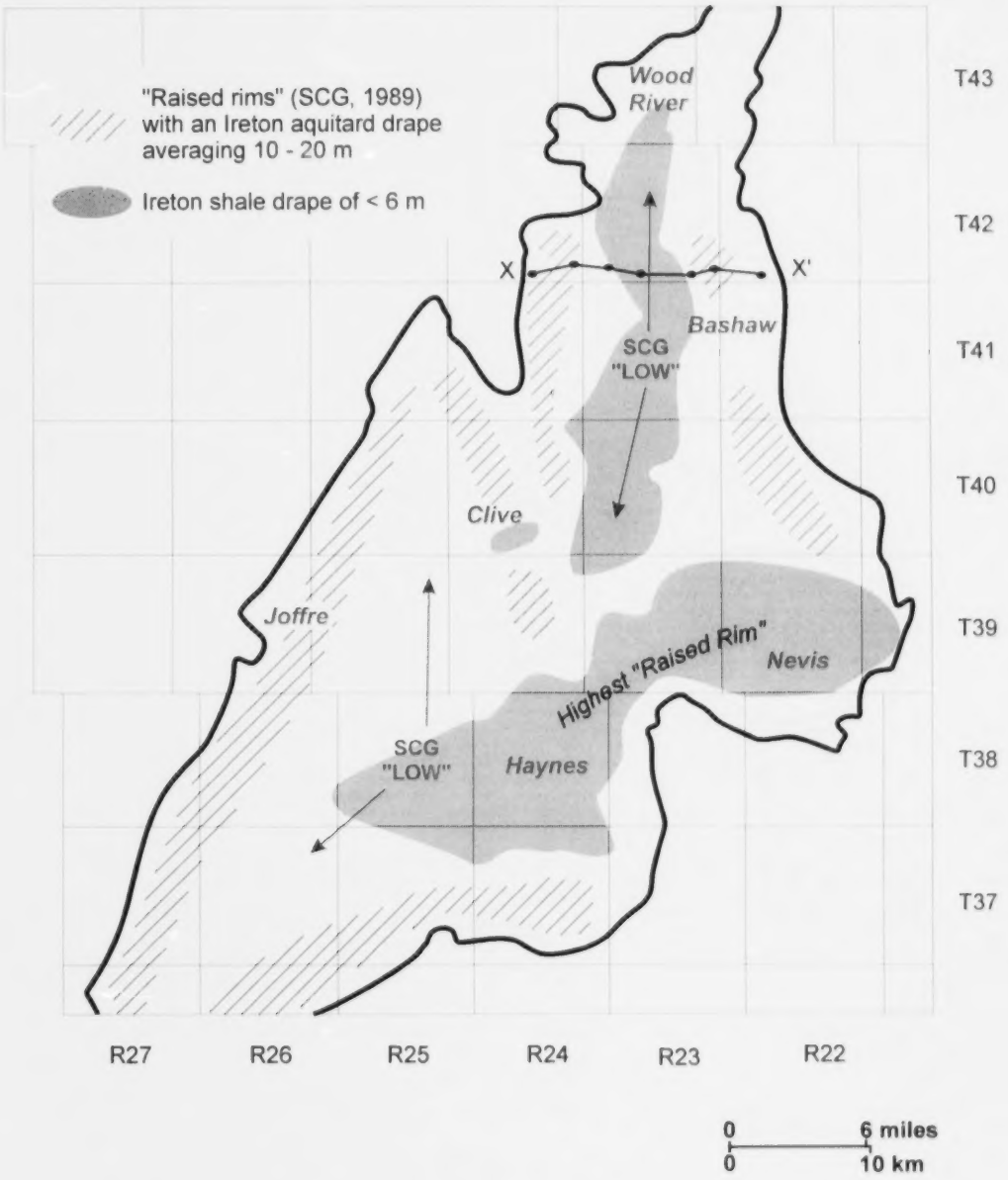

Figure 2.6: A map indicating the Ireton aquitard thickness over the "raised rims" of the Bashaw Reef Complex (striped areas), which are inferred to be paleotopographic highs by SCG (1989), and areas of < 6 m Ireton aquitard thickness (grey shading), which are considered by this study to have had the highest depositional relief. SCG "lows" are also indicated. The Haynes and Nevis "raised rims" are considered the highest topographic feature at the end of sediment deposition of the Leduc Formation in both this study and SCG (1989).

1989) related to a rapid relative rise in sea-level. In the study area, there is good evidence for hardgrounds and erosive(?) lags between the Ireton aquitard and the lower Nisku Formation on the eastern margin of the reef complex, where glauconitic grains are present, but in other places the contacts are gradational and some are of questionable origin.

2.3 Paleotopographic "Lows" in the Interior of the Bashaw Reef Complex?

A notable feature of the Bashaw Reef Complex are the paleotopographic "lows" described by SCG (1989) from a Leduc Formation isopach map (Figure 1.4). These "lows" are located in the interior of the reef complex and approximately coincide with a thin Ireton aquitard drape (<6 m; Figure 2.6) which is mostly conformable over the Leduc Formation. Surrounding these "lows" are the so-called "raised rims" on the margins of the reef complex (SCG, 1989) which are typically draped by >10 m of Ireton aquitard (Figure 2.6). The "raised rims" in the Nevis and Haynes areas in the south east, however, have a much thinner veneer of Ireton aquitard (Figure 2.6) and are considered by SCG (1989) to have been the highest depositional feature at the end of sediment deposition of the Leduc Formation.

A thickening of the Ireton aquitard over most of the margins is inconsistent, however, with the idea that the reef complex formed a "raised rim" to the margins, because aquitard thicknesses over a "raised rim" should intuitively be thinner not thicker than the paleotopographic "lows" because of higher wave energy conditions reducing sediment (clay) accumulation. The Ireton aquitard thicknesses, however, suggest that the lows of the reef complex were in fact topographically higher than the "rims" at the end of sediment deposition of the Leduc Formation, and similar in height to the Nevis and Haynes areas (Figure 2.6).

In spite of this inconsistency, the SCG (1989) study concluded that the margins of the reef complex were shallow features because they are now structurally higher than the interior. However, it is likely that there was greater differential compaction affecting the interior of the reef complex relative to the margins, *e.g.*, Redwater reef (Mossop, 1972). Such differential compaction is to be expected because seaward margins are commonly strengthened by cementation due to a higher flux of seawater being pumped

through by waves and tides (James *et al*, 1976). For example, in the Devonian Golden Spike and Rainbow reefs, up to about 70% by volume of early marine cement is found in the reef margins (Walls and Burrowes, 1985). Cementation processes would also explain the presence of the highs of the Clive and Alix areas (Figure 2.1) located within the interior of the reef complex. These highs are developed around a re-entrant known as the Clive Channel (Figure 2.1) where it was likely that open-marine water was focused into the reef interior (SCG, 1989) enabling cementation.

In the Bashaw Reef Complex, there is no direct evidence to support differential compaction because the uppermost Leduc Formation displays poor zonation between reefal and lagoonal facies in the marginal areas, and no core is available from the interior "low" areas. A similar pattern of discontinuous reef growth was also observed in the Upper Leduc Formation of the Redwater and Golden Spike reefs (Klovan, 1964; McGillivray and Mountjoy, 1975). However, these studies showed that despite the lack of sediment differentiation in the Upper Leduc Formation, during sediment deposition of the Middle Leduc Formation, there was a more continuous "rigid" reef framework at the margins of the reef complex. This "rigid" framework was likely to be the supporting structure that created the raised rim observed in the Redwater reef (Mossop, 1972). A similar situation, therefore, may have occurred in the Bashaw Reef Complex and would explain the present-day structural variation seen between the margins and the interior.

Furthermore, construction of a cross section with a younger datum, the Calmar Formation, elevates the reef interior to a level higher than that of the margins (Figure 2.7). The choice of the Calmar Formation as a datum was considered questionable by Gilhooly (1987) because of its variable thickness, however, its thickness is uniform over the central part of the complex. Another effect that could influence the validity of a cross section, using the Calmar Formation as a datum, is the dissolution of the upper Nisku Formation evaporites which could "raise" portions of the Leduc Formation in the cross section, however, this is unlikely to have affected the whole cross section.

2.4 Differential Relief of Reef-Complex Margins.

Another anomalous feature of the isopach map of the Leduc Formation is the apparent ~40 m height difference between the "raised rim" on the north and west margins,

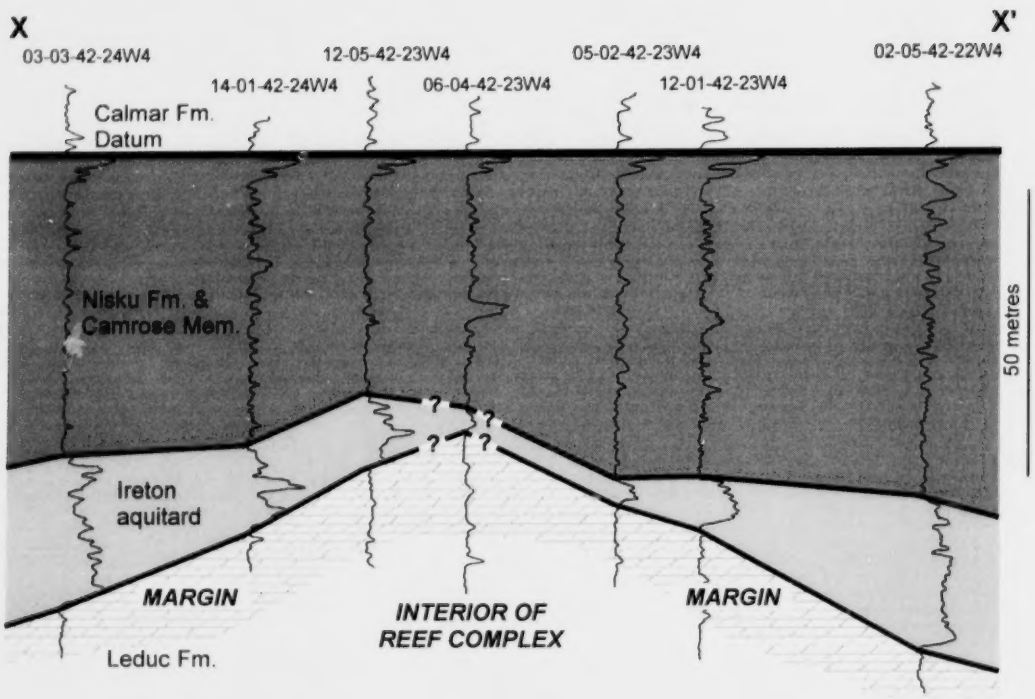

Figure 2.7: A cross section demonstrating the raised interior of the Bashaw Reef Complex to that of the reefal margin at the time of Calmar Formation sediment deposition. This suggests that the reefal margins may have been submerged and affected by similar processes as modern shelf-edged reefs. Clay/silt-rich lenses within the interior of the reef complex (see gamma-ray curves) suggest that the margins may have "drowned" earlier (see text for discussion). The line of cross section X to X' is shown in Figure 2.6.

and the rim on the southeast of the reef complex in the Nevis and Haynes area (Figure 2.1). The differential relief between the margins of the reef complex is likely to have been present during sediment deposition of the Leduc Formation because the Ireton aquitard mimics this relief; a compacted Ireton aquitard of 10 - 20 m thickness covers the north and west margins, whereas in the southeast, Ireton aquitard thicknesses are close to zero (Figure 2.6). The present-day variation in relief between the margins of ~40 m may not be that dissimilar, therefore, to the relief that existed at the end of Leduc Formation sedimentation, if the Ireton aquitard was uncompacted. Possible explanations for the development of this relief are those of erosion, syndepositional faulting, differential compaction, and relative rises of sea level causing reef backstepping. Erosion is an unlikely explanation for the ~40 m relief now present between the reef margins of the north and west and those of the southeast, because there is no evidence of extensive erosion, subaerial or subaqueous, between the Leduc Formation and the Ireton aquitard. Syndepositional faulting probably had only a minor effect, and is unlikely to have affected one margin and not the others. Compaction is also unlikely to have generated such differential relief, especially as the majority of compaction likely postdates sediment deposition of the Leduc Formation. It is therefore hypothesized that much of the difference in relief between the margins is probably occurred as a result of relative rises in sea level causing reef backstepping on the Bashaw Reef Complex.

Evidence in support of reef backstepping is that Leduc Formation sediments of a much deeper environment should be preserved in cores from the north and west margin, compared to the shallower southeast, if an ~40 m differential relief existed prior to the deposition of the sediments of the Ireton aquitard over the reef complex. Core data, however, shows that the north and west margins consisted of shallow water sediments, with evidence of reef associated organisms (*e.g.*, tabular, hemispherical stromatoporoids), although they were probably not quite as shallow as the "patch reefs" to the southeast. Nevertheless, assuming most organic accretion took place in shallower waters of <40 m, the reef organisms of the north and west margins were unlikely to have existed contemporaneously with those of the southeast. This implies that the demise of the Bashaw Reef Complex did not occur simultaneously across the reef complex and that reef backstepping likely occurred; the reefal organisms of the northern and western margins

probably died slightly earlier during sediment deposition of the Leduc Formation, whereas the southeastern "patch reefs" were able to continue growing, producing up to ~40 m of relief.

A possible explanation as to why the reef margins of the north and west died earlier than the southeast could be related to an initial difference in height of the margins, as indicated by the slightly deeper-water reefal facies of the north and west margins, compared to the shallower "patch reef" facies of the southeast. During a relative rise in sea level, an initial difference in the heights of the margins might have led to an earlier demise of the deeper-water reefal organisms by taking them out of the photic zone at a faster rate than the shallower "patch reefs" which could keep-up or catch-up with sea level rise. Within the northern and western areas, sharp contacts and some lag deposits occur between the Leduc Formation and Ireton aquitard that could be interpreted as indicators of a drowning surface (Schlager, 1989).

Terrigenous clastic smothering is considered unlikely to have been the direct cause of reef demise because it probably would have killed the entire reef complex, and would not therefore generate such differential relief. However, in conjunction with a relative rise in sea level, clay sedimentation would occur in the deeper areas (below fairweather wave base). This could also account for the marked increase in clay content seen within the uppermost Leduc Formation of the Nevis and Haynes areas, and the highs in the interior of the reef complex (see gamma-ray "kicks" in Figure 2.7). These areas may have been periodically covered with clays and silts stirred up from the nearby drowned areas during storms, creating clay/silt-rich lenses within the reefal areas.

The initial difference in height of the reef complex may have developed because of storm-related processes. Within a modern reef environment around the island of Grand Cayman, Blanchon (1995) has shown that storms have a significant impact on the height of accretion of submerged shelf-edge reefs. On the storm-exposed margins of the island, where fragile corals are periodically "pruned" by storm waves, reefs only grow up to ~20 m below sea level. On the leeward margin, however, the lower wave energies during storms enable the shelf-edge reef to grow to within ~12 m of the surface. In the Bashaw Reef Complex, similar storm processes may have hit the reef complex from the north, enabling the less exposed southeastern margin to accrete closer to sea level, whereas the

west and north margins were "pruned" by storm waves. Indirect evidence in support of a dominant storm influence from the north can be inferred from the greater fetch that was available for the generation of storm winds across the northern part of the East Shale Basin (Figure 1.1). In addition, the dominant ocean currents for the East Shale Basin are estimated to be from the north (tabulated by Stoakes: 1980, Table 1, p.390), and may also have been controlled by winds from the north. Therefore, it is likely that major storms, and therefore waves, would have tended to approach from the north.

2.5 Synopsis.

The isopach lows of the Leduc Formation (SCG, 1989) appear to represent differentially compacted sediments of the interior of the reef complex. These lows were once probably similar in height to the southeastern margin of the Nevis and Haynes areas, and were therefore higher than the other present-day "raised rim" margins (Figure 2.8). This is also suggested by the fact that the other "raised rim" margins of the reef complex, during at least the uppermost Leduc Formation, were represented by deeper-water reefal facies, in contrast to the slightly shallower "patch reef" facies of the Nevis and Haynes areas, and perhaps that of the interior of the reef complex. Such differential reef accretion can be accounted for, or is consistent with, a storm-induced process. This likely prevented the north and west margins from accreting to near sea level, and is a similar process to that which affects modern shelf-edged reefs (Hubbard *et al.*, 1986; Blanchon, 1995). The Nevis and Haynes margins (as well as the interior of the reef complex) were sheltered from the dominant storm fetch and were able to grow closer to sea level. Near the end of Leduc Formation sediment deposition, the deeper western and northern margins were unable to keep up with a relative rise(s) in sea level and consequently drowned. The shallower southeastern margin "patch reefs" and reef interior survived longer developing ~40 m of relief. However, it is likely that cementation occurred in the margins of the reef complex that meant the interior of the reef complex was more affected by subsequent differential compaction. Thus a "raised" margin developed around the reef complex and the Nevis and Haynes areas developed an apparent ~40 m relief to that of the north and west margins.

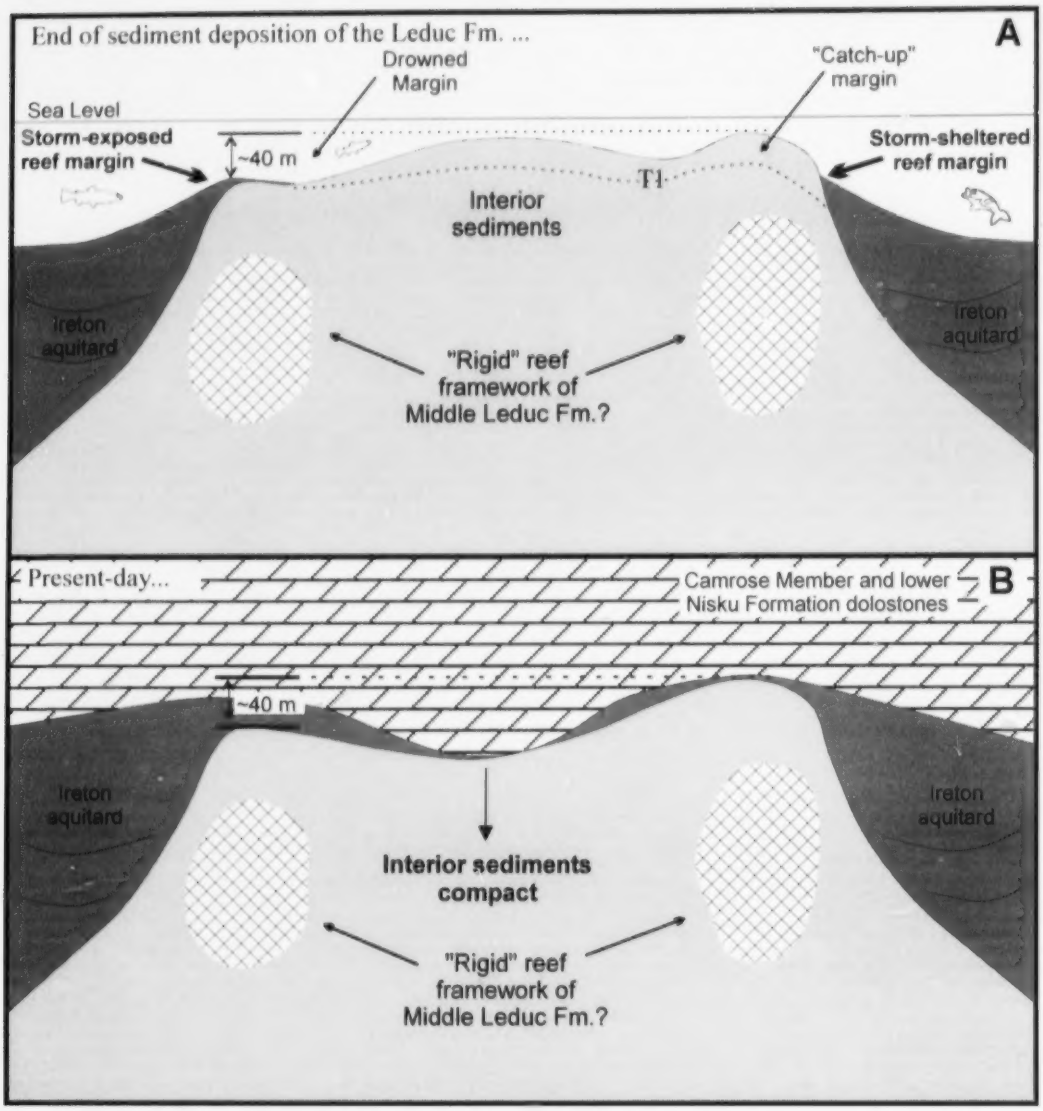

Figure 2.8: A schematic of the Bashaw Reef Complex showing differential reef accretion and compaction of the interior of the reef complex. Diagram A depicts the demise of the storm-exposed reef margin with a rise in sea level at time line T1, the storm-sheltered margin continues to grow as does the reef interior. Diagram B indicates the present-day relief of the Bashaw Reef Complex, with a greater Ireton aquitard thickness over the storm-exposed "raised" margin than the interior of the reef complex, or the storm-sheltered margin which now has ~ 40 m of relief over the storm-exposed margin.

CHAPTER 3

DIAGENESIS

This chapter presents the results of the first diagenetic study of the Bashaw area as a whole. An understanding of the diagenesis of the area is an essential component in the determination of hydrocarbon migration and breaching characteristics. One other diagenetic study in the Bashaw area deals with the Joffre Field (Al-Bastaki *et al.*, 1995a). The diagenesis and paragenetic history of the area has been established through detailed core, thin section, and geochemical analysis (Figure 3.1). Many of the diagenetic phases are similar in appearance to some of the phases described from the Leduc Formation and Nisku Formation reefal facies of central Alberta (*e.g.*, Machel and Anderson, 1989; Amthor *et al.*, 1993; Drivet, 1993), and those of the sabkha/tidal-flat environments of the Birdbear Formation of Saskatchewan (Whittaker and Mountjoy, in press). Major influences on fluid migration and pore generation include: replacement dolomitization, late-stage dolomite and anhydrite cementation, and fracturing and dissolution events. Replacement dolomitization, however, appears to have had the most significant impact on fluid migration and pore generation in the Bashaw area.

3.1 Petrographic and Geochemical Characteristics.

3.1.1. Limestones

The eastern flank of the Bashaw Reef Complex, in the area of well 3-15-41-22W4 (Figure 1.2), generally consists of marine grainstones and floatstones, and is the only area comprised of limestone. Interparticle porosity is dominantly filled by sparry calcite cements, ranging in size from fine to coarse crystalline. In some cases the sparry calcite cement is partially dolomitized, and some fractures are lined with dolomite cements. The fauna includes: crinoids, brachiopods, and scattered coral and stromatoporoid debris. Peloidal grains are also abundant (~100 μm in diameter).

Isotopic analyses (methodology in Appendix I) of two limestones from well 3-15-41-22W4 yielded $\delta^{18}O$ values of -5.4 and -6.8‰ (PDB) and $\delta^{13}C$ values of +3.3 and

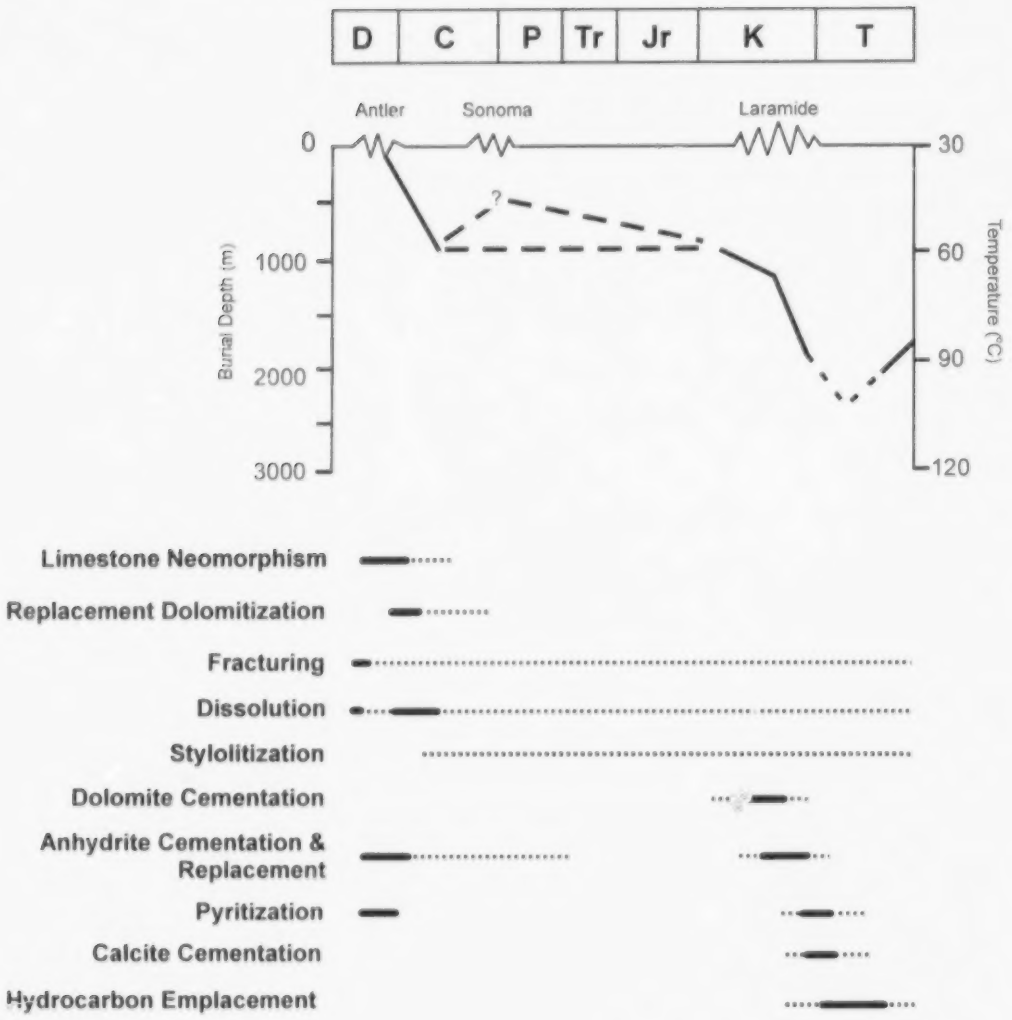

Figure 3.1: A paragenetic sequence for the Bashaw area, coupled with a generalized burial history (modified from Whittaker and Mountjoy, in press). In the paragenetic sequence, the thicker lines represent the periods when these processes were most likely to have occurred. Dotted lines indicate the probable range of time over which these processes *may* have occurred.

+2.7‰ (PDB) (Figure 3.2; Table 3.1).

3.1.2. Matrix replacement dolomites

Matrix replacement dolomites form the most abundant diagenetic phase in the area, obliterating all evidence of the precursor limestone, except that of well 3-15-41-22W4. The approximate spatial extent of the matrix dolomites in the Bashaw area was determined using core and well log data. Three types of replacement dolomite were identified and classified according to crystal-size distribution (unimodal/polymodal) and crystal-boundary shape (planar/nonplanar) (Sibley and Gregg, 1987; Figure 3.3).

T1: A cryptocrystalline (1 - 4 μm) unimodal dolomite (Figure 3.4a) that forms a mosaic with extremely low intercrystalline porosity of inclusion-rich, light brown dolomite with a homogeneous orange-red cathodoluminescence. No crystal boundaries could be discerned. T1 dolomite is present in the upper Nisku Formation evaporitic sediments and is fabric retentive (*e.g.*, cryptalgal laminations).

T2: A very fine- to fine-crystalline (4 - 30 μm), planar-subhedral, unimodal dolomite (Figure 3.4b) that is present as a mosaic with low intercrystalline porosity of inclusion-rich, brown/grey dolomite. Cathodoluminescence is red-orange and less luminescent than T1 dolomite. T2 dolomite is almost exclusively present in the Ireton aquitard, but also occurs locally in the Leduc Formation and lower Nisku Formation where it is gradational with T3 dolomites. T2 dolomite, in general, preserves the original sediment fabric.

T3: Fine- to coarse-crystalline (30 - 400 μm), planar-subhedral(euhedral), polymodal dolomite. This broad category is essentially a composite of the Type 1 and Type 2 dolomites described by Amthor *et al.* (1993) from the adjacent Rimbey-Meadowbrook reef trend. Gradations are seen between T3 crystals that are grey (inclusion-rich), subhedral, and fine crystalline (Figure 3.4c), to clear, euhedral, and coarse crystalline (Figure 3.4d). Inclusions form a "speckled" nucleus in many crystals and are more prevalent in smaller crystals. T3 dolomite is present both as a mosaic with low intercrystalline porosity of subhedral crystals, or as a more porous mosaic of euhedral crystals. Euhedral crystals are typically less cloudy and display clear rims adjacent to

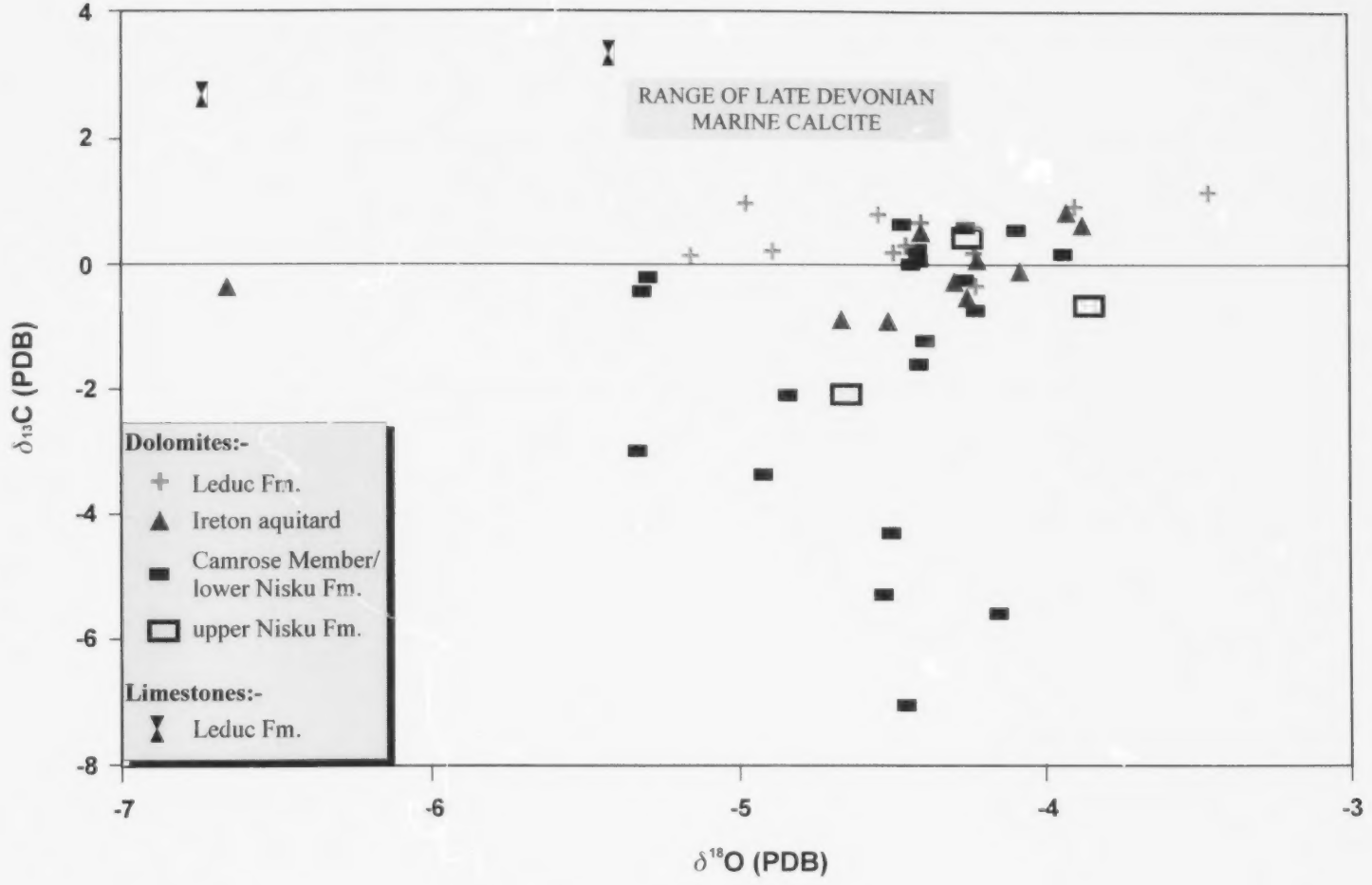

Figure 3.2: Plot of $\delta^{13}C$ versus $\delta^{18}O$ isotope values for replacement dolomites and two limestone samples. The range for Late Devonian marine calcite was taken from Carpenter *et al.* (1991).

Well Location	Depth (ft or m)	Interval	Delta 18O	Delta 13C	Dolomite Type	Organic-rich Y/N
4-17-39-21W4	5448 ft	u.Nisku	-3.8	-0.7	T1	N
4-17-39-21W4	5500 ft	u.Nisku	-4.2	-0.7	T3	N
4-17-39-21W4	5520 ft	l.Nisku	-4.9	-2.1	T2	Y
4-17-39-21W4	5523 ft	l.Nisku	-4.5	-7.0	T3	Y
4-17-39-21W4	5530 ft	l.Nisku	-4.1	-5.6	T3	Y
4-17-39-21W4	5540 ft	Leduc	-5.0	0.9	T3	N
5-33-40-24W4	1823 m	l.Nisku	-4.4	0.0	T3	N
5-33-40-24W4	1826.3 m	l.Nisku	-3.9	0.1	T3	N
5-33-40-24W4	1832.5 m	l.Nisku	-4.4	0.0	T3	N
5-33-40-24W4	1836 m	Ireton aq.	-4.3	-0.3	T2	N
5-33-40-24W4	1858 m	Leduc	-5.1	0.2	T3	N
5-33-40-24W4	1860 m	Leduc	-4.9	0.2	T3	N
16-26-39-24W4	1844 m	Cam/l.Nisku	-4.4	0.2	T3	N
16-26-39-24W4	1848.4 m	Ireton aq.	-4.1	-0.1	T3	N
16-26-39-24W4	1856.5 m	Ireton aq.	-4.4	0.6	T2	N
16-26-39-24W4	1858 m	Leduc	-4.5	0.3	T3	N
6-22-38-24W4	6148 ft	Camrose	-4.2	0.6	T3	N
6-22-38-24W4	6168 ft	Ireton aq.	-3.9	0.8	T3	N
6-22-38-24W4	6173 ft	Ireton aq.	-3.9	0.6	T2	N
6-22-38-24W4	6200 ft	Leduc	-4.2	-0.3	T3	N
2-15-38-24W4	6134 ft	l.Nisku	-4.1	0.5	T3	N
2-15-38-24W4	6154 ft	Camrose	-4.2	0.4	T3	N
2-15-38-24W4	6160 ft	Camrose	-4.4	0.2	T3	N
2-15-38-24W4	6168 ft	Ireton aq.	-4.4	0.6	T2	N
2-15-38-24W4	6170 ft	Leduc	-4.2	0.2	T3	N
3-15-41-22W4	5542 ft	u.Nisku	-4.6	-2.1	T1	Y
3-15-41-22W4	5547 ft	Ireton contact	-4.5	-4.3	T2	N
3-15-41-22W4	5634 ft	Ireton aq.	-4.5	-0.9	T2	N
3-15-41-22W4	5758 ft	Ireton aq.	-6.6	-0.3	T2	N
3-15-41-22W4	5844 ft	Leduc	-5.4	3.3	Lmst.	N
3-15-41-22W4	5853 ft	Leduc	-6.8	2.7	Lmst.	N
10-18-40-26W4	6827 ft	l.Nisku	-4.4	-1.2	T3	N
10-18-40-26W4	6834 ft	l.Nisku	-5.3	-0.4	T3	N
10-18-40-26W4	6842 ft	Ireton aq.	-4.6	-0.8	T2	N
13-29-40-22W4	5474 ft	l.Nisku	-4.9	-3.3	T3	Y
13-29-40-22W4	5478 ft	l.Nisku	-4.5	-5.2	T3	Y
13-29-40-22W4	5506 ft	Ireton aq.	-4.2	0.1	T3	N
13-29-40-22W4	5532 ft	Leduc	-4.5	0.8	T3	N
16-2-40-24W4	1917.5 m	Ireton aq.	-4.2	-0.5	T3	N
16-2-40-24W4	1929.2 m	Leduc	-4.4	0.7	T3	N
16-2-40-24W4	1930.5 m	Leduc	-3.9	0.9	T3	N
6-12-39-22W4	5402 ft	l.Nisku	-4.2	-0.3	T3	N
6-12-39-22W4	5427 ft	l.Nisku	-5.3	-0.2	T3	N
6-12-39-22W4	5435 ft	l.Nisku	-4.4	-1.6	T3	Y
6-12-39-22W4	5447 ft	Camrose	-4.5	0.6	T3	N
6-12-39-22W4	5464 ft	Leduc	-4.5	0.2	T3	N
6-12-39-22W4	5490 ft	Leduc	-3.5	1.1	T3	N
11-9-44-24W4	5792 ft	l.Nisku	-5.3	-3.0	T3	Y

Table 3.1: Sample location, depth, and isotopic composition of replacement dolomite (Types T1, T2, and T3), and two limestone samples. The presence of organic matter appears to correspond to a more restricted, hypersaline facies with lower carbon-13 values.

Matrix Replacement Dolomite Types

T1

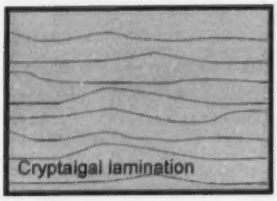

- cryptocrystalline (1-4μm)
- unimodal
- very dense (low porosity) mosaic
- orange/red cathodoluminescence

T2

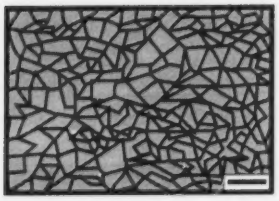

- very fine to fine crystalline (4-30μm)
- planar-subhedral
- unimodal
- dense mosaic
- brown/grey (inclusion-rich)
- red/orange cathodoluminescence

T3 (Types 1 & 2)

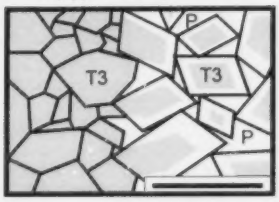

- fine to coarse crystalline (30-400μm)
- planar-subhedral (euhedral)
- polymodal
- porous to dense mosaic
- clear to grey
- red/orange cathodoluminescence with dark blotches

Pore-lining Dolomite Cement Types

C1 (Type 3)

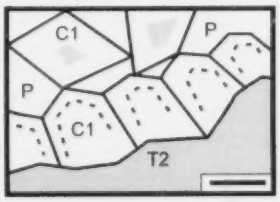

- coarse crystalline (100-700μm)
- planar-subhedral (euhedral)
- clear to cloudy white
- zonation
- dull orange/black cathodoluminescence that varies with zonation

C2 (Type 5)

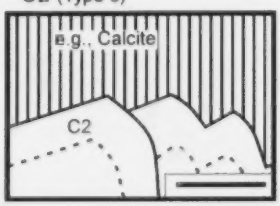

- coarse to very coarse crystalline (400-1400μm)
- non-planar (saddle)
- curved crystal faces and sweeping extinction
- homogeneous red cathodoluminescence

Figure 3.3: Five dolomite textures observed in the Bashaw area (Leduc Fm. to upper Nisku Fm.). Classification scheme is compared with dolomite Types 1,2,3, and 5 of Amthor et al. (1993). "P" is an abbreviation for pore space. T1 dolomite has no discernible crystal size; the scale bar for T2 dolomite is 30 μm; and the scale bars of T3, C1, and C2 dolomites are 500 μm.

FIGURE 3.4: Photomicrographs of matrix replacement dolomite types.

a) Cryptocrystalline dolomite **T1** (T1), with some coarser T2 dolomite (T2) distributed in an algal laminite facies. 3-15-41-22W4, 5542 ft, plane polarized light. Scale bar = 300 μm.

b) Low porosity, fine crystalline (20-30 μm), planar-subhedral **T2** dolomite. 16-36-41-23W4, 1726 m, plane polarized light. Scale bar = 100 μm.

c) Low porosity, medium crystalline (~100 μm), planar-subhedral **T3** dolomite. Note the inclusion-rich cores to many of the crystals. 16-26-39-24W4, 1858 m, plane polarized light. Scale bar = 100 μm.

d) Porous, medium crystalline (~150 μm), planar-subhedral(euhedral) **T3** dolomite (centre of picture), encompassed by less porous T3 dolomite. Intercrystalline pore-space is black. Note the clear crystal rims adjacent to pore-space and the better developed crystal faces. 6-12-39-22W4, 5447 ft, cross-polarized light. Scale bar = 100 μm.

Figure 3.4: Photomicrographs of matrix replacement dolomite types.

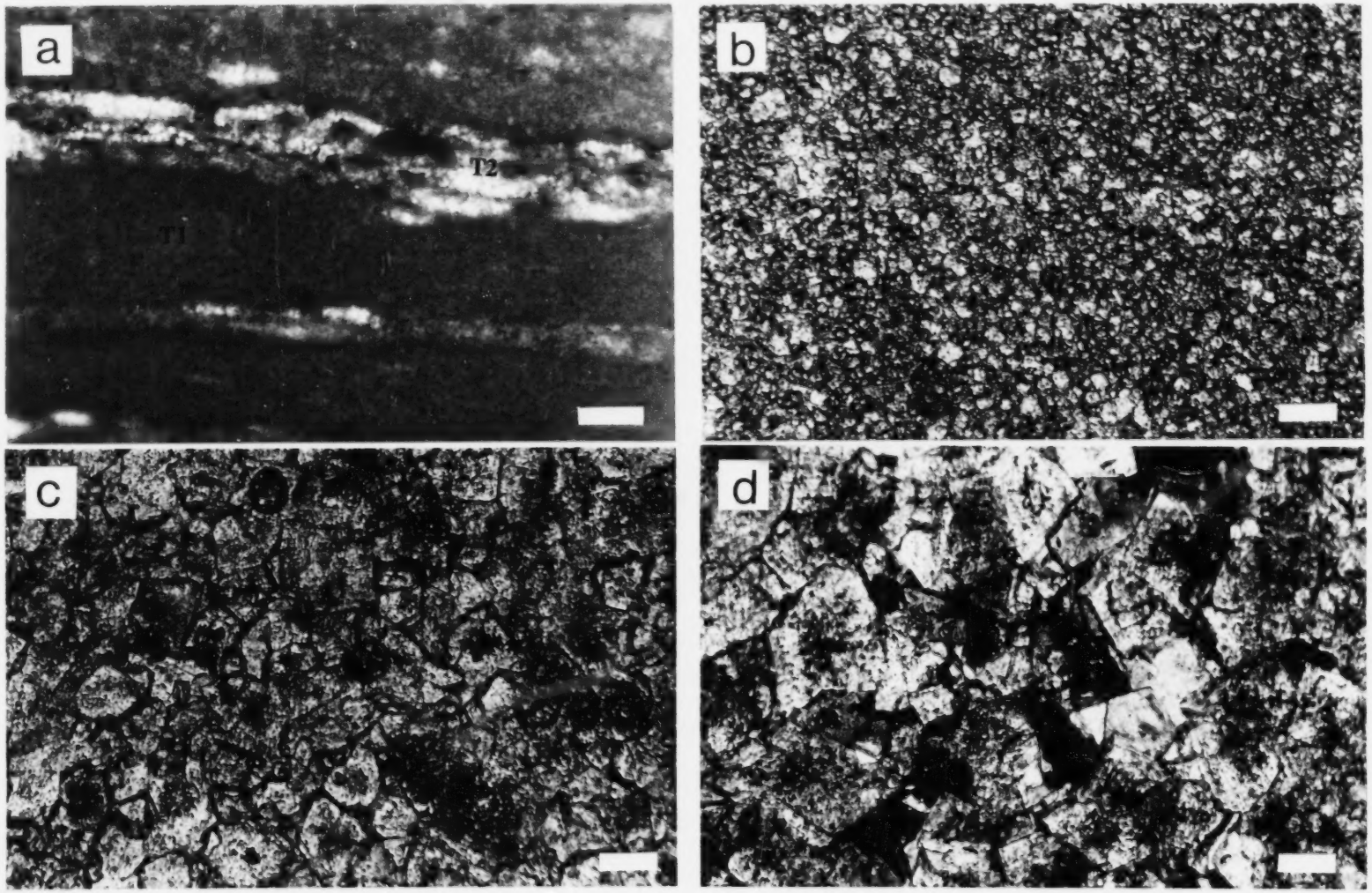

pore-spaces. Cathodoluminescence of T3 dolomite is red-orange, with dark biotches, and is very similar to T2 dolomite. T3 dolomite is typically found in the Leduc Formation, Camrose Member and lower Nisku Formation facies, but also occurs in the Ireton aquitard where the carbonate content is high. With increasing crystal size, T3 dolomite becomes less fabric retentive. In particular, the replacement dolomites in the Leduc Formation are generally more coarsely crystalline, vuggy, and less fabric retentive than replacement dolomites of the Camrose Member and lower Nisku Formation (see Figure 4.6).

Most replacement dolomites are non-ferroan and predate high-amplitude stylolites. Within or near the Ireton aquitard (typically > 20% clay content), ferroan dolomite is present, as indicated by potassium ferricyanide staining.

Stable isotopic analyses of the matrix dolomites have $\delta^{18}O$ values ranging from -3.8 to -5.5‰ (PDB), with one sample at -6.7‰ (Figure 3.2; Table 3.1), and $\delta^{13}C$ values range from +1 to -7‰ (PDB) (Figure 3.2; Table 3.1).

Matrix dolomites are pervasive throughout the Nisku Formation, the Ireton Formation drape, and most of the upper portions of the Leduc Formation. The Leduc Formation reef margin in well 3-15-41-22W4 was observed to be partially dolomitized. Well log analysis found only one well with photoelectric absorption (P_e) data penetrating the Cooking Lake (well 16-36-41-23W4) and revealed that dolomitization extended no further than the lowermost Leduc Formation.

3.1.3. Pore-lining dolomite cements

Pore-lining dolomite cements form a volumetrically minor percentage (<5%) of the bulk-rock composition. They do, however, form a significant porosity-reducing phase, typically lining or in some cases occluding moldic, vuggy, or fracture porosity. Two dolomite cement types are present, C1 and C2 (Figure 3.3), that postdate matrix dolomites.

C1: Coarse-crystalline (100 - 700 μm) planar-subhedral(euhedral) dolomite (C1 dolomite of Drivet, 1993; Type 3 dolomite of Amthor *et al.*, 1993). This dolomite type is usually clear to cloudy white, and typically displays zonation (Figure 3.5a). Cathodo-luminescence is mottled dull orange/black, but may range from black to bright red where

FIGURE 3.5: Photomicrographs of pore-lining dolomite cement types.

a) Coarse crystalline (~300 μm), planar-euhedral **C1** dolomite cement (C1), lining moldic porosity. Anhydrite cement occludes the pore space (An). 8-8-42-23W4, 1792 m, cross-polarized light. Scale bar = 100 μm.

b) Cathodoluminescence of **C1** cement (C1). Note the zonation from yellow to black (arrow). Covering the C1 cement syntaxially is a later saddle (C2) dolomite cement, with a slightly brighter red luminescence. Black area to the right is pore-space. 2-15-38-24W4, 6168 ft. Scale bar = 250 μm.

c) Very coarse crystalline (~700 μm), planar-saddle **C2** dolomite cement (whole picture). Note the curved crystal faces. P = pore-space. 6-12-39-22W4, 5490 ft, plane polarized light. Scale bar = 300 μm.

d) Cathodoluminescence of **C2** cement (C2), with brighter red luminescence than C1 cement (C1), occluding the very centre of a moldic pore — also displays some zonation (arrow). C1 cement fills up most of the moldic pore and also displays zonation. T3 dolomite is present in the periphery (T3). 16-2-40-24W4, 1929.2 m. Scale bar = 250 μm.

Figure 3.5: Photomicrographs of pore-lining dolomite cement types.

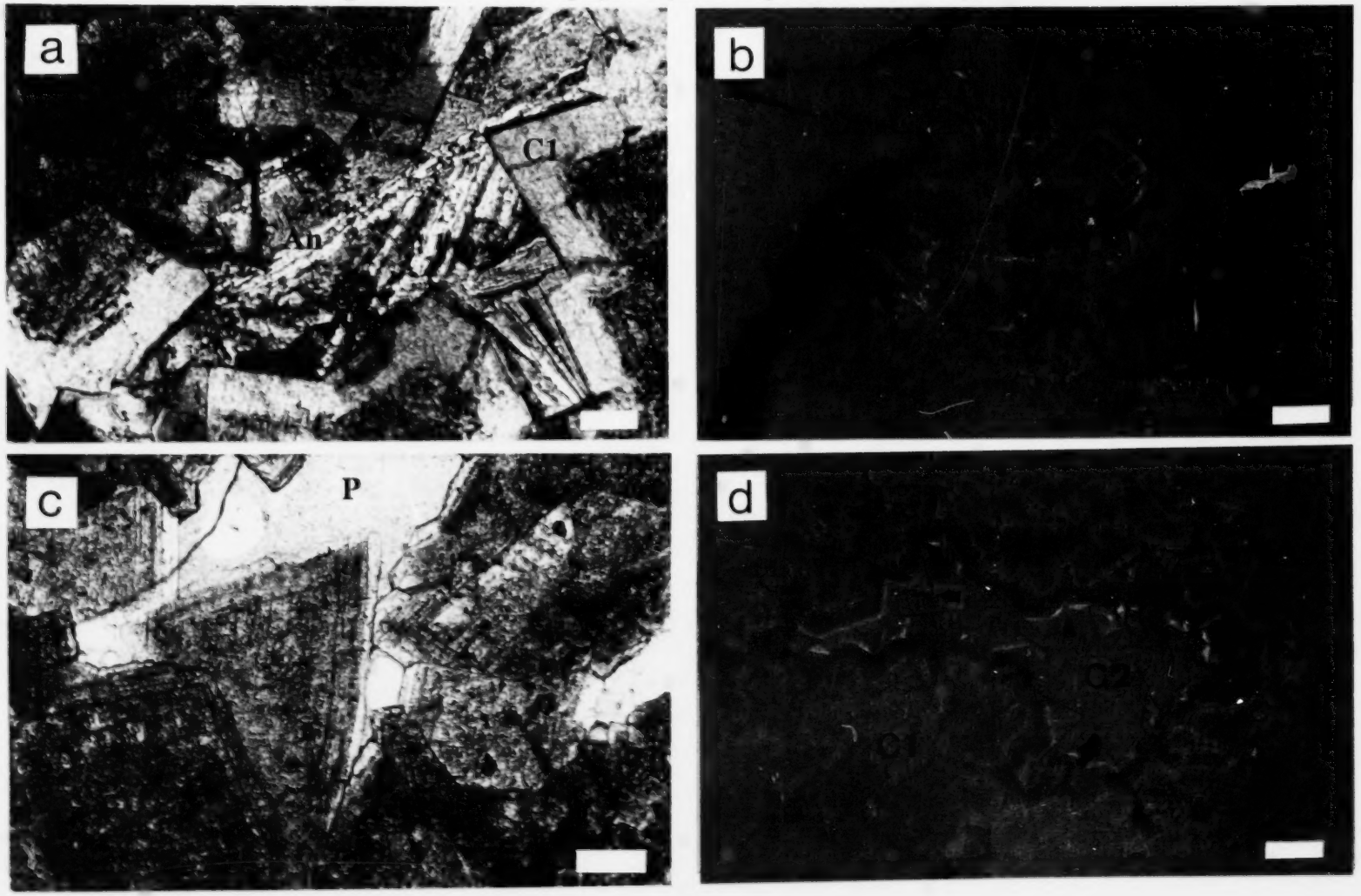

zonation is prevalent (Figure 3.5b). C1 dolomite occurs throughout the study area within the more porous, fossiliferous units.

C2: Coarse- to very coarse- crystalline (400 μm - 1.4 mm) non-planar (saddle) dolomite (C2 dolomite of Drivet, 1993; Type 5 dolomite of Amthor *et al.*, 1993). This dolomite type is characterized by curved crystal faces (Figure 3.5c) and sweeping extinction, and has a homogeneous red cathodoluminescence (Figure 3.5d). Saddle (C2) dolomite is less common than C1 dolomite and was present in only eight thin sections from the Leduc Formation and Camrose Member, and postdates C1 dolomite.

3.1.4. Anhydrite phases and calcite cements

In the Bashaw area anhydrite is found both as a "primary" matrix (*i.e.*, in the sabkha and lagoonal environments of the upper Nisku Formation), and as a late pore-lining/occluding cement or replacement phase within the dolostones of the Leduc Formation, Camrose Member and lower Nisku Formation. There is a greater abundance of late anhydrite in the lower Nisku Formation/Camrose Member (up to 30%) than the Leduc Formation (<10%). Anhydrite is rarely present in the Ireton aquitard except, however, where the Ireton aquitard drape is particularly thin.

Within the upper Nisku Formation, "primary" matrix anhydrite is present as a mesh of felted, finely crystalline (~30 μm long), anhedral fibres (Figure 3.6a). In contrast, the late anhydrite of the underlying units have a more varied crystal-size and form that ranges from finely crystalline to 1 - 2 cm, and from fibrous to blocky, anhedral to euhedral crystals (Figure 3.6b). All anhydrite types are non-luminescent.

Although the majority of the late anhydrite postdates the dolomite cements (C1 and C2), relationships are not clear, and some of the anhydrites may have precipitated prior to or during the precipitation of the dolomite cements. Replacement anhydrite can be determined from the floating "islands" of dolostone present within the anhydrite (Figure 3.6c), and is more prevalent in the lower Nisku Formation/Camrose Member. Late anhydrite is commonly associated with stylolites, late pyrite, late calcite, and some crystals contain oil inclusions.

Late calcite cements are typically developed as large poikilotopic crystals (~10 - 15 mm) that occlude pore-space. Precipitation of this calcite was synchronous with, or

FIGURE 3.6: Photographs of other diagenetic phases.

a) Finely crystalline (~30 μm long), mesh of felted "primary" matrix anhydrite (An) within a sediment also comprised of peloidal T2 dolomite (T2). 4-17-39-21W4, 5448 ft, cross-polarized light. Scale bar = 100 μm.

b) Coarsely crystalline, blocky, late anhydrite cement/replacement, randomly oriented. 6-12-39-22W4, 5490 ft. Scale bar = 300 μm.

c) Core photograph of late anhydrite cement/replacement of T3 dolomite. Anhydrite cement (An) is a white colour in the bottom of the picture and is seen to have also replaced medium brown T3 dolomite (T3), toward the top of the picture, that has itself replaced what appears to be tabular stromatoporoids(?). The light brown floating "islands" of dolomite crystals (Is) within the anhydrite indicate the replacive nature of the sulphate-rich fluids. 11-21-39-26W4, 5934 ft. Scale = dime coin.

d) Late poikilotopic calcite cement (pinkish) that also replaced late anhydrite along cleavage planes (Cl). Oil inclusions are present in the calcite (In), as well as lining fractures that have developed subsequent to calcite precipitation (Fr). 16-2-40-24W4, 1917.5 m, cross-polarized light. Scale bar = 100 μm.

e) T3 matrix dolomite (T3) that has been fractured (Fr), solution enlarged (dissolved), and then overgrown with C1 dolomite cement (C1). Dissolution is indicated by the corrosion of the T3 dolomite (Ds). 12-3-43-23W4, 5647 ft, plane polarized light. Scale bar = 100 μm.

f) Late fracture (Fr) that cross-cuts C1 dolomite cement (C1) and is filled with anhydrite cement (An). 16-26-39-24W4, 1844 m, cross-polarized light. Scale bar = 100 μm.

Figure 3.6: Photographs of other diagenetic phases.

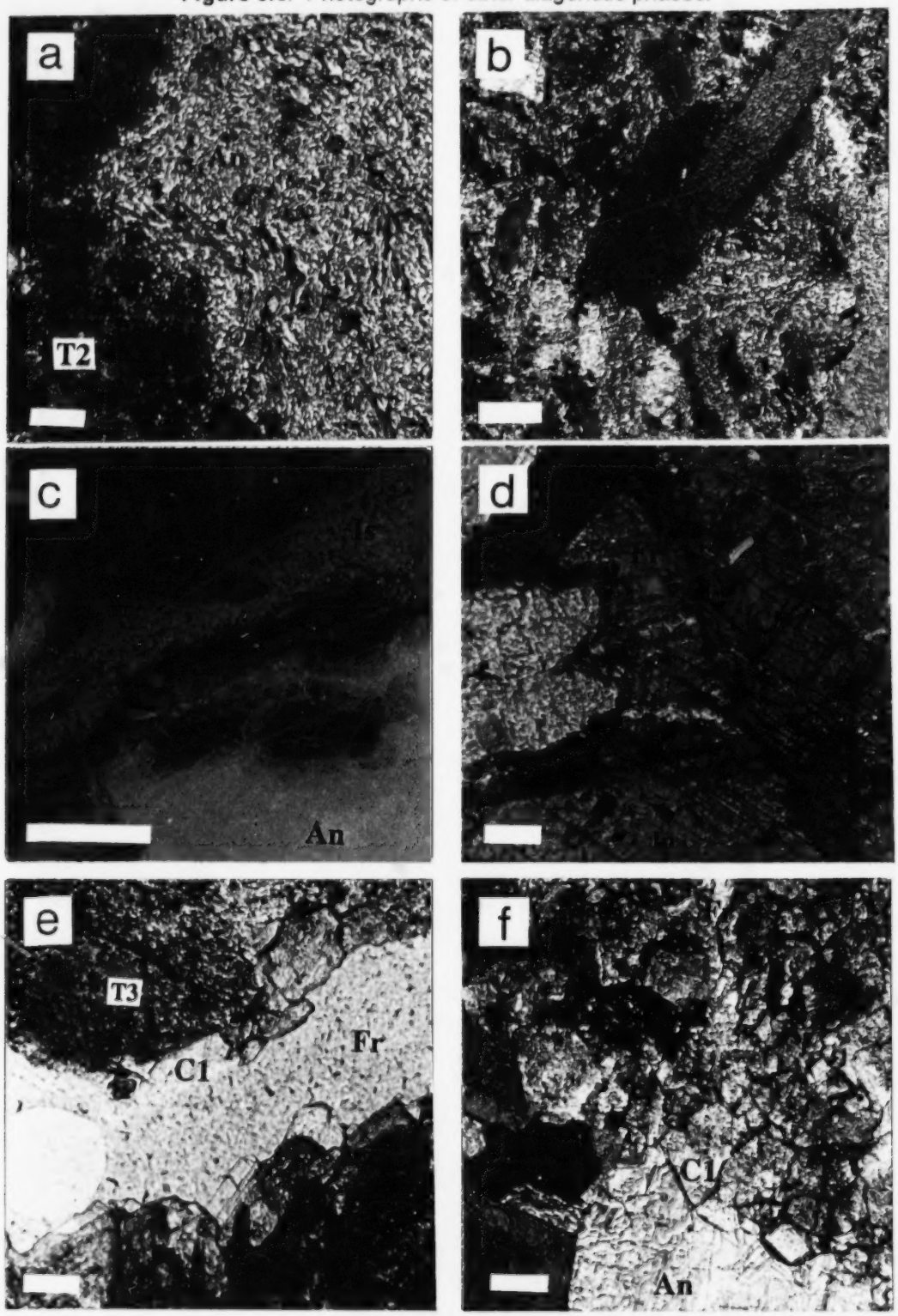

postdates late anhydrite, with some calcite containing oil inclusions. Later fractures that cross-cut the calcite crystals also show oil-stain (Figure 3.6d). The distribution of late calcite cements within the Bashaw area was not determined, however, late calcite is present in the Nisku Formation, Leduc Formation, and where the Ireton aquitard thins.

3.1.5. Fracturing and dissolution

Multiple phases of fracturing and dissolution are evident across the study area. The greatest density of fractures occurs in the Leduc Formation dolostones, and to a slightly lesser extent in the lower Nisku Formation and Camrose Member. The Ireton aquitard, however, appears to be less affected with only a few cores displaying fractures where the Ireton aquitard is thin and more carbonate-rich. The oldest fractures are sediment-filled fractures (*e.g.*, neptunian dykes) seen in the upper Nisku Formation, and within the Leduc Formation of the Nevis area.

The earliest major phase of dissolution was the leaching of allochems from the fossiliferous facies that were replacively dolomitized producing moldic and vuggy porosity (see Chapter 4, Figure 4.6). The next phase of fracturing and dissolution occurred after replacement dolomitization but prior to the C1 and C2 dolomites, as evidenced by the corrosion of replacement dolomite crystals along the fracture walls and solution enlargement of the fractures (Figure 3.6e). A subsequent phase of fracturing and dissolution also occurred after the precipitation of the dolomite cements but prior to, or during, late anhydrite and calcite precipitation. Fractures that are lined by late anhydrite or calcite and cross-cut the dolomite cements are evidence for the later timing of these fractures (Figure 3.6f). Finally, fractures are seen to postdate all cementation phases and are lined by oil/bitumen (Figure 3.6d).

3.1.6. Other diagenetic products

Sutured stylolites are a common feature in the carbonate-rich units, ranging from high to low amplitude. Sutured stylolites postdate replacement dolomites. Dissolution seams (wispy stylolites) dominate the more clay-rich Ireton aquitard and form as swarms or are wrapped around carbonate nodules.

Pyrite occurs both as an early and late-stage diagenetic phase. Early pyrite is

disseminated throughout the Ireton aquitard and as coarser cubes within the storm-generated facies of the lower Nisku Formation. Late pyrite is associated with stylolites and late calcite cements.

Hydrocarbon emplacement is the last major diagenetic phase found in the area, present as oil droplets or bitumen within fractures and moldic, intercrystalline, and vuggy porosity.

3.2 Discussion.

3.2.1. Early diagenesis

Limestones

The pervasive nature of the replacement dolomitization in the area has obliterated most of the precursor limestones — only Leduc well 3-15-41-22W4 retains partially dolomitized precursor limestones.

Marine calcite cements were the principal early diagenetic phase present. Isotopic analyses of similar marine calcite cements from the Nevis D-3B reef "pinnacle" (see Figure 4.1) revealed that the cements have a $\delta^{18}O$ signature of -4.8 to -10‰ PDB trending from a Late Devonian seawater to that of meteoric water (Carpenter and Lohmann, 1989; p. 808). Isotopic analyses made in this study also show that there is a similar alteration, although the analyses were an averaged signature of the limestone components (Figure 3.2). This isotopic alteration is most likely to have occurred prior to replacement dolomitization in the area, because any alteration of the limestones subsequent to the dolomitization would also likely have affected the $\delta^{18}O$ signatures of the dolomites. Ruling out the possibility that calcite alteration postdated replacement dolomitization is not possible, however, because the more stable dolomite phase could theoretically remain unaffected by later diagenetic fluids, therefore only altering the calcites.

The $\delta^{13}C$ signatures of the limestones have not been affected by meteoric alteration and compare well with the estimated Late Devonian marine calcite signature of +2 to +3‰ (Carpenter *et al.*, 1991).

3.2.2. Replacement dolomitization

In order to determine the most likely origin to the replacement dolomites in the study area, information is required as to the approximate spatial distribution of the replacement dolomites, the stratigraphy of the area, the petrography, and the geochemistry of the dolomites. Replacement dolomitization in the study area occurred prior to sutured stylolitization and was therefore likely to have developed in the first few hundred metres of burial, and during the Frasnian/Famennian. In addition, planar crystal faces of the replacement dolomite also is consistent with an early origin to the replacement dolomite because planar crystal faces are thought to form at temperatures below 50 - 100°C (Gregg and Sibley, 1984; Sibley and Gregg, 1987).

The spatial distribution of replacement dolomite can often assist in explaining which dolomitization process has affected an area. Different processes generate distinctive distribution patterns (Figure 3.7) (Tucker and Wright 1990; Amthor *et al.*, 1993; Kaufman, 1994). A schematic of the spatial distribution of the replacement dolomites in the vicinity of the study area (Figure 3.8) indicates that dolomitization was generally pervasive down to the base of the Leduc Formation in the Bashaw Reef Complex. This is a similar distribution to that reported from the nearby Erskine, Innisfail and Wimborne fields (Figure 1.1) (Andrichuk, 1958a; White and Charles, 1958; Brennan and Warden, 1959). Notably, however, the Duhamel Leduc Formation reef, which is part of the Bashaw reef trend (Figure 1.1; shown schematically in Figure 3.8), consists of limestone (Andrichuk, 1961), as does the Nevis D-3B reef (Figure 4.1; Carpenter and Lohmann, 1989), and both are covered by a thicker drape of Ireton aquitard (>25 m) than the main reef complex. The carbonate in the Ireton Formation of the surrounding East Shale Basin (Figure 1.1) is also predominantly calcite, with only the uppermost carbonates being dolomitized (McCrossan, 1961; Campbell and Oliver, 1968).

The restricted distribution pattern of the replacement dolomites in the study area (Figure 3.8) is consistent with early dolomitization via refluxing, dense, hypersaline fluids from the overlying formations of either the upper Nisku Formation or Wabamun Group (Figure 3.7). In particular, the lack of dolomite in the Duhamel and Nevis D-3B reefs, which are covered by a thicker drape of Ireton aquitard, and the dolomitization of only the uppermost portions of the Ireton Formation in the basin, are consistent with brine

Dolomitizing Models	Application to the Bashaw area
A. Coastal Mixing 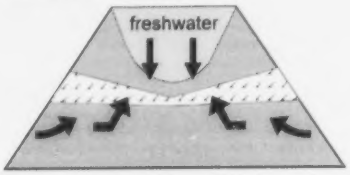	- Dolomitization by coastal mixing could have affected parts of the Leduc Fm., however, coastal-mixing is unlikely to have affected the overlying units due to increasing aridity at the time of their deposition.
B. Seawater 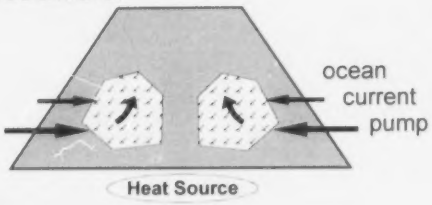	- Thermal convection or ocean current pumping of seawater could have caused dolomitization of parts of the platform and reefal facies in the area. However, it cannot account for the dolomitization of the uppermost Ireton Fm. in the basinal areas, nor the lack of dolomite in the Duhamel reef.
C. Regional-Scale Flow 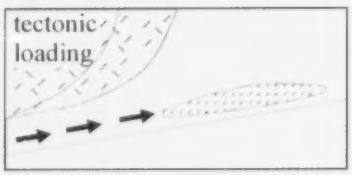	- Dolomitization by regional-scale flow warrants that the regional aquifer in the area (the Cooking Lake Foramtion) be dolomitized — it is mostly limestone.
D. Burial Compaction 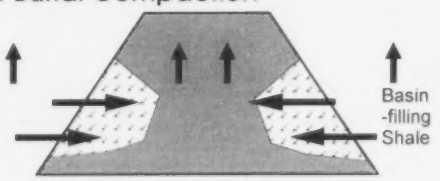	- Dolomitization by burial compaction should effect areas adjacent to the "shale" basin. However, well 3-15-41-22W4, the Duhamel reef, and the D-3B "pinnacle" are limestone.
E. Reflux 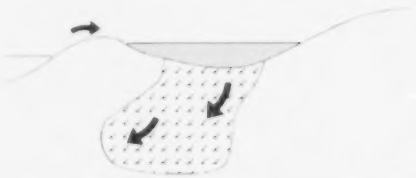	- Dolomitization by reflux is accounted for by stratigraphy, dolostone distribution, petrography, and geochemical evidence.

Figure 3.7: Various dolomitizing models and their application to the Bashaw area. Diagrams modified from Tucker and Wright (1990), Amthor *et al.* (1993), and Kaufman (1994).

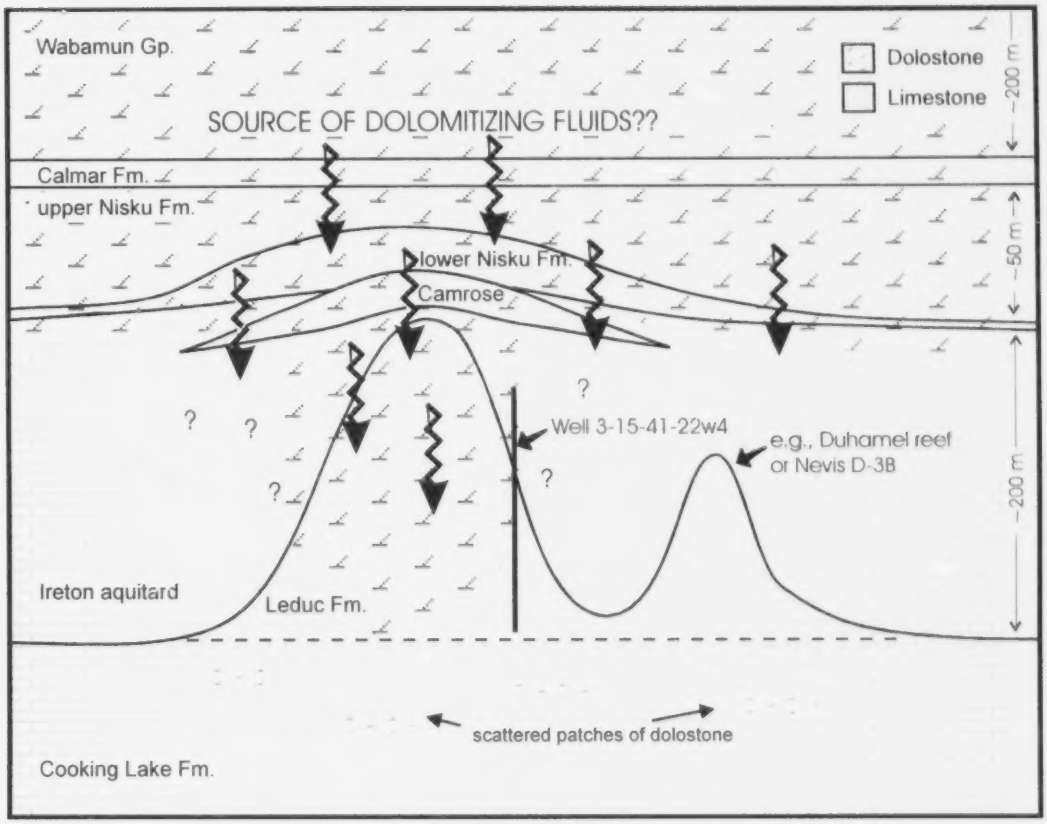

Figure 3.8: Schematic of estimated dolostone distribution in the Bashaw area, with brine reflux dolomitization originating from the upper Nisku Formation/Wabamun Group.

reflux dolomitization. Further evidence consistent with this hypothesis is the crypto-crystalline T1 dolomite present within the upper Nisku Formation that is common to penecontemporaneous hypersaline dolomite environments (McKenzie, 1981; Machel and Mountjoy, 1986), as well as the geochemical evidence of the replacement dolomite (discussed later). However, the influence of coastal-mixing dolomitization and seawater dolomitization cannot be totally discounted and may have occurred locally within platform and reef facies.

Brine reflux as the chief dolomitization process would further limit the timing of replacement dolomitization to have occurred at depths <~250 - 450 m (Figure 3.7). It also suggests that during early burial the Ireton aquitard overlying the Bashaw Reef Complex (<25 m) was permeable to the dolomitizing fluids. The more finely crystalline texture of the T2 dolomite of the Ireton aquitard is probably related to the higher clay content of the aquitard causing an increase in the number of dolomite nucleation sites and reducing pore-space for crystal growth (Gregg and Sibley, 1984: Sibley and Gregg, 1987).

The reflux hypothesis for the whole Bashaw area is similar to that proposed for the dolomitization of the Nisku Formation in the Joffre area and the Birdbear Formation to the southeast of Bashaw (Al Bastaki *et al.* 1995b; Whittaker and Mountjoy, in press). However, brine reflux dolomitization in the Bashaw area contrasts with the regional-scale dolomitization model proposed for the adjacent Rimbey-Meadowbrook reef trend (Amthor *et al.*, 1993), and therefore further research is necessary to determine the extent of the influence of reflux dolomitization on Leduc Formation reefs.

Geochemical interpretation of replacement dolomites

The $\delta^{18}O$ values for the replacement dolomites of the study area (-3.8 to -5.5‰) are similar to those of replacement dolomites in the Joffre area, the Birdbear Formation, and the Nisku Formation of the Enchant area in southeastern Alberta (Al Bastaki *et al.* 1995b; Tan and Mountjoy, 1995; Whittaker and Mountjoy, in press; Figure 3.9), but are 1.4 to 5.5‰ more negative than hypothetical Upper Devonian marine dolomite (Amthor *et al.*, 1993), as well as dolomites of hypersaline environments (Figure 3.9) — dolomites associated with hypersalinity from both the modern and ancient preserve a $\delta^{18}O$

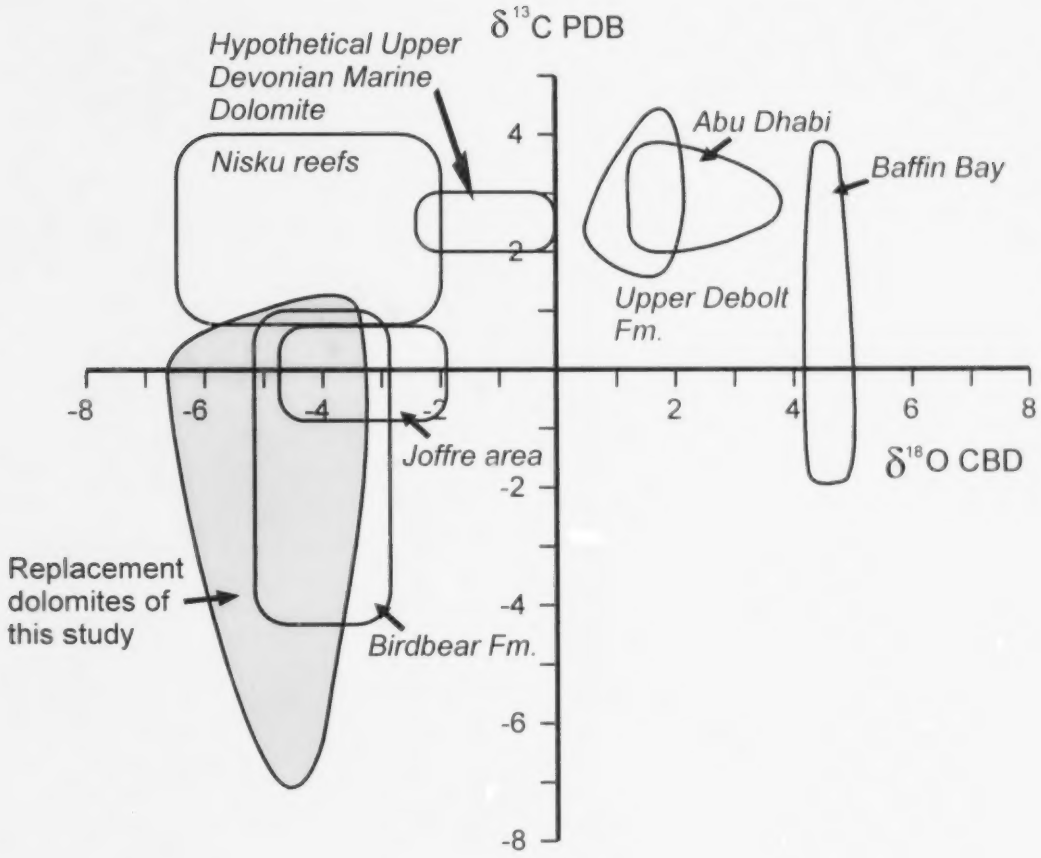

Figure 3.9: Comparison of $\delta^{13}C$ and $\delta^{18}O$ isotope compositions of replacement dolomites from the Bashaw area and other studies. The replacement dolomite isotope range for this study is shaded grey. Hypersaline isotope signatures include recent examples from Abu Dhabi (McKenzie, 1981), Baffin Bay (Behrens and Land, 1972), and the Paleozoic Mississippian Upper Debolt Formation (Packard, 1992). Time-equivalent dolostones to the Bashaw area are those of the Nisku Formation in the Joffre area (Al-Bastaki *et al*, 1995b), the Nisku Fm. reefs in the West-Pembina area of central Alberta (Machel and Anderson, 1989), and the Birdbear Formation to the southeast of Bashaw (Whittaker and Mountjoy, in press). The estimated isotopic range for Upper Devonian marine dolostones is taken from Amthor *et al.* (1993).

enrichment (due to evaporation), typically >0‰ PDB (McKenzie, 1981; Behrens and Land, 1972; Packard, 1992; Figure 3.9). Therefore, ^{18}O isotopic evidence of hypersalinity (and reflux) is no longer present in the Bashaw area, even in the T1 dolomite which was the most likely to have formed in a hypersaline environment. However, replacement dolomites of the Joffre area and the nearby Birdbear Formation, which are similarly depleted in ^{18}O, are also purported to be of reflux origin based on strontium data (Al Bastaki *et al.* 1995b; Whittaker and Mountjoy, in press; Figure 3.9). Replacement dolomites in the Bashaw area could therefore have had an evaporative $\delta^{18}O$ signature that was later altered by recrystallization and the $\delta^{18}O$ values reset to their present values (-3.8 to -5.5‰). This is a similar conclusion to that reached by Al Bastaki *et al.* (1995b) for the Joffre area and Whittaker and Mountjoy (1995) for the Birdbear Formation dolomites. One $\delta^{18}O$ value (-6.7‰), however, appears not to have been "reset" and is from a sample taken from the Ireton aquitard on the eastern flank of the reef complex (well 3-15-41-22W4). This value may reflect conditions associated with its peripheral location to the main dolomitizing pathway (Figure 3.7). It is also likely that the off-reef Ireton aquitard was less permeable to dolomitizing fluids and therefore the lower water/rock interaction preserved a $\delta^{18}O$ value more closely related to that of the ^{18}O-depleted precursor limestone.

The $\delta^{13}C$ values of the replacement dolomites from the Bashaw area are depleted compared to hypothetical Upper Devonian marine dolomite of +2.5 ± 1.0‰ (Amthor *et al.*, 1993; Figure 3.9). Other Devonian reefs, however, are comparable to this hypothetical value (Machel and Anderson, 1989; Amthor *et al.*, 1993; Drivet, 1993; Figure 3.9), and appear to closely mimic the precursor limestone $\delta^{13}C$ signature, typical of the Late Devonian (Carpenter *et al.*, 1991). This suggests that there is almost no fractionation between calcite and dolomite (*e.g.*, McKenzie, 1981), and that $\delta^{13}C$ values are difficult to alter — unless they are affected by a high water/rock interaction (*e.g.*, Marshall, 1992). Unaltered $\delta^{13}C$ signatures of limestones in a well that displays O-isotope evidence of meteoric alteration (well 3-15-41-22W4) confirm the strong preservation potential of the $\delta^{13}C$ signature. The negative $\delta^{13}C$ shift of replacement dolomites from the Bashaw area, therefore, is unlikely to be explained by the dolomitizing

fluids mimicking the $\delta^{13}C$ signature of the meteorically-altered precursor limestone.

The most plausible explanation for the depleted $\delta^{13}C$ values is that they reflect the $\delta^{13}C$ composition of the dolomitizing fluid which refluxed from the upper Nisku Formation or Wabamun Group. The most depleted $\delta^{13}C$ values (-1 to -7‰) are from a cryptalgal laminite facies of the upper Nisku Formation and a storm facies of the Camrose Member/lower Nisku Formation, both of which developed in meso- to hyper-saline, restricted conditions. Pore fluids associated with greater environmental restriction, such as hypersaline conditions, are commonly depleted in ^{13}C (Lloyd, 1964) either due to increased microbial respiration (Patterson and Walter, 1994), incorporation of ^{12}C-enriched CO_2 from the atmosphere (Lazar and Erez, 1992), or incorporation of organogenic carbon from the decomposition of organic matter (Marshall, 1992). These ^{13}C-depleted fluids from the upper Nisku Formation or Wabamun Group probably refluxed into the underlying units, and with a relatively high water/rock interaction implied by the pervasive nature of the dolomitization, lowered the precursor limestone $\delta^{13}C$ values of the underlying units from around +2 to +3‰, originally (Carpenter *et al.*, 1991), to negative $\delta^{13}C$ values. $\delta^{13}C$ values of the individual formations (Figure 3.10) suggest that there may also have been a slight trend of decreasing water/rock interaction as the fluids percolated into deeper formations, with Leduc Formation $\delta^{13}C$ values being the least altered from the Late Devonian $\delta^{13}C$ signature.

Ferroan Dolomite

The restricted occurrence of iron-rich replacement dolomites within the Ireton aquitard interval suggests that the Fe^{+2} ions were sourced locally from clay particles. Theoretically, Fe^{+2} ions could be released by two possible mechanisms. The first, and most likely is that the Ireton aquitard experienced reducing conditions which made Fe^{+2} ions available during very early diagenesis (*e.g.*, when passing through the nitrate/sulphate reduction zones). Early diagenetic pyrite indicates that reducing conditions were indeed prevalent in the Ireton aquitard during very shallow burial (Hesse, 1990).

Alternatively, later-stage Fe^{+2}-rich fluids could have been generated during the conversion of smectite-illite within the Ireton aquitard (McHargue and Price, 1982).

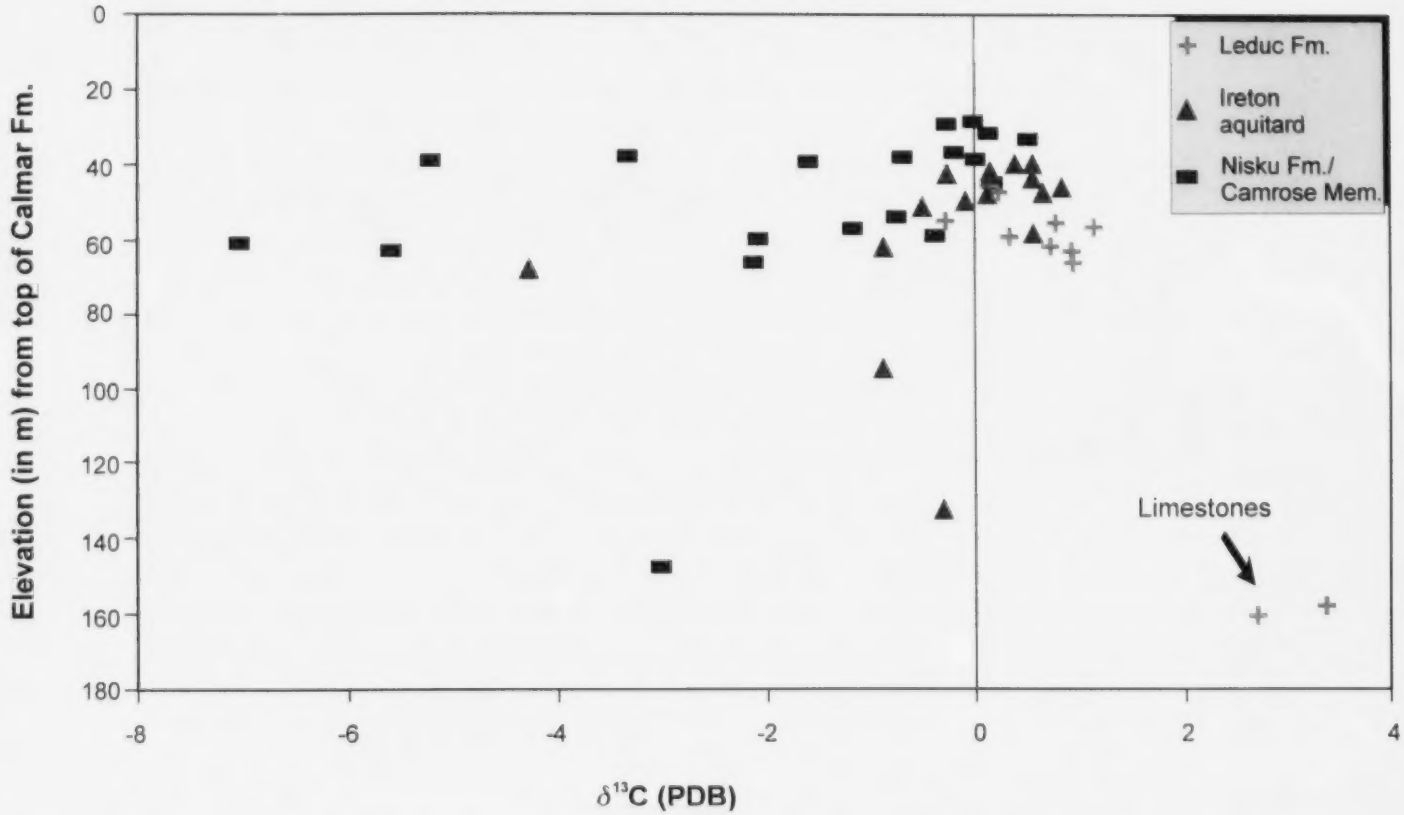

Figure 3.10: Plot of $\delta^{13}C$ of all replacement dolomites versus elevation from the top of the Calmar Formation. Note the trend toward more positive values from the Nisku Formation down into the Leduc Formation. Two limestone $\delta^{13}C$ values are approximately that of the original Upper Devonian carbon signature.

Conversion must have occurred prior to, or during, replacement dolomitization in order for the Fe^{+2} to be absorbed into dolomite crystal structure, at depths less than ~250 - 450 m (Figure 3.7). Estimates of smectite-illite conversion, however, suggest that the conversion occurs at temperatures between 50°C (Lahann, 1980) and 125°C (Boles and Franks, 1979). These temperatures correspond to burial depths of 700 - 3100 m, using a geothermal gradient of ~30°C/km (Hitchon, 1984), and indicates that the smectite-illite conversion and release of Fe^{+2} ions is less likely to have been responsible for the ferroan dolomite.

3.2.3. Cement phases

Dolomite cementation

The relationship of the C1 and C2 cements to the overall paragenetic sequence (Figure 3.1) was determined solely from cross-cutting relationships within the study area, as no stable isotope data were collected. C1 cements were precipitated prior to C2, but both postdate/or were synchronous with stylolitization and predate hydrocarbon migration. Similar cement types and cross-cutting relationships are present in the Leduc Formation Rimbey-Meadowbrook reef trend (Amthor *et al.*, 1993; Drivet, 1993). These Rimbey-Meadowbrook late-stage dolomite cements yielded more negative $\delta^{18}O$ values than the replacement dolomites of that area, which likely indicate deeper burial conditions (Machel, 1987; Amthor *et al.*, 1993; Drivet, 1993). Fluid inclusion data of Drivet (1993) constrained the timing of cementation to burial depths reached during the Laramide orogeny (Late Cretaceous to early Tertiary; Figure 3.1). The close similarity between the cement types of the Rimbey-Meadowbrook reef trend to those of the Bashaw area suggest that the C1 and C2 cements of the Bashaw area may have been precipitated in the same time interval. A suggested origin for the C1 and C2 cements is that of pressure solution of an earlier phase of dolomite and its reprecipitation into pore space at slightly higher temperatures (Machel, 1987; Amthor *et al.*, 1993). Planar C1 dolomite is likely to have precipitated from slightly lower temperatures fluids due to its planar crystal faces, whereas the curved crystal faces of the C2 dolomite apparently indicate that slightly higher temperatures above a critical roughening temperature (of around 50 – 100°C) were present during crystal growth (Gregg and Sibley, 1984; Sibley and Gregg, 1987).

Anhydrite cementation and replacement

The source of anhydrite in the Bashaw area is probably from the evaporite units of the upper Nisku Formation and Wabamun Group. Fluids causing dissolution of these "primary" anhydrites may have percolated down into the underlying units, precipitating as cements and replacing dolostones. This is supported by the fact that a greater abundance of anhydrite is present in the lower Nisku Formation and Camrose Member (up to 30%), compared to the Leduc Formation (<10%), and only increases in abundance within the Leduc Formation where the Ireton aquitard is thin, therefore suggesting that anhydrite was likely percolating from the overlying evaporites. The greater abundance of replacement anhydrite in the lower Nisku Formation/Camrose Member also suggests that the sulphate saturated fluids were more "aggressive" in these formations. Gilhooly (1987) documented evidence of early solution-collapse breccias in the evaporite sequences of the upper Nisku Formation and suggested that some sulphate-rich fluids were probably mobilized soon after burial. But thin sections reveal that most of the anhydrite cements present today postdate dolomite cementation. Later subsurface dissolution of evaporites in the Bashaw area is supported by evidence of salt dissolution of the Wabamun Group in the Rumsey area (Figure 1.1) during the Late Cretaceous (Oliver and Cowper, 1983). Fluid inclusions of oil in late anhydrite cements also constrain their emplacement to the Late Cretaceous and Tertiary (Figure 3.1), as migration of oils in the Devonian of the WCSB is thought to have taken place during the Late Cretaceous to Early Tertiary (Deroo *et al.*, 1977).

3.2.4. Pore generation

Pore generation in the Bashaw area can be categorized into three major pore systems that developed at different times during the diagenetic history of the area.

Pore system 1: Interparticle and early fracture porosity. Limestone interparticle pore-space was developed during sedimentation. In addition, early fractures (*e.g.*, neptunian dykes) enhanced porosity in some formations and were likely related to early lithification. Subsequently, sedimentary and diagenetic processes have rendered this pore system ineffective to fluid migration today.

Pore system 2: Intercrystalline, moldic, and vuggy porosity. Replacement

dolomitizing fluids during the latest Frasnian to Famennian likely utilized the interparticle pore network of the precursor limestone (Pore system 1) in order to generate pervasive intercrystalline porosity of the matrix dolomites present in the dolostones today. Extensive dissolution of the most fossiliferous facies generating vuggy and moldic porosity also probably occurred at the same time, or soon after, replacement dolomitization. This cause-effect relationship was concluded from the fact that calcite allochems in the Leduc Formation limestone did not show any significant signs of leaching (*e.g.*, well 3-15-41-22W4). Similar conclusions were reached by Machel and Anderson (1989) for the Nisku Formation reefs, Kaufman *et al.* (1991) for the Swan Hills Formation, and Amthor *et al.* (1993) for the Rimbey-Meadowbrook reef trend. The less fossiliferous units of the upper Nisku Formation and Ireton aquitard were generally less affected by dissolution.

Pore system 3: Fracturing and dissolution. Late-stage fracturing and dissolution could have occurred at any time after replacement dolomitization, however, it is most likely that the main episodes of fracturing were either related to phases of compaction of the interior of the Bashaw Reef Complex, or perhaps by faulting associated with rapid burial during the Laramide orogeny. If dolomite cements lining these fractures are indeed Laramide in origin, then some of this fracturing potentially took place between replacement dolomitization (Late Devonian) and dolomite cementation (Cretaceous). Later anhydrite/calcite-lined fractures and open-fractures are likely to have occurred in the Cretaceous/Tertiary as they cross-cut everything. As a result of these fracturing episodes, changes in the migration pathways and fluid chemistry were likely to have occurred which may have resulted in dissolution occurring at the same time as fracturing, as well as concomitant precipitation of various cement products.

A significant feature of the fracturing and dissolution events within the Bashaw area is that they appear to have affected the coarser grained dolostones of the Leduc Formation to a greater degree than those of the lower Nisku Formation and Camrose Member. There is a notable absence, however, of fractures in the Ireton aquitard where only a number of wells are fractured. This is probably a result of the clay content of the Ireton aquitard providing greater ductility to the unit. Only where the carbonate content of the Ireton aquitard is high are fractures present (*e.g.*, well 14-2-39-22W4). The

evaporites of the upper Nisku Formation also appear to behave in a similar ductile manner.

Later hydrocarbon migration into the Bashaw area occurred utilizing pore systems 2 and 3, with pore system 3 providing enhanced communication via fractures between moldic, vuggy, and intercrystalline porosity of pore system 2.

3.2.5. Compaction

The effects of compaction on the Bashaw Reef Complex can be interpreted from isopach maps of the Ireton aquitard and Leduc Formation (compare Figures 5.1 and 2.1). There is about 60 m of differential relief between the interior "lows" of the reef complex and the highest reefal margins. This relief is probably a result of the greater mechanical and chemical compaction of the "finer" reef interior sediments to that of the cemented reef margins. Effects of compaction in the other formations is less conspicuous than in the Leduc Formation probably due to the relatively thin development of the Ireton aquitard drape, lower Nisku Formation, and Camrose Member.

Evidence of early mechanical compaction has been obliterated by replacement dolomitization. A study of compaction in fine grained shallow-water limestones by Shinn and Robbin (1983), however, showed that there is up to 50% porosity reduction in the first 300 m of burial, with only minor mechanical compaction thereafter. Chemical compaction, however, is evident in many cores in the form of high and low amplitude stylolites that postdate replacement dolomitization. The onset of stylolitization may have occurred during the first tens of metres of burial (Meyers and Hill, 1983), but more likely continued to develop under several hundred metres of overburden as burial continued.

Studies of the Rimbey Meadowbrook reef trend and the Redwater reef (Mossop, 1972; O'Connor and Gretener, 1974) demonstrate that the timing of compaction of the interior of the reef complexes occurred in two main stages: 1) prior to development of the pre-Cretaceous unconformity; and 2) during the Late Cretaceous to early Tertiary. It is therefore likely that there were similar stages and timing of compaction in the Bashaw Reef Complex. Compaction may have begun as early as during sedimentation in the Ireton and Nisku formations (*e.g.*, Bonnie Glen; O'Connor and Gretener, 1974), however, the cross-section in Figure 2.7 shows that the reef interior in the northern part of the

Bashaw complex still had a positive relief to that of the margins at the time of sediment deposition of the Calmar Formation and therefore compaction of the interior occurred later. Any compaction prior to the formation of the pre-Cretaceous unconformity can probably be attributed solely to mechanical compaction, with chemical compaction dominating the second stage, during the Late Cretaceous. Although, depending on the amount of overburden that existed prior to the unconformity, chemical compaction may also have had a greater effect on porosity reduction during the first stage of compaction.

3.3 Synopsis.

The Bashaw area has undergone a complex diagenetic history (Figure 3.1). However, only a certain number of these diagenetic events have influenced later hydrocarbon migration. These include: replacement dolomitization, late-stage dolomite and anhydrite cements and replacements, and late fracturing and dissolution events.

Replacement dolomitization via the hypothesized process of reflux dolomitization created matrix dolomites with abundant intercrystalline, moldic, and vuggy porosity (Pore system 2). Dolomitization was pervasive into the Leduc Formation and indicates that the more fine-grained Ireton aquitard was fully permeable to dolomitizing fluids. The higher clay content of the Ireton aquitard, however, resulted in the generation of a more finely-crystalline and less porous replacement dolomite (T2), that is less permeable to fluids today. Later cementation and replacement by dolomite and anhydrite reduced porosity throughout the study interval, however, there is a notable absence of these diagenetic products in the Ireton aquitard, except where it is thin. The effects of fracturing and dissolution during burial diagenesis are most pronounced in the Leduc Formation, and to a lesser extent in the lower Nisku Formation/Camrose Member, and has enhanced the permeability of these units (Pore system 3). The Ireton aquitard, however, is rarely fractured, except in some locations where it is thin. Hydrocarbon migration has therefore utilized pore networks 2 and 3, with some reduction in permeability and porosity due to late-stage cements.

CHAPTER 4

HYDROCARBON RESERVOIR DATA

In this chapter, general information concerning the present-day hydrocarbon reservoirs is presented to better assess hydrocarbon breaching of the Ireton aquitard. Information includes: the structure of the area, reservoir characteristics, trapping styles, reservoir production, and hydrocarbon types.

4.1 Pool Distribution, Structure, and Hydrocarbon Column Heights.

A close spatial association exists between the pools of the lower Nisku Formation/Camrose Member and the Leduc Formation that can be used to infer possible communication (Figures 4.1 and 4.2; *e.g.*, GSC, 1988; Rostron, 1995). Cross sections A-A′, B-B′, and C-C′ illustrate the structural attitude of the formations studied in the Bashaw area (Figures 4.3, 4.4, and 4.5). Across the region there is a $<1^{\circ}$ angle of dip toward the south-west that is visible in dip-section C-C′ (Figure 4.5). The influence of reef morphology, differential compaction, and anhydrite dissolution on the present-day structure of the study area are also visible in these cross sections (Figures 4.3, 4.4, and 4.5). Where possible, core data were used to provide the most accurate formation/interval picks. However, well logs, particularly gamma-ray and neutron logs, were used to distinguish between "impure" carbonate and anhydrite. The picks of the Camrose Member were more problematic and required a combination of core information and the interpretation of shallowing-upward cyclicity in gamma-ray logs for the most accurate pick.

Most of the pools in the study area have both an oil/water and gas/oil contact within the reservoirs (Figures 4.3, 4.4, and 4.5). Exceptions include the oil-filled Wood River and Joffre fields, and the Nevis gas field. The hydrocarbon column heights for a number of the pools in the study area are also tabulated in Table 4.1 (Alberta Society of Petroleum Geologists (ASPG), 1960, 1966, and 1969). The column heights are generally less than 30 m (100 feet), but where there is up-dip termination of both the lower Nisku

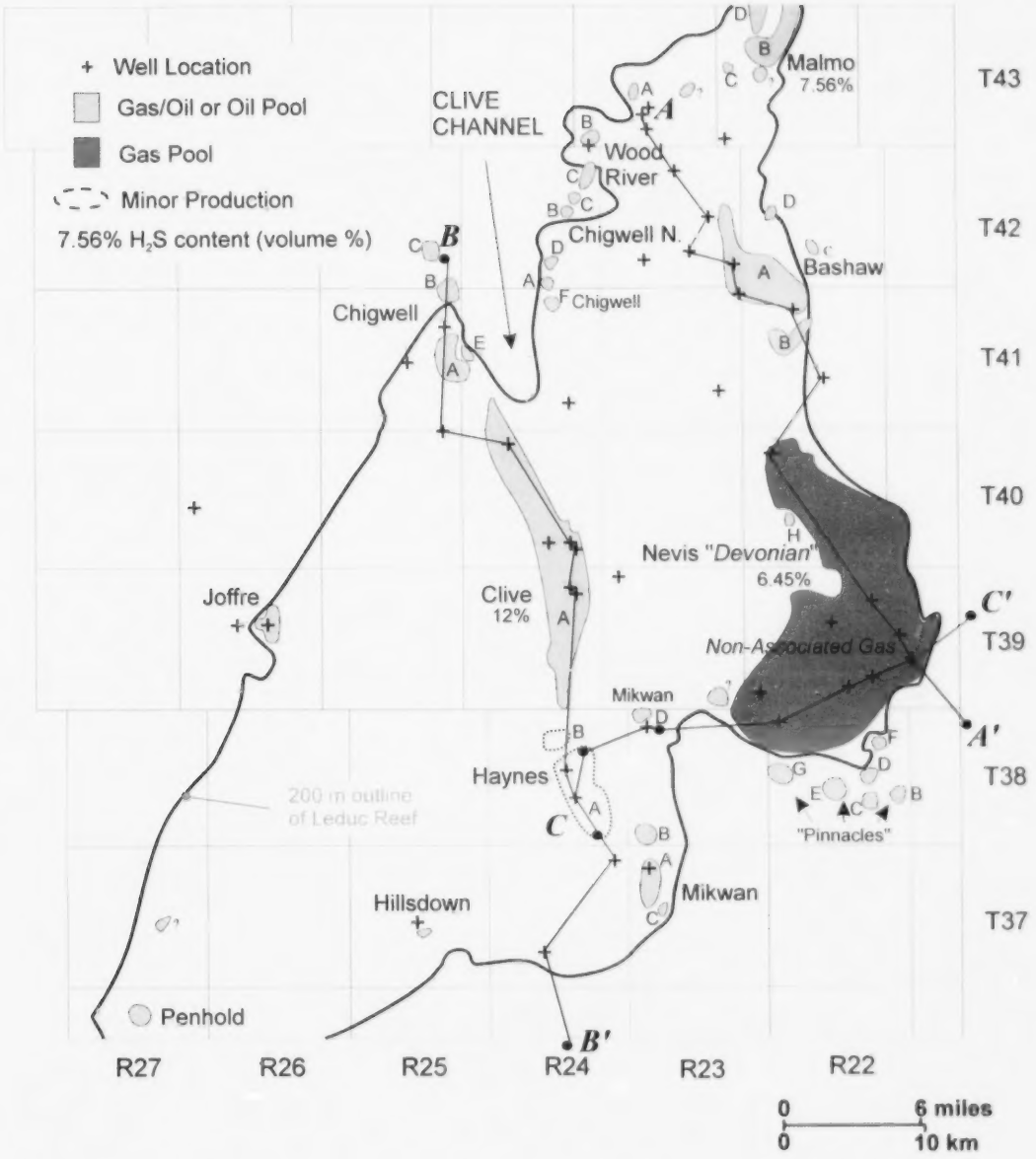

Figure 4.1: Detailed outline of Leduc Formation (D-3) hydrocarbon pool locations, and H_2S content. Data extracted from the CD-ROM version of the Alberta Energy Resources Conservati on Board (AERCB) well database by CDPubco (Calgary), Alberta Society of Petroleum Geologists (ASPG, 1960, 1966, and 1969), and T.Geier (Ulster Petroleums Ltd., pers. comm.) for the Clive field H_2S values. Locations are shown of cross sections A-A', B-B', and C-C' (Figures 4.3, 4.4, and 4.5).

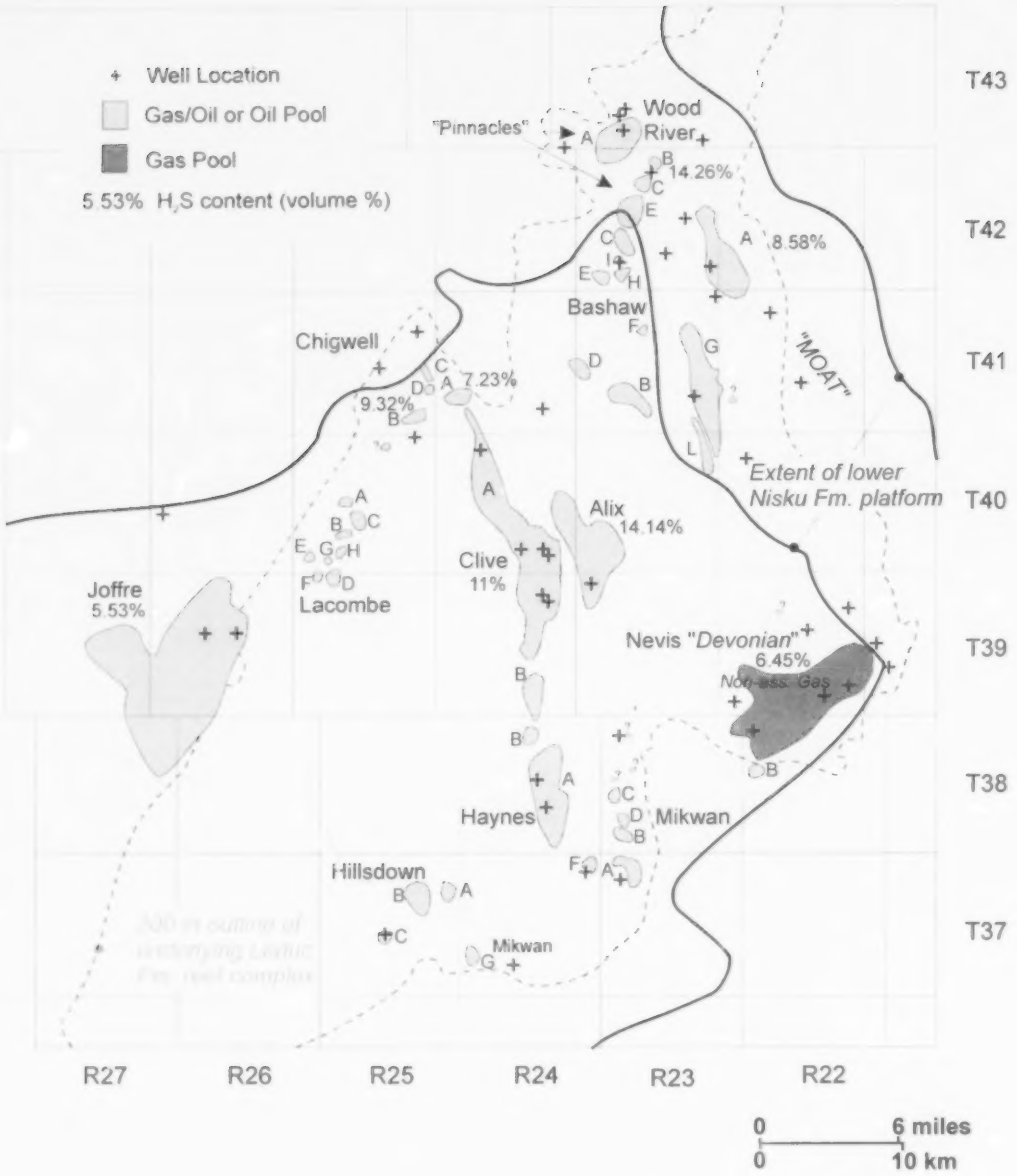

Figure 4.2: Detailed outline of lower Nisku Formation and Camrose Member (D-2) hydrocarbon pool locations, and H_2S content. Data extracted from the CD-ROM version of the AERCB well database by CDPubco (Calgary), Alberta Society of Petroleum Geologists (ASPG, 1960, 1966, and 1969), and T.Geier (Ulster Petroleums Ltd., pers. comm.) for Clive field H_2S values.

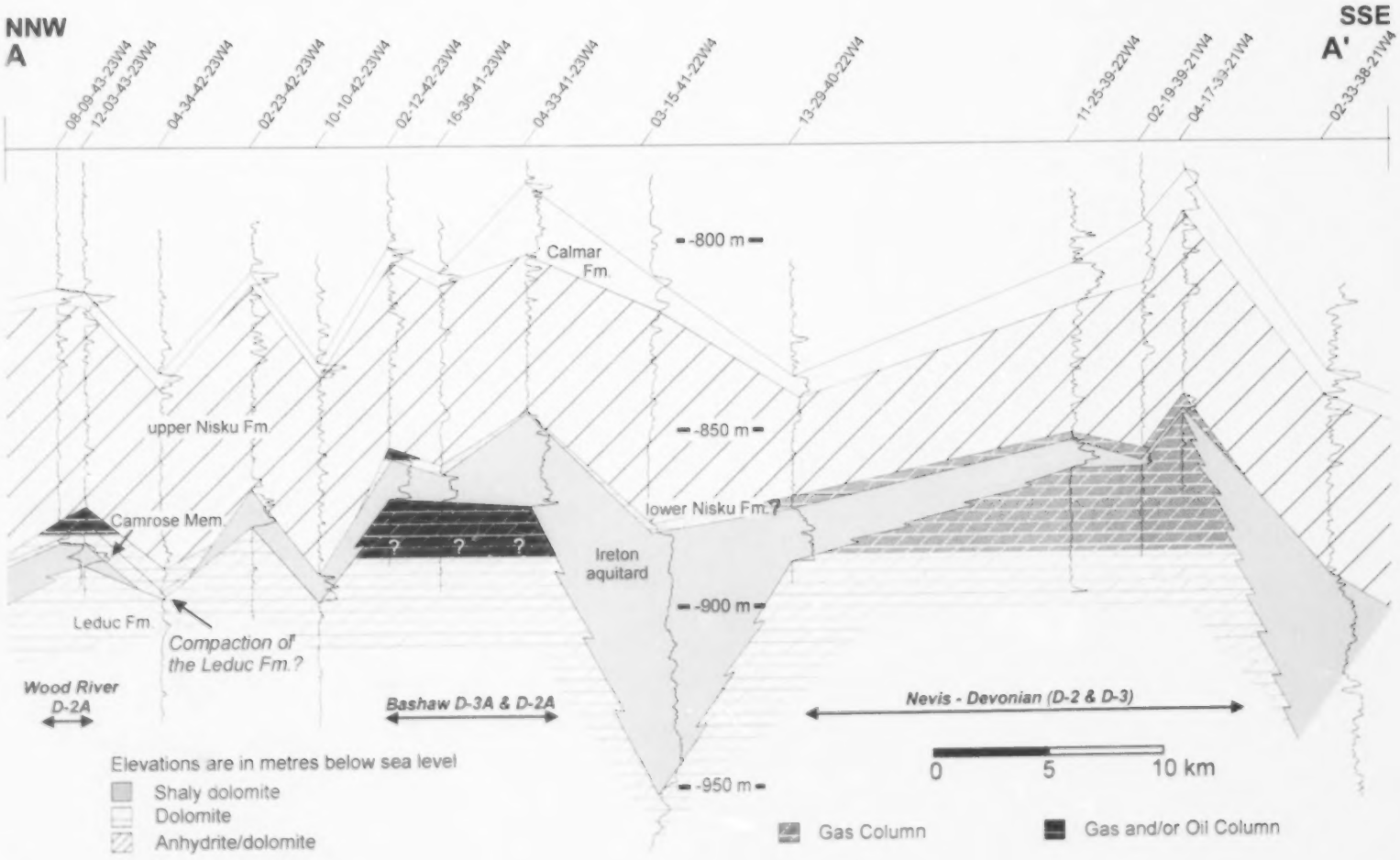

Figure 4.3: Structural cross section A-A' indicating the present-day reservoir accumulations and approximate hydrocarbon column heights (gross pay). All log signatures are gamma-ray. Line of cross section is shown in Figure 4.1.

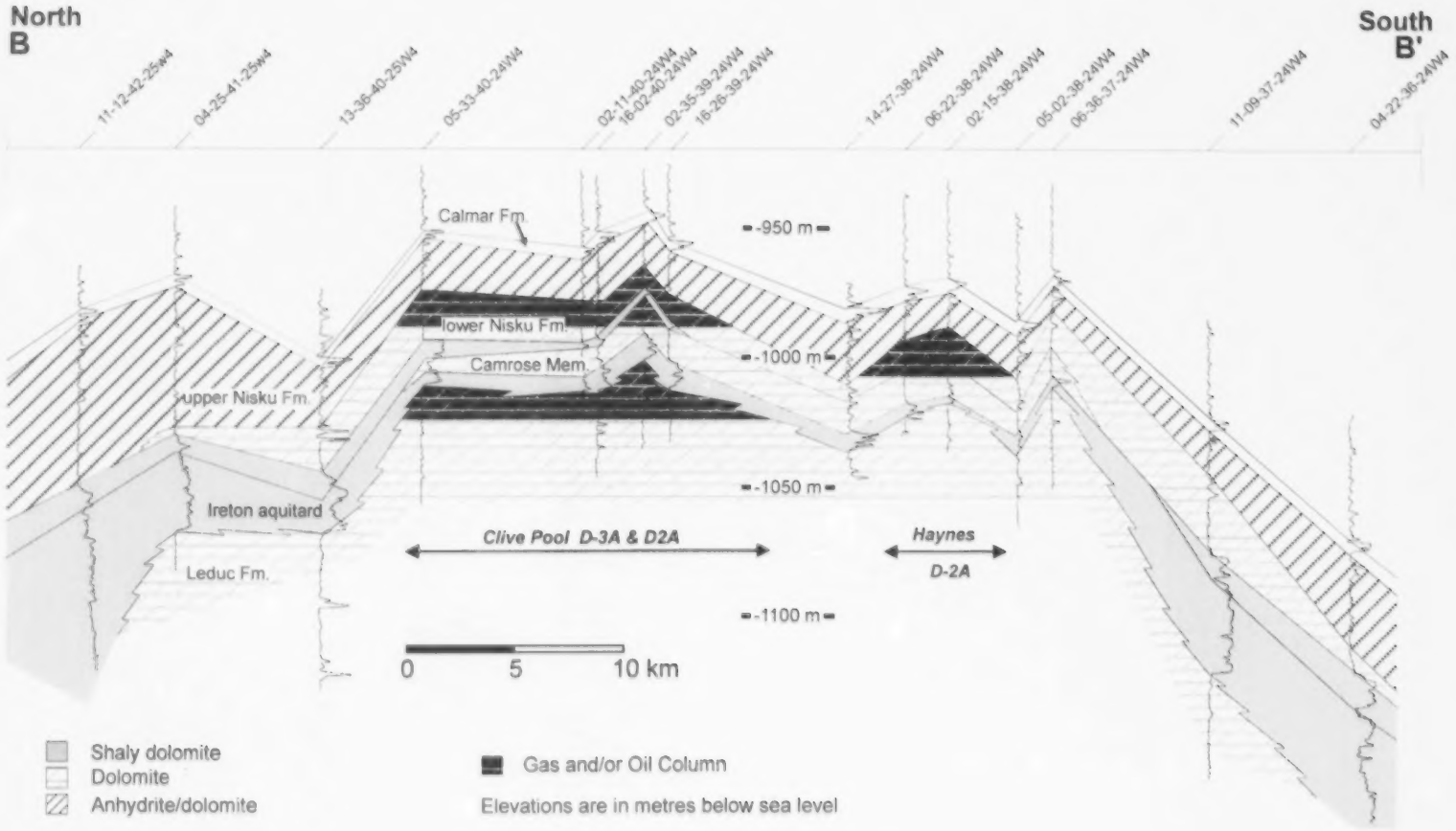

Figure 4.4: Structural cross section B-B' indicating the present-day reservoir accumulations and approximate hydrocarbon column heights (gross pay). All log signatures are gamma-ray. Line of cross section is shown in Figure 4.1.

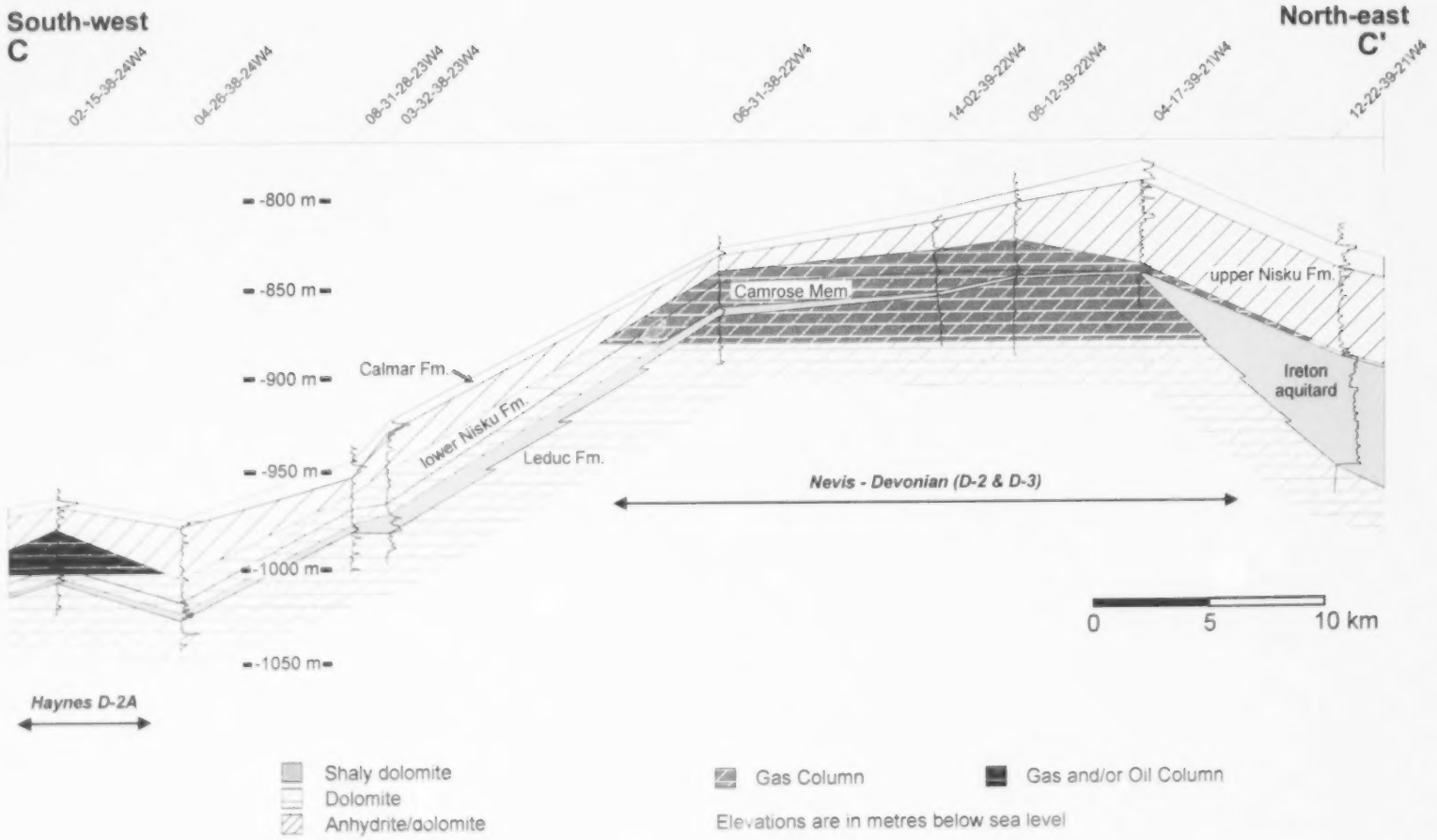

Figure 4.5: Structural cross section C-C' indicating the present-day reservoir accumulations and approximate hydrocarbon column heights (gross pay). All log signatures are gamma-ray. Line of cross section is shown in Figure 4.1.

Field	Pool	Hydrocarbon column thicknesses			Associated/non associated gas
		Gas column (m)	*Oil column (m)*	*Total (m)*	
Alix	D-2	5	5	10	ass.
Chigwell	D-2A		5	5	ass.
	D-2B		5	5	ass.
Clive	D-2A	15	8	23	ass.
	D-3A	19	8	27	ass.
Haynes*	D-2A	~14	~7	21	ass.
Joffre	D-2		21	21	no gas
Malmo	D-3A	20	22	42	ass.
Nevis	D-2	37		37	non ass.
	D-3	41		41	non ass.
Wood River	D-2A		11	11	no gas
	D-2B		16	16	no gas

* Column height for the Haynes field was interpreted from data provided by Murphy Oil Company, Calgary

Table 4.1. Hydrocarbon column thicknesses (gross pay) for a number of the pools in the Bashaw area. Information extracted from ASPG (1960, 1966, and 1969).

Formation platform and Leduc Formation reef complex against evaporites and Ireton aquitard, respectively, the columns are in the order of 30 - 60 m (100 - 200 feet) (*e.g.*, in the Nevis and Malmo fields, Table 4.1 and Figure 4.3).

4.2 Reservoir Characteristics.

4.2.1. Leduc Formation

The Leduc Formation (D-3) dolostones have excellent reservoir characteristics, with good moldic, vuggy, and intercrystalline porosity (*e.g.*, Figure 4.6a) that extend well below the present-day pay zones. D-3 pools have high permeabilities, and porosities in the order of 5 - 15%, that have enabled recoveries of 25 - 65% (ASPG, 1960). Visual estimates of porosity, from core logging, suggest that there is a facies control on porosity development similar to the Homeglen-Rimbey fields of the southern Rimbey-Meadowbrook reef trend (Drivet, 1993). Skeletal grainstones and stromatoporoid/coral facies are all visibly more porous than skeletal packstones and wackestones. Nevertheless, it is likely that many of the facies observed in the uppermost Leduc Formation also have good reservoir characteristics. Porosity loss in the uppermost Leduc Formation is commonly a result of anhydrite cementation.

4.2.2. Nisku Formation and Camrose Member

Nisku Formation and Camrose Member (D-2) production is predominantly from lower Nisku Formation and Camrose Member dolostones. These units are contiguous over much of the reef complex and are developed to a maximum thickness of ~50 m within the Bashaw area. The Camrose Member usually forms the lowermost 10 m to the reservoir interval. However, in the Clive area, where argillaceous carbonates and calcareous shales of the Ireton Formation onlap the reef complex, the Camrose Member forms a separate reservoir interval (T.Geier, Ulster Petroleums Ltd., pers. comm.) (Figure 4.4).

Porosity types in the D-2 reservoirs are dominantly moldic and intercrystalline, and are less vuggy than the Leduc Formation dolostones (Figure 4.6b). Average pool porosities range from 3 - 10% with recoveries of 20 - 50% (ASPG, 1960). These values are lower than those of the Leduc Formation and may be an effect of the less fabric-

FIGURE 4.6: Characteristic reservoir rocks of Leduc Formation and Camrose Member/ lower Nisku Formation pay zones.

a) Leduc Formation core with extensive porosity development in the form of moldic (Mo), intercrystalline (Ic), fracture (Fr), and vuggy (V) porosity. Note that virtually no fossil is left unleached and, therefore, facies identification is difficult. 16-2-40-24W4, 1929.5 m. Scale = dime coin (17 mm).

b) Camrose Member core, with relatively low porosity that is typical of the lower Nisku Formation and Camrose Member facies. Minor open moldic (Mo) is present, with much of the porosity that was generated during replacement dolomitization being occluded by late anhydrite cement (An). Note that fossil preservation (present in this picture as wafer to banded stromatoporoids) is much greater in the lower Nisku Formation/Camrose Member than the Leduc Formation. 16-2-40-24W4, 1915.5 m. Scale = dime coin (17 mm).

c) Non-facies selective, late anhydrite cements. Porosity is occluded by anhydrite (An) in the bottom of the picture, with open moldic porosity at the top of the picture — within the same facies (lower Nisku Formation). Presumably, cementation was controlled by preferred fluid conduits through the facies and was not a pervasive process. 14-2-39-22W4, 5375 ft. Scale = dime coin (17 mm).

Figure 4.6: Characteristic reservoir rocks of Leduc Formation and Camrose Member/lower Nisku Formation pay zones.

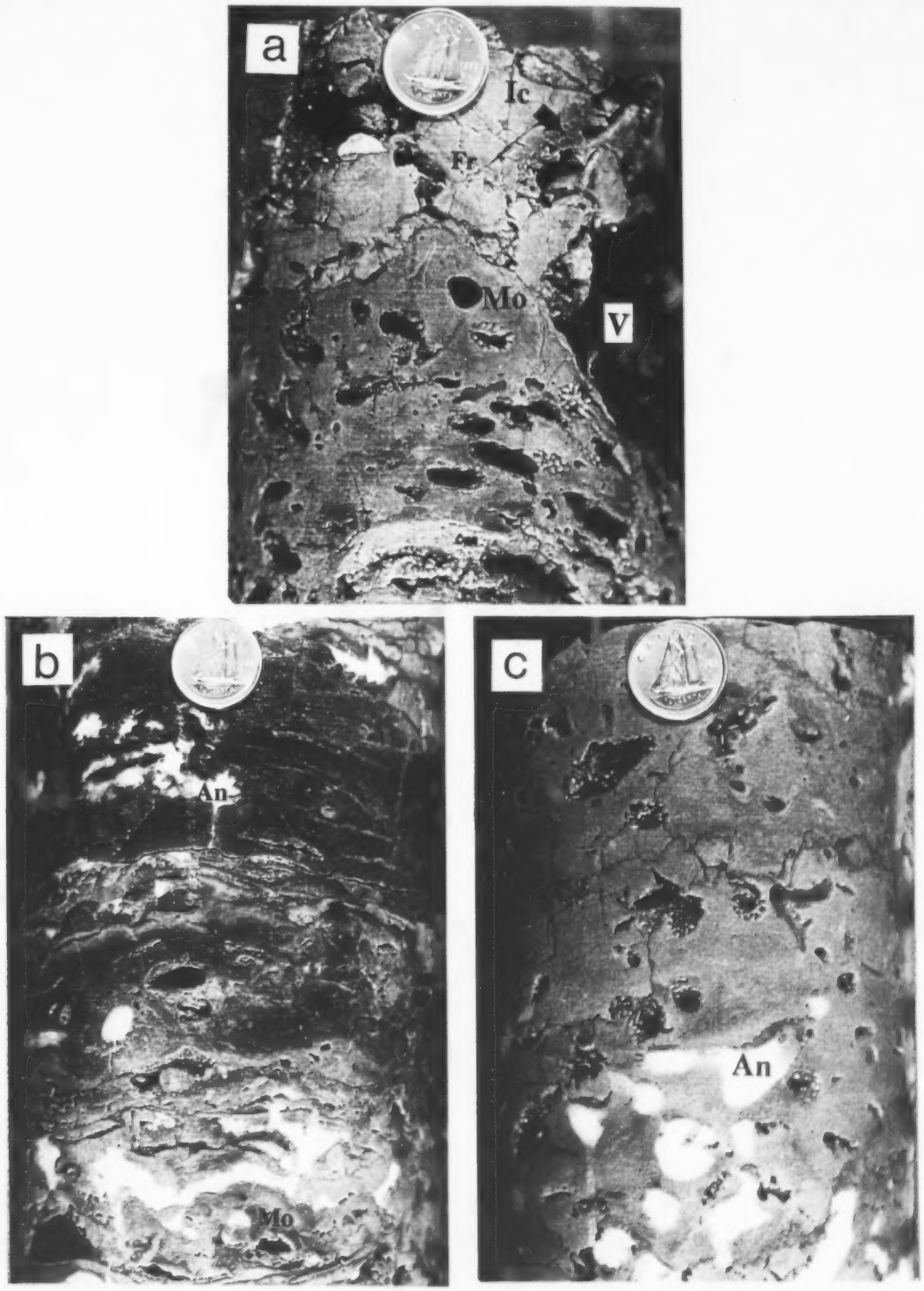

destructive nature of matrix replacement dolomitization within the lower Nisku Formation and Camrose Member platform facies. Variations in either the facies or perhaps the effects of early diagenetic alteration (prior to dolomitization) in the lower Nisku Formation and Camrose Member, to those of the Leduc Formation, could possibly have resulted in lower porosity during replacement dolomitization. Late anhydrite cements are a major cause of further porosity reduction, probably due to the nearby sourcing from the overlying evaporite sequences (upper Nisku Formation and Wabamun Group). Anhydrite cementation appears to be a non-facies selective process that leaves occluded moldic porosity adjacent to open moldic porosity within the same facies (Figure 4.6c), causing reservoir heterogeneity.

4.3 Trapping Styles.

4.3.1. Leduc Formation (D-3) pools

There is a strong correlation between the location of the Leduc Formation pools to that of the present-day relief associated with the Bashaw Reef Complex (compare Figure 4.1 with Figures 4.3, 4.4, and 4.5). In most cases, the Leduc Formation pools are located within closures related to topographic highs along the top of the reef complex, with some pools possibly being close to spill-point, *e.g.*, the Nevis and Clive D-3A pools (ASPG, 1960 and 1969). As discussed in Section 2.3, many of the topographic highs were probably developed through differential compaction, except in the Haynes and Nevis areas which appear to have "survived" as the highest portions of the reef complex. The "sealing" unit is generally the Ireton aquitard which provides a nearly continuous top and lateral aquitard, except in a few locations where its thickness thins to <1 m. Thus, most traps within the reef complex can be classified as stratigraphic (reefal) traps (Rittenhouse, 1972) with structural enhancement by differential compaction. Pools are also located off the reef complex within "pinnacle" reefs, *e.g.*, the "pinnacles" south of Nevis (Figure 4.1), and the reefs of New Norway and Duhamel to the north of the study area (Figure 1.1).

One trapping anomaly is found within the Bashaw Reef Complex, in what is commonly referred to as the Nevis "Devonian" pool (undifferentiated between D-2 and D-3 production horizons; Figures 4.1 and 4.2), which appears to have a common gas/water contact between the D-2 and D-3 production horizons. Such a phenomenon

would suggest that hydraulic communication exists between the two production horizons for this type of equilibrium to occur, especially as the Ireton aquitard thins to <6 m over the pool (Figure 2.6). It also suggests that trap closure is principally within the Nisku Formation. Similarly, the Haynes pool has <6 m of Ireton aquitard drape (Figure 2.6) and although production is typically thought to be occurring from both D-2 and D-3 production horizons, it is mostly occurring in the D-2 horizon with only minor production from the Leduc Formation (Figure 4.1).

4.3.2. Nisku Formation/Camrose Member (D-2) pools

Nisku Formation/Camrose Member trapping styles are less clearly defined than D-3 pools. The lower Nisku Formation and Camrose Member are contiguous over much of the area, except in the area of the Clive field where argillaceous carbonates and calcareous shales of the Ireton Formation separate the two units (Figure 4.4). "Sealing" of the D-2 pools is typically by the facies transitions from the carbonate reservoirs into the less permeable upper Nisku Formation evaporites, or the argillaceous carbonates/calcareous shales of the Ireton Formation (*e.g.*, Clive field). Therefore, like the Leduc Formation, D-2 pools also are stratigraphic traps. Closure along these facies transitions was mainly controlled by compactional drape as the Leduc Formation (and Nisku Formation) differentially compacted. In particular, many of the D-2 pools can be seen to directly overly the present-day highs of the Leduc Formation (compare Figure 4.2 with Figures 4.3, 4.4, and 4.5). Facies transitions within the platform from high to low permeability facies, as well as the occurrence of porosity plugging late dolomite and anhydrite cements, also complicate trap characterization. The close proximity of the upper Nisku Formation evaporites provides a likely source of anhydrite for extensive cementation of the platform facies, enabling diagenetically controlled entrapment. This is best seen in the Joffre field (Al-Bastaki *et al.*, 1995b), but may also have occurred in other fields, *e.g.*, the Clive field (T.Geier, pers. comm.).

Basinward of the lower Nisku Formation platform, traps are situated within "pinnacle" thamnoporoid-dominated reefs surrounded by "sealing" evaporite units, *e.g.*, Wood River area (Dixon *et al.*, 1991) (Figure 4.2). The Bashaw D-2 A, G, and L pools, located to the east of the platform margin (Figure 4.2), are pooled within a thinly-

developed, banded, fine and coarse crystalline dolostone that developed beneath the "Moat" area (Figure 4.2). Trapping of these pools developed due to compactional drape of the Ireton aquitard, creating dip reversal to the east.

4.4 Reservoir Production Data.

For this study concerned with aquitard integrity, the most useful reservoir information is that of the pool pressure, production, and injection history. This data can provide indications that, on a production time-scale, hydrodynamic communication exists between reservoirs separated by an aquitard. For example, the pressure decline curve of a D-2 pool can be compared with that of a D-3 pool to see if their decline rates are similar or if the effects of water injection or hydrocarbon production in one pool effects another. However, when such information does not indicate communication during production, there still may be communication on a geologic time-scale. This may be determined from initial pool pressure and drill stem test data.

The pressure-decline production histories of the Clive D-2A and D-3A pools, Haynes pool (which is principally producing from the D-2 level), Bashaw D-3A pool, and Alix D-2 pool (Figures 4.1 and 4.2) are given as examples in Figure 4.7 (ERCB, 1986). A close match can be seen between the pressure histories of the Haynes pool and the two Clive pools. All had a noticeable increase in rate of pressure decline after 1976, followed by a subsequent decrease in the rate of decline after 1979 (Figure 4.7). This provides reasonable evidence to conclude that all three pools are in hydrodynamic communication and that consequently there is hydrocarbon breaching of the Ireton aquitard near these pools on a production time-scale. The pressure decline curve of the Alix D-2 pool, however, shows a marked increase in pressure after 1974 due to the shutting-in of a number of wells (ERCB, 1979-1986) that is not reflected in the pressure decline curves of the other pools, even in the adjacent (1 km west) Clive D-2A pool (Figure 4.2). This suggests that on a production time-scale the Alix pool is in isolation of the other pools, and that probably there is permeability impedance in the lower Nisku Formation platform (via facies transitions or diagenetic plugging) between the Alix and Clive D-2A pools. The Bashaw D-3A pool (located approximately 20 km to the northeast (Figure 4.1)) has a similar decline curve to that of the Haynes and Clive pools. However, it does not show

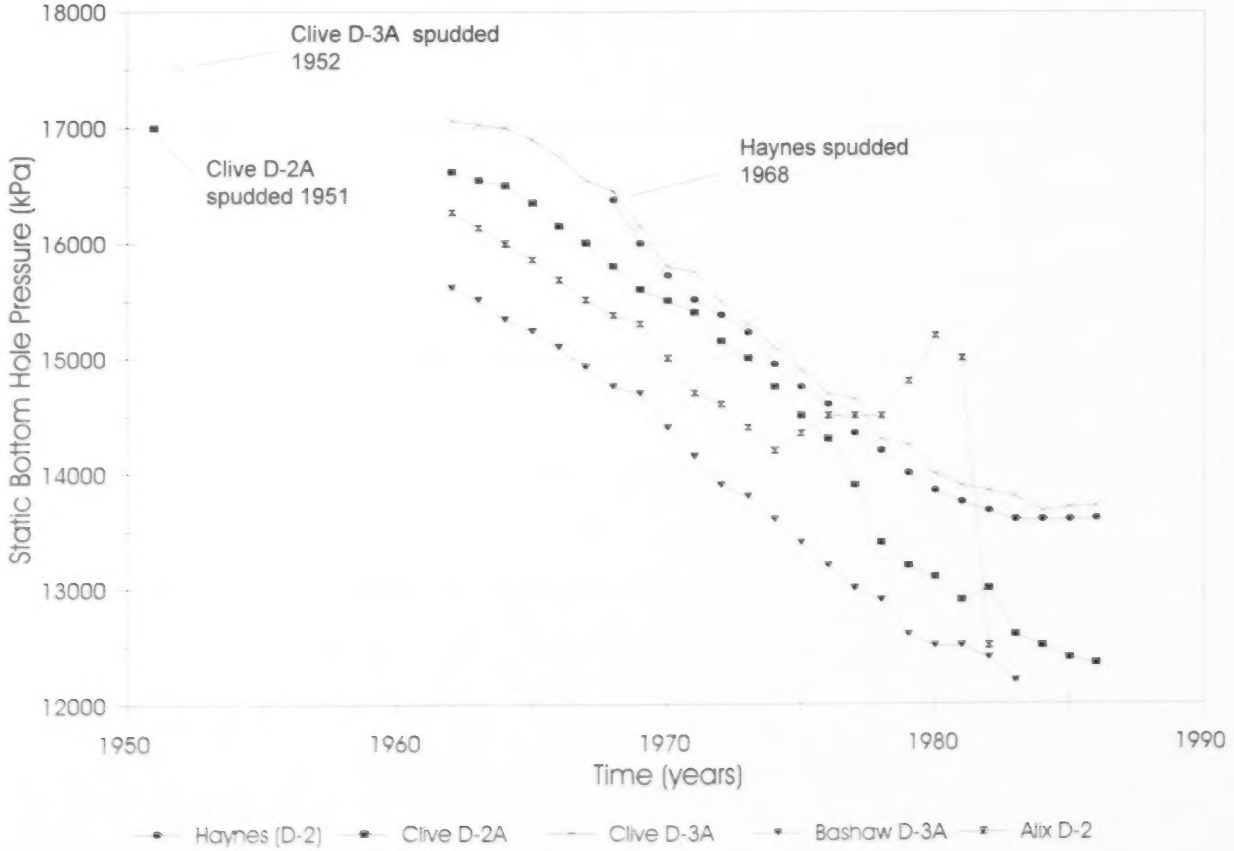

Figure 4.7: Pressure-decline curves of the production histories of the Haynes (D-2), Clive D-2A, Clive D-3A, Bashaw D-3A, and Alix D-2 pools.

the more subtle variations in pressure gradient that were used to match the Haynes and Clive pools. Therefore no conclusions can be drawn regarding communication on a production time-scale between the Haynes and Clive pools and that of the Bashaw D-3A pool. Nevertheless, the data do not discount the possibility that communication may exist on a production time-scale over this distance, as unfortunately the data are unable to distinguish between the "noise" of production of the Bashaw area and that of the production effects in the Haynes and Clive areas.

Hydraulic communication on a geologic time-scale through the Ireton aquitard exists in the Haynes and Clive area, as indicated by a pressure/elevation plot (p/z) of the initial pool pressures in the Clive area (Figure 4.8), and a pressure/depth plot (p/d) of well 6-22-38-24W4 in the Haynes area (Figure 4.9). The initial oil pressures of the Clive D-2A and D-2B pools are close to the initial, undisturbed formation pressures, as these pools were among the first to be drilled in the Bashaw reef area (1951 and 1952, respectively (Figure 4.7)). The measured vertical pressure-gradient between these two oil-pools corresponds exactly with the density-corrected (~209,000 mg/l brine for the Bashaw area) nominal gradient of 11.2 kPa/m (Paul, 1994). A brine gradient was used as the best approximation of the hydrostatic fluid gradient for the area because the influence of the hydrocarbons in the pools on this gradient is only minor because of the relatively small hydrocarbon column heights present. Such a precise correlation in fluid gradient between reservoirs separated by an aquitard suggest that there is pressure communication, at least over geologic time, between the reservoirs. Even taking the oil and gas phases into consideration, the pressure difference between the two Clive pools is not marked enough to argue that the two pools are hydraulically isolated. The nominal gradient in well 6-22-38-24W4 of the Haynes pool (Figure 4.9) is also very close to the two measured pressure-test values (water phase only) from the D-2 and D-3 horizons. The slight off-set in the measured pressure values from the nominal gradient could, however, be an effect of drawdown from the Clive pools which had already been producing for over 17 years (Haynes was discovered in 1968). Nevertheless, the correlation is also strong for the Haynes area, like the Clive area, which suggests that geologic communication between the D-2 and D-3 horizons across the Ireton aquitard does exist in this area of the Bashaw Reef Complex.

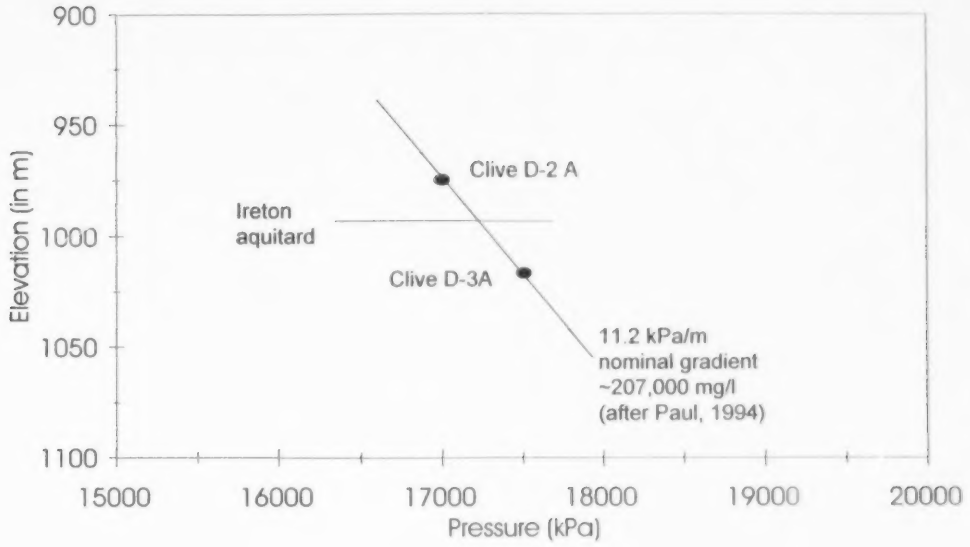

Figure 4.8: Pressure-Elevation plot of the initial pressures in the Clive D-2A and D-3A pools.

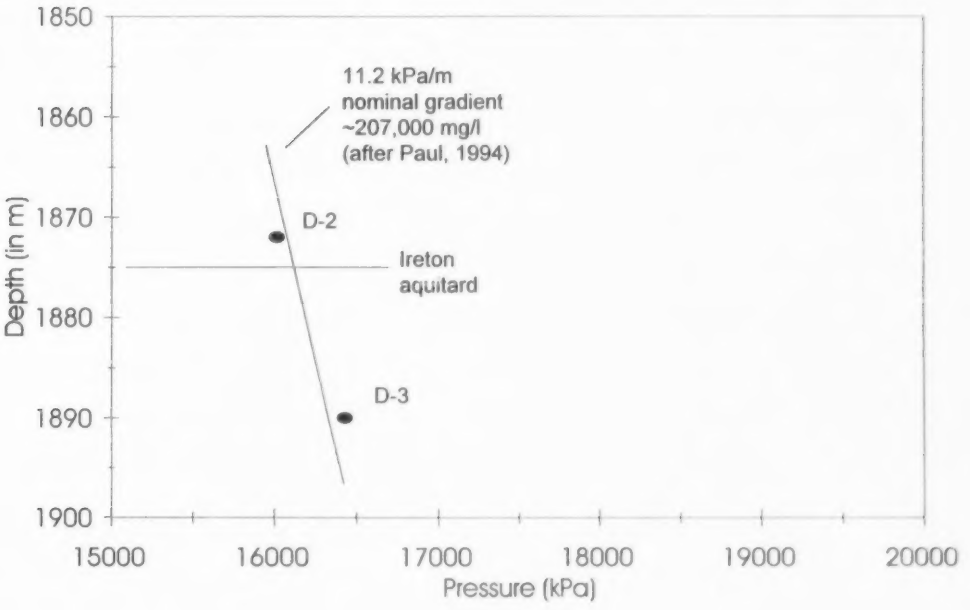

Figure 4.9: Pressure-Depth plot from D-2 and D-3 production horizons of well 6-22-38-24W4 in the Haynes area.

4.5 Hydrocarbon Data.

Oil to source rock correlations by Stoakes and Creaney (1985) identified the organic-rich, basinal carbonates of the Duvernay Formation (Figure 1.3) as the principal source rock for the oil accumulated within the Leduc Formation of the Bashaw area. Maturation studies indicate that the Duvernay source rocks are just within the oil window throughout the study area, and that their maturity increases to the southwest (Stoakes and Creaney, 1985). Oils in the Nisku Formation/Camrose Member pools are also believed to have a Duvernay origin, as suggested by: the similar API gravities of the Nisku Formation oils with those of the Leduc Formation oils (~40 API)(ASPG, 1960); the close spatial association of the Nisku Formation/Camrose Member pools with the Leduc Formation (Rostron, 1995); and hydrogeological data (Paul, 1994; Rostron, 1995). More detailed oil-oil correlations by the petroleum companies working the Bashaw area have confirmed a predominantly Duvernay origin to the oils of the Leduc and Nisku formations. However, some pools (*e.g.*, the D-2 pools situated east of the lower Nisku Formation platform (Figure 4.2)) are believed to have a signature that is perhaps a mixture of Duvernay-sourced oil with oil(s) from some other hitherto unidentified source(s) (T.Cadrin, PanCanadian Petroleum Ltd., pers. comm.).

A significant volume of H_2S has also been recorded from a number of pools in the area (Figures 4.1 and 4.2) (ASPG, 1960, 1966, 1969). Unfortunately no H_2S data is available for some of the pools, and other reference sources sometimes quote H_2S percentages quite different to that of the ASPG (confidential reports; T.Geier, pers. comm.). Nevertheless, a broad variation in the H_2S content of the pools is observed, from values as low as 0.6 volume percent, to a high of 14.14 volume percent. Therefore most pools are considered to be "sour". Two processes could account for the presence of H_2S: thermochemical sulphate reduction (TSR) and bacterial sulphate reduction (BSR). Percentages of H_2S >10%, that are commonly present in the Bashaw area, are considered to preclude the possibility that the H_2S was formed by *in situ* BSR (Machel *et al.*, 1995). H_2S generated via the process of TSR, however, requires a minimum temperature of ~100 - 140°C (Machel *et al.*, 1995). These temperatures correspond to minimum burial depths of ~2700 - 4000 m, assuming normal geothermal gradients. The Bashaw Reef Complex, however, is unlikely to have been buried to depths greater than ~2500 m (Figure 3.1), and

therefore reservoir temperatures have never been high enough for *in situ* TSR. The most likely explanation, therefore, is that H_2S was sourced allochthonously. One possible origin is that the H_2S migrated from a source further downdip (southwest). The presence of H_2S in the Innisfail and Wimborne Fields to the southwest (Figure 1.1), and an abundance of sour gas in the deeper Upper Devonian reservoirs further to the southwest support a likely southwesterly origin to the H_2S in the Bashaw area. The deeper Upper Devonian H_2S reservoirs are also presumed to be of TSR origin (Krouse *et al.*, 1988), and would therefore tend to suggest a TSR origin to the H_2S present in the Bashaw area. An alternative hypothesis, however, is that H_2S may have migrated through deep-reaching faults from hitherto unidentified hydrocarbon reservoirs underlying the Upper Devonian in the Bashaw area or farther to the southwest. Evidence is accumulating as to the presence of basement faulting in the WCSB that may have been periodically reactivated during the history of the WCSB (Edwards *et al.*, 1995). For example, Haines (1960) has suggested that lead-zinc deposits present in the Duhamel, New Norway, and Malmo reefs (Figure 1.1), to the north of the study area, may have a hydrothermal origin possibly controlled by faults.

CHAPTER 5

THE IRETON AQUITARD

The Ireton aquitard provides the principal control to cross-formational fluid flow within the study area. An assessment of the integrity of this aquitard requires two levels of observation, a micro- and macro-scale. On a macro-scale, this chapter describes the sedimentology of the Ireton aquitard that was deposited directly over the Bashaw Reef Complex, and is followed by a micro-scale analysis in an effort to identify more precisely breaching locations of this aquitard.

Data presented in this chapter indicates that hydrocarbon breaching is likely to have occurred across the Ireton aquitard within the Bashaw area. Breaching locations are related to variations in the Ireton aquitard facies and the effects of dolomitization on porosity distribution within the Ireton aquitard.

5.1 Sedimentology.

Within the study area, the Ireton aquitard was deposited as a nearly continuous drape over the reef complex, and generally consists of tight, green, shaly carbonates. The Ireton aquitard is most easily recognized on gamma-ray logs because the clay content in the Ireton aquitard causes a pronounced "kick" in the gamma response in contrast to the underlying and overlying Leduc Formation and Camrose Member/lower Nisku Formation carbonates. Unfortunately, there are difficulties in recognizing the Ireton aquitard on logs where the aquitard drape thins to <~4 m. For example, the presence of clay/silt-rich lenses within the uppermost parts of the Leduc Formation, that were possibly generated during storm events and derived from nearby "drowned" areas of Ireton aquitard sedimentation, can easily be confused with the laterally continuous Ireton aquitard on logs. It is therefore necessary to look at core (where available) to determine which gamma "kicks" are produced by the Ireton aquitard. In general, the storm-generated, clay-rich lenses contrast from the Ireton aquitard by having a higher clay content, are "greener" in appearance, and are located within reefal sediments.

5.1.1. Thickness and composition

The distribution of the Ireton aquitard over the reef complex was mapped in detail by Rostron (1995) using gamma-ray logs from over 1000 wells, and modified using data gathered in this study. The isopach map of the Ireton aquitard (Figure 5.1) reveals that over the central and southeastern part of the reef complex there is <6 m of aquitard drape. Within the <4 m contour interval, 28 wells were identified by Rostron (1995) to have no Ireton aquitard. Toward the margins of the reef complex the Ireton aquitard thickness increases to ~25 m, before thickening rapidly into the surrounding basin (~200 m thick). Minor modifications to the isopach map (Figure 5.1), however, are necessary because of the difficulty in accurately defining the Ireton aquitard contacts without core control. This Ireton aquitard distribution appears to reflect deposition over the inferred Bashaw reef morphology (Figure 2.6), with the highest parts of the Leduc Formation being draped by the thinnest Ireton aquitard.

Mineralogic compositions of the basinal shales/carbonates in the Ireton Formation were first reported by McCrossan (1961) and expanded upon by Campbell and Oliver (1968). Generally, the basinal Ireton Formation is composed of calcite (in the lower parts of the succession), dolomite (in the upper parts), illite, quartz, and chlorite, and minor pyrite. Over the Bashaw Reef Complex, bulk X-Ray diffraction and thin section analyses confirmed the presence of dolomite, illite, quartz, and pyrite. No precursor marine limestone was present. Locally, anhydrite and late poikilotopic calcite cements are also present, especially where the Ireton aquitard drape is thin. The detrital carbonate component of the Ireton aquitard is probably sourced from reefal areas within the basin (McCrossan, 1961), whereas the majority of clay and quartz is derived from an extrabasinal, northerly source (Stoakes, 1980).

Variation in the carbonate content of the Ireton aquitard across the reef complex has been determined by dissolving the Ireton aquitard samples in acid. The analytical procedure is outlined in Appendix I and the results are tabulated in Table 5.1. An attempt to contour these data (Figure 5.2) is restricted, however, because of insufficient data in some areas. Average values were determined when more than one analysis was performed in a particular well. However, not all sample values are representative of the aquitard, and some were omitted. For example, data from thin, discontinuous lenses

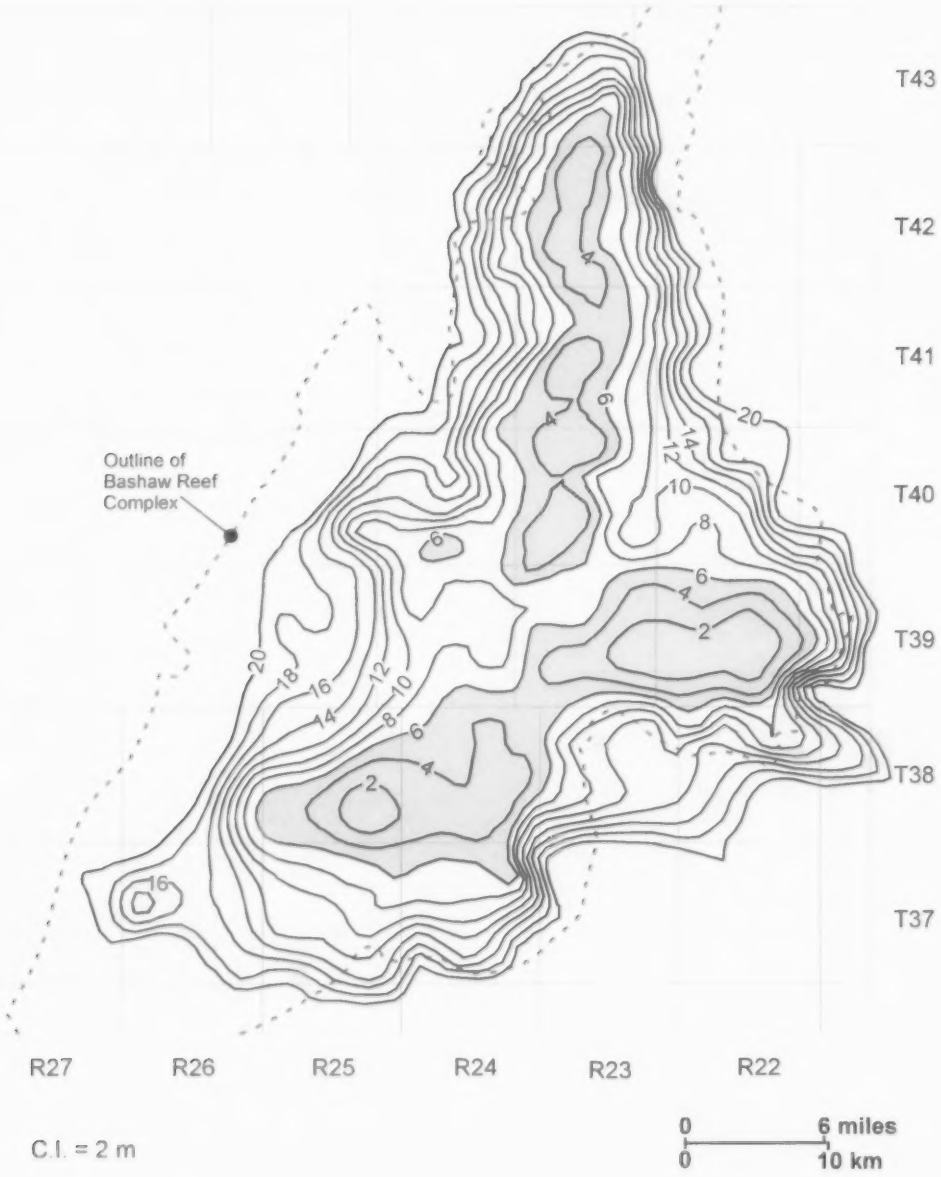

Figure 5.1: Detailed isopach map of the Ireton aquitard over the Bashaw Reef Complex (modified from Rostron, 1995). Light grey shaded areas indicate an Ireton aquitard thickness of < 6 m.

Location	Depth	Average Ireton aquitard facies	Thickness of aquitard (m)	Position from top of aquitard (m)	% Carbonate	Average % for each well
11-9-37-24W4	2031.5m	Lower slope	45	42.4	43	43
6-36-37-24W4	1835m	Upper slope	4	1.8	95	95
16-16-37-25W4	6790ft	Lower/Upper	9	3.0	94	82
16-16-37-25W4	6800ft	Lower/Upper	9	6.1	72	82
16-16-37-25W4	6808ft	Lower slope	9	8.5	78	82
6-31-38-22W4	5589ft	Upper slope	6	1.2	90	90
8-31-38-23W4	1800m	Upper slope	5	2.7	84	84
2-15-38-24W4	6168ft	Platform	1	0.3	88	88
6-22-38-24W4	6168ft	Upper slope	4	2.4	76	71
6-22-38-24W4	6169ft	Upper slope	4	2.7	67	71
6-22-38-24W4	6173ft	Upper slope	4	4.0	70	71
14-2-39-22W4	5391ft	Platform	1	0.3	93	96
14-2-39-22W4	5393ft	Platform	1	0.9	98	96
11-25-39-22W4	5519ft	Upper slope	4	0.2	94	94
10-31-39-23W4	5991ft	Platform	3	1.8	95	95
16-26-39-24W4	1847.6m	Upper slope	10	1.2	93 (a)	78
16-26-39-24W4	1848.4m	Upper slope	10	1.8	64	78
16-26-39-24W4	1849m	Upper slope	10	2.4	89	78
16-26-39-24W4	1856.5m	Upper slope	10	9.1	82	78
2-35-39-24W4	1837m	Upper slope	9	3.0	53	67
2-35-39-24W4	1841.5m	Upper slope	9	7.0	81	67
10-22-39-26W4	2112m	? Lower/Basin	46	45.4	59	59
13-29-40-22W4	5484ft	Lower slope	10	1.2	66	75
13-29-40-22W4	5506ft	Lower slope	10	7.9	83	75
16-2-40-24W4	1917.5 m	Upper slope	9	1.8	95	85
16-2-40-24W4	1925.3 m	Upper slope	9	7.6	77	85
16-2-40-24W4	1926m	Upper slope	9	8.2	83	85
2-10-40-24W4	6196ft	Upper/Lower	2	0.2	64	64
5-33-40-24W4	1836m	Lower slope	17	1.0	63	63
3-15-41-22W4	5634ft	Basin	98	25.6	57	48
3-15-41-22W4	5648ft	Basin	98	29.9	58	48
3-15-41-22W4	5758ft	Basin	98	63.4	36	48
3-15-41-22W4	5768ft	Basin	98	66.4	41	48
4-33-41-22W4	5726ft	Lower slope	24	1.2	53	53
16-36-41-23W4	1726m	Upper slope	5	2.7	54	54
6-25-41-25W4	6270ft	Lower Slope	c.30	1.5	94 (a)	76
6-25-41-25W4	6273ft	Lower Slope	c.30	10.7	73	76
6-25-41-25W4	6305ft	Lower Slope	c.30	20.4	79	76
2-12-42-23W4	5660ft	Lower slope	9	1.2	70	66
2-12-42-23W4	5663ft	Lower slope	9	2.1	61	66
12-3-43-23W4	5635ft	Lower slope	4	1.8	52	52
12-10-43-23W4	1673.5m	Lower slope	10	4.3	88	70
12-10-43-23W4	1679.5m	Lower slope	10	9.8	52	70
11-9-44-24W4	5800ft	Basin	91+	1.2	58	63
11-9-44-24W4	5829ft	Basin	91+	10.1	67	63

Table 5.1: Percentage carbonate content data for each Ireton aquitard sample, and an average carbonate percentage for the Ireton aquitard of each well. (a) = anomalous value.

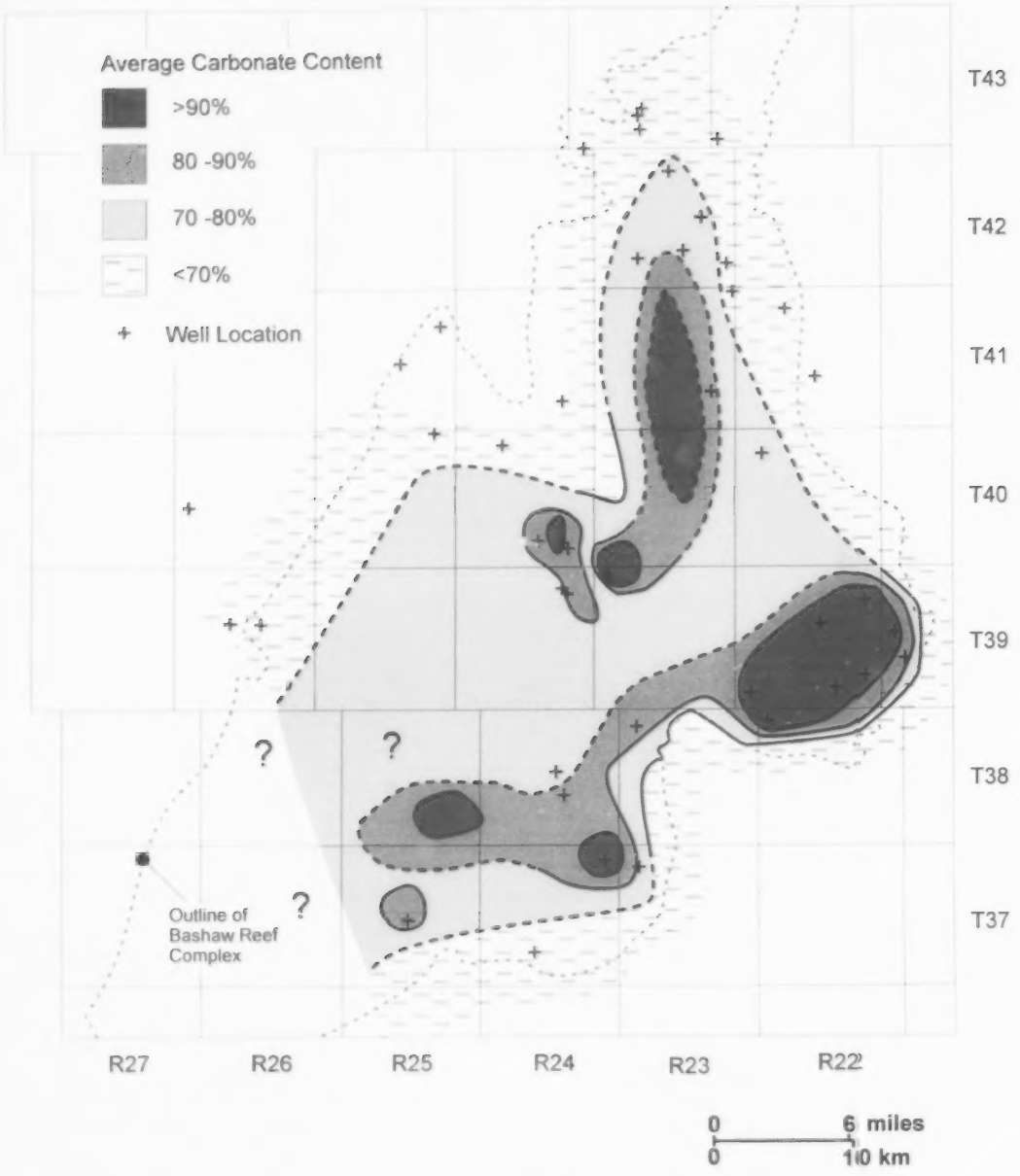

Figure 5.2: An approximate distribution map of the average percentage carbonate content present within the Ireton aquitard over the Bashaw Reef Complex. Carbonate contents have been inferred (dashed lines) in areas of no/limited data, based on a trend of decreasing carbonate content with increasing Ireton aquitard thickness.

(either carbonate-rich or poor) were omitted, as were those samples taken from near the gradational upper or lower contacts between the Leduc Formation or the Camrose Member/lower Nisku Formation where bioturbation was found to mix the sediments above and below the contacts.

A comparison of the carbonate percentage map (Figure 5.2) with the isopach map of the Ireton aquitard (Figure 5.1) reveals a fairly close trend of increasing aquitard thickness with decreasing carbonate content, which can be directly related to reef morphology at the end of sediment deposition of the Leduc Formation. For example, the zones with >90% carbonate content coincide with the <6 m contour interval and paleotopographic highs of the Leduc Formation.

5.1.2. Facies and facies distribution

Facies identification in the Bashaw area was based on a detailed facies analysis of the Ireton Formation by Stoakes (1980). Stoakes (1980) produced a regional-scale model of Ireton facies and depositional environments that developed as a series of clinoforms that prograded across the basin from east to west. Sedimentation along the clinoforms was characterized by periods of either predominantly clay/silt deposition or predominantly carbonate deposition/accretion (Stoakes, 1980). Stoakes (1980) proposed an essentially eustatic control on sedimentation within the basin, where most clay/silt deposition occurred during periods of slow rises in sea level or sea level stillstands, and carbonate deposition during rapid rises. During periods of rapid rises in sea level, the fluvial estuaries which supplied clay/silt were flooded and most of the terrigenous sediment supply was shut-off from the basin. This probably led to the development of hardground surfaces across the basin and the formation of carbonate-rich layers. In suitable water depths, calcareous organisms were able to proliferate on the clinoforms because of the lower levels of clastic input within the basin.

The Ireton aquitard in the Bashaw area was deposited along a reef-to-basin profile with four major environments of deposition, each with particular facies associations (Figure 5.3). These are:

i) *Platform*: Two facies types are typical of the platform environment; crinoidal

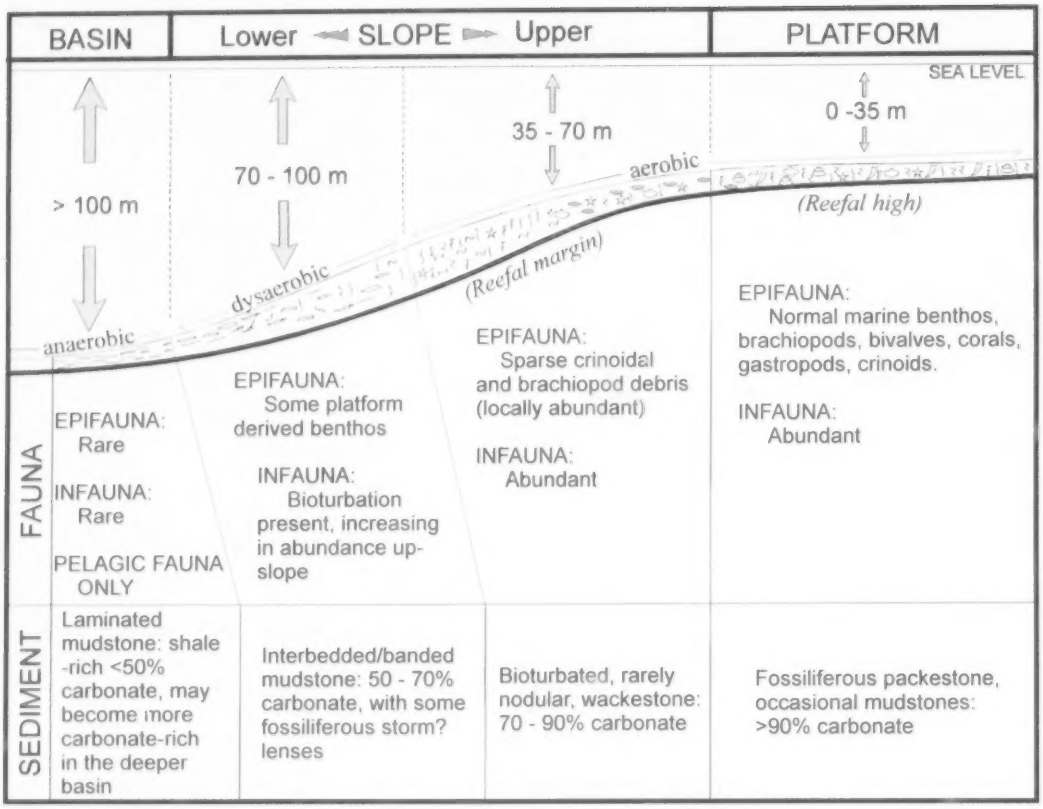

Figure 5.3: Depositional environments and associated facies of the Ireton aquitard along an idealized sloping profile, from reefal high to basin, including approximate water depths and oxygen content at the sediment/water interface (modified from Stoakes, 1980).

packstones in a green, clay-rich matrix (Figure 5.4a), and bioturbated mudstones (Figure 5.4b). The mudstones most likely developed due to some environmental restriction on the platform, *e.g.*, within an intertidal to supratidal setting (Stoakes, 1980). Carbonate content is typically greater than 90% (Figure 5.2) and developed in water depths of 0 - 35 m (Figure 5.3; Stoakes, 1980). These facies are rarely seen in core on the Bashaw Reef Complex as they are located toward the periphery of the topographic highs of the Leduc Formation where there was mainly zero aquitard deposition.

ii) *Upper Slope*: Just down-slope of the platform, there is a sharp decrease in fossil content into a very intensely bioturbated wackestone, with rare nodules (Figure 5.4c). Thin lenses of packstones are locally abundant and are probably derived from the platform via storm-related processes. Carbonate content averages between 70 - 90% and water depths (Stoakes, 1980) probably ranged between 35 - 70 m (Figure 5.3).

iii) *Lower Slope*: Towards the base of the slope the bioturbation intensity decreases, reflecting a gradual transition into dysaerobic conditions (Figure 5.3; Stoakes, 1980). Sedimentary laminations/bedding are developed as interbedded or banded mudstones of shaly carbonates (Figure 5.4d). As on the Upper Slope, marine benthos are rare and present mainly in storm-generated lenses. Water depths were probably between 70 - 100 m, with the carbonate content decreasing to 50 - 70%.

iv) *Basin*: Laminated mudstone facies with up to 50% carbonate content are present in a basinal environment (Figure 5.4e). These likely formed in anaerobic conditions, in water depths in excess of 100 m (Figure 5.3; Stoakes, 1980). The basinal environment is present in the off-reef areas and onlap the reef complex only slightly. Infauna and epifauna are rare, with mainly pelagic fauna being deposited.

These four environments represent a slight modification to the depositional environments proposed by Stoakes (1980) for the clay/silt-rich basinal clinoforms. The distribution of these environments (Figure 5.5) was constructed by determining the dominant facies type observed in each core. The distribution pattern of Ireton aquitard facies (Figure 5.5) shows a strong correlation to the percentage carbonate map (Figure 5.2). For example, the platform environment corresponds with a high carbonate content which then increases in carbonate content downslope. This trend correlates with a greater

FIGURE 5.4: Typical facies of the Ireton aquitard.

a) *Platform environment*: Crinoidal packstone in green clay-rich matrix. Rarely present on the reef complex. 6-12-39-22W4, 5442 ft. Scale bar = 17 mm.

b) *Platform environment*: Bioturbated mudstone with typically >90% carbonate content. Black tubular shapes indicate burrowing activity, with organic(?) lining. Large-amplitude stylolites are also present. 2-15-38-24W4, 6169 ft. Scale = dime coin (17 mm).

c) *Upper Slope environment*: Bioturbated wackestone with rare preservation of lamination and no visible fauna. Poorly developed nodules are also present (N). Carbonate content ranges between 70-90%. 11-25-39-22W4, 5534. Scale = dime coin (17 mm).

d) *Lower Slope environment*: Interbedded/banded mudstone within a dysaerobic environment, preserving organic-rich laminated layers (O). Carbonate content ranges between 50-70%. At the base of the picture there is a bioturbated hard/firmground surface. 3-15-41-22W4, 5624 ft. Scale = dime coin (17 mm).

e) *Basin environment*: Laminated mudstone with up to 50% carbonate content within a dysaerobic/anaerobic environment. 16-36-41-23W4, 1723.8 m. Scale = dime coin 177 mm).

Figure 5.4: Typical facies of the Ireton aquitard.

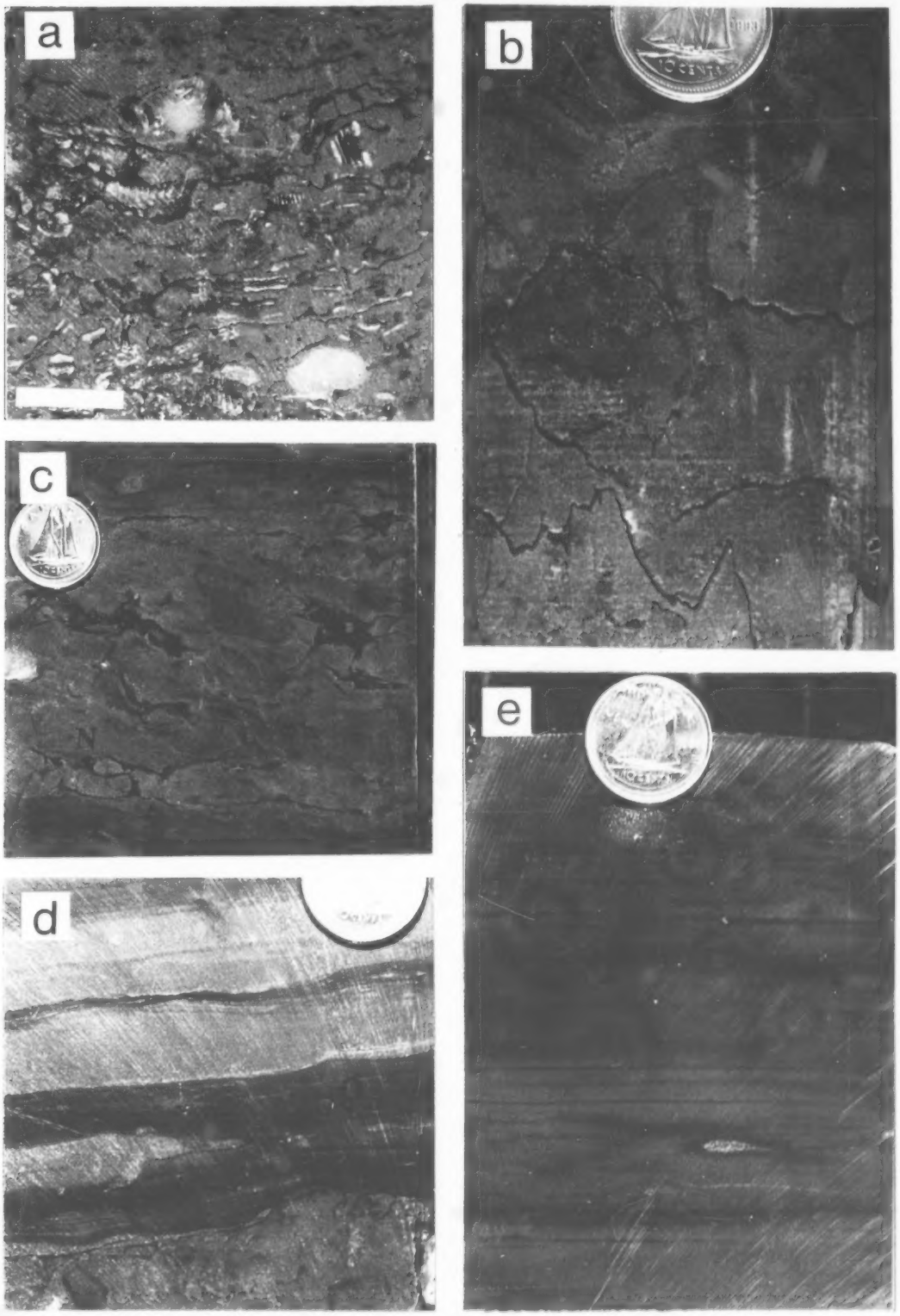

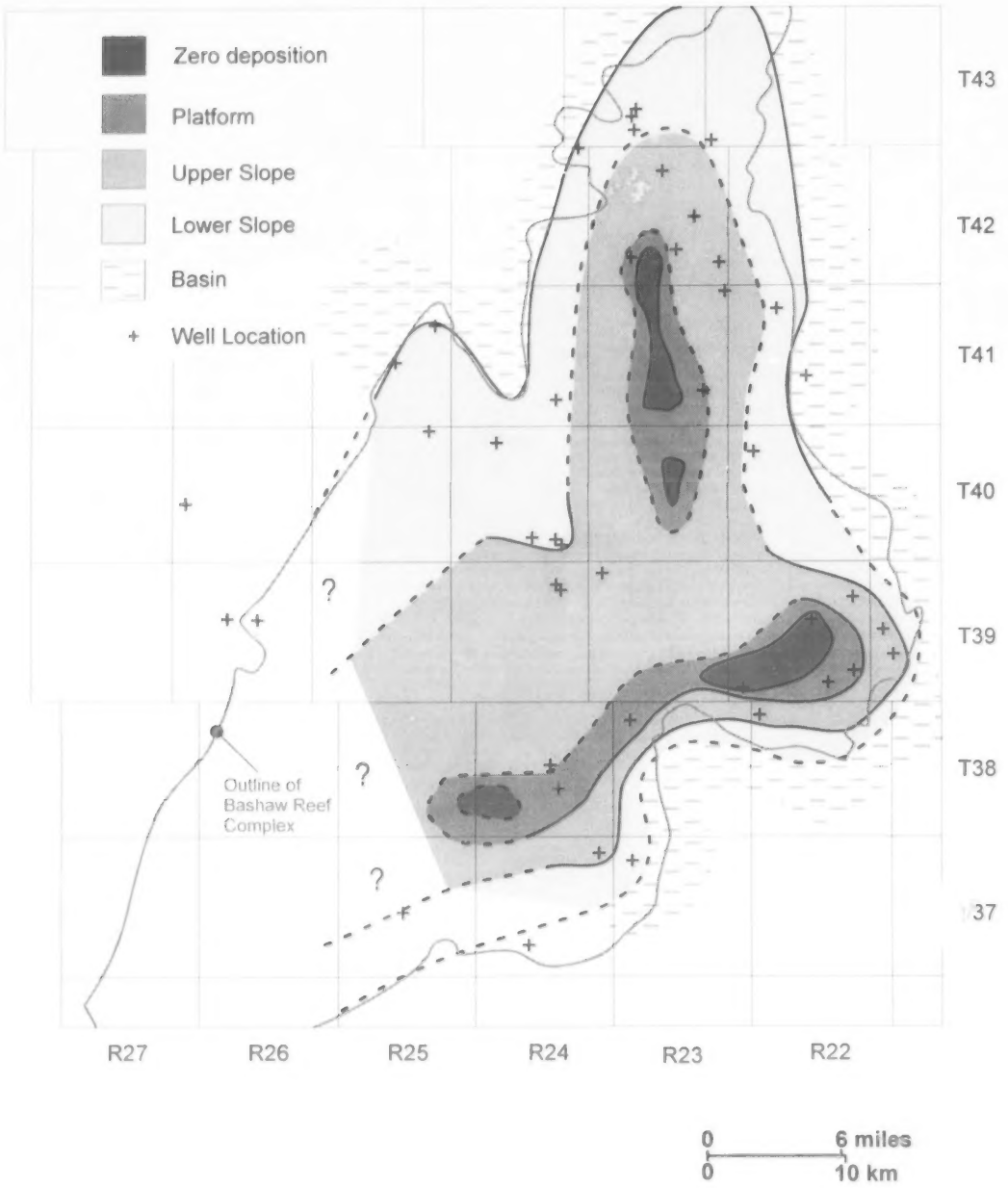

Figure 5.5: Distribution map of the Ireton aquitard environments over the Bashaw Reef Complex. Some environments have been inferred (dashed lines) in areas of no/limited data, based on a trend of increasing depositional water depth with increasing Ireton aquitard thickness. Areas of zero deposition were taken from Rostron (1995), who used well log data to contour the Ireton aquitard thickness/distribution.

thickness of Ireton aquitard being deposited in the down-slope environments (compare Figure 5.5 with Figure 5.1).

5.1.3. Discussion

Over the Bashaw Reef Complex, an increase in Ireton aquitard thickness correlates with a general decrease in the carbonate content and a progression from platform to basinal environments. These features can be directly linked to the underlying topography of the Leduc Formation. Topographic highs of the Leduc Formation (Figure 2.6) coincide spatially with thins of the Ireton aquitard, high carbonate percentages, and platform-related facies. Over the reefal highs, water energies were likely too turbulent for steady clay sedimentation, therefore, carbonate accretion continued in these areas and thin platform facies developed at the peripheries. Water depth and ocean turbulence were the principal controls on clay/silt deposition and the types of facies that were deposited across the reef complex.

The relatively high carbonate content of the Ireton aquitard across the reef complex is substantially higher than the carbonate content of the Ireton Formation clinoforms in the basin (Campbell and Oliver, 1968, p.62). This is probably in part due to the local sourcing of detrital carbonate from those parts of the reef complex that continued to accrete (*e.g.*, in the Haynes and Nevis areas) while other areas of the reef complex were "drowned" and draped by the Ireton aquitard. The present-day carbonate content of the Ireton aquitard, however, may also have increased through diagenetic processes such as early(?) and late calcite cementation and replacement dolomitization.

The Ireton aquitard over the reef complex was probably deposited during a number of incremental (or gradual) rise(s) in sea level, with the backstepping of reef growth (see Section 2.4) and the onlapping of Ireton aquitard onto the reef complex, in what appears to be an overall transgressive event (Figure 5.6). The rise(s) in sea level likely resulted in fewer shallow-water locales for carbonate-accreting organisms to exist on the reef complex and eventually "drowned" the reef complex.

5.2 Petrologic and Petrophysical Data.

The close spatial relationship that exists between the Leduc Formation (D-3) pools

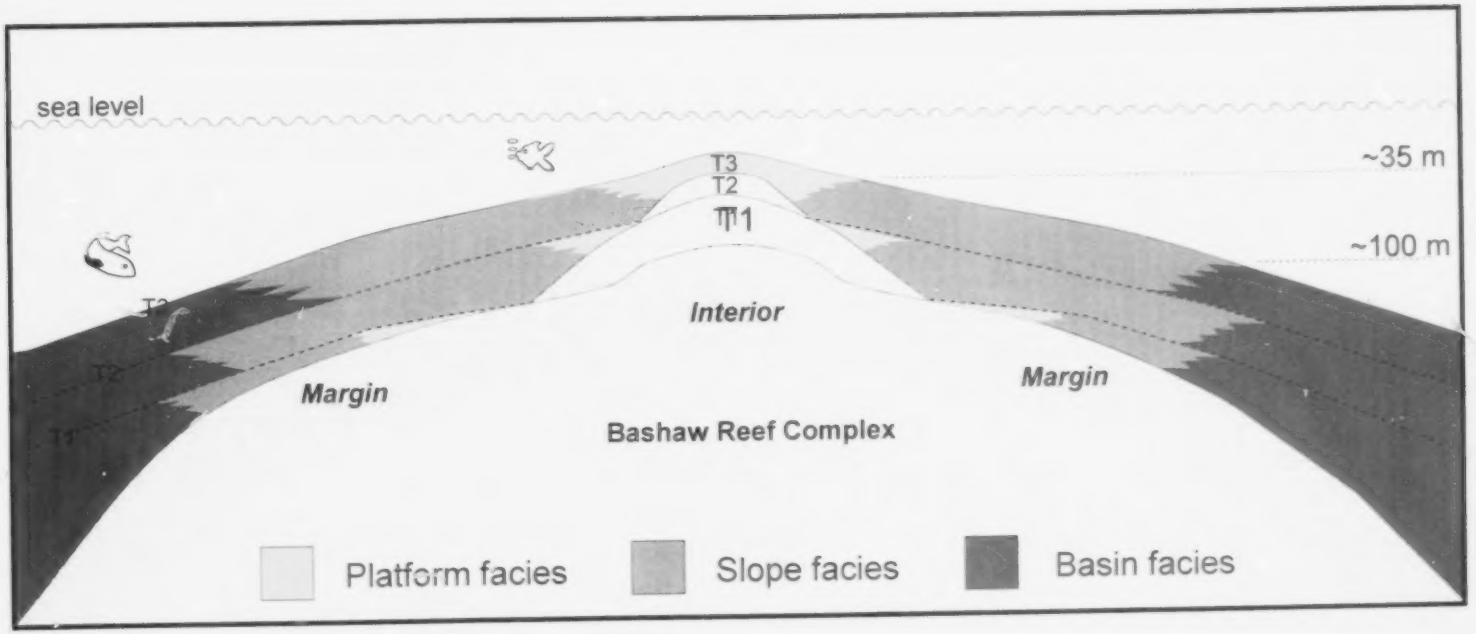

Figure 5.6: A schematic of Ireton aquitard deposition over the Bashaw Reef Complex. T1 to T3 represent imaginary timelines of an overall backstepping/transgressive style of sedimentation. Each incremental rise in sea level (or gradual rise) saw a reduction in the area of reef growth, and eventually the reef complex was "capped" by Ireton aquitard by the time of T3.

and Nisku Formation (D-2) pools has led to speculation that the Ireton aquitard provides an ineffective seal to hydrocarbon entrapment (GSC, 1988; SCG, 1989; Creaney and Allan, 1990; Rostron, 1995). Hydraulic communication between the reservoirs is suggested to have occurred either in areas where the Ireton aquitard is absent, through fractures, or where the Ireton aquitard drape is particularly thin. Speculation as to where breaching occurs is based on hydrogeologic data and Ireton aquitard isopach maps. These indirect lines of evidence, however, are unable to determine how, or indeed if, hydrocarbons actually breached the Ireton aquitard in the Bashaw area. It therefore becomes necessary to look at cores of the Ireton aquitard in order to discern physical evidence of breaching.

5.2.1. Hand sample and thin section analysis

The first approach to identifying physical evidence of breaching locales is to examine hand samples of the Ireton aquitard core and look for visible evidence of oil migration, *i.e.*, oil/bitumen lined fractures or pores. However, only in one well (well 14-2-39-22W4), in the Nevis "Devonian" gas field, was a continuous network of oil/bitumen stained fractures observed in the Ireton aquitard (Figure 5.7a). Thin section analysis was therefore required to observe, on a finer scale, the possible presence of oil within the Ireton aquitard using transmitted-light and fluorescence microscopy. Thin section analysis confirmed the presence of oil/bitumen and the type of pore system that facilitated migration, *i.e.*, a combination of fracture, intercrystalline, and moldic porosity (Table 5.2; *e.g.*, Figure 5.7).

Two factors should be considered, however, before concluding that the residue within a particular thin section is migrated oil. These are:

1) the apparent oil/bitumen in thin section could in fact be detrital organic matter or a residue associated with stylolite formation; and

2) the Ireton aquitard could be a potential source-rock generating its own oil/bitumen residue seen in the thin section (evaluated using Rock-Eval Pyrolysis).

Detrital organic matter and stylolitic residues generally can be distinguished from oil/bitumen by transmitted-light microscopy based on the fact that these residues are not

FIGURE 5.7: Recognition of hydrocarbon breaches in the Ireton aquitard.

a) Hand sample evidence of an oil breach through the Ireton aquitard in well 14-2-39-22W4 (5392 ft) from the Nevis "Devonian" gas pool. Hair-line fractures transmitted oil through this tight mudstone, fanning out into intercrystalline porosity (Ic) (near bottom). Later-on this area seems to have been diagenetically resealed (see 5.7c). Scale = dime coin (17 mm).

b) Intercrystalline porosity within the Ireton aquitard (16-2-40-24W4, 1917.5 m) that is fully occluded by oil/bitumen (O), and distinct from that of the adjacent stylolite (St) in the (thin section enlarged?) fracture. Plane polarized light. Scale = 40 μm.

c) Fluorescence photograph of an Ireton aquitard fracture with oil stain that fluoresces yellow/orange (centre of picture). The light-blue fluorescence also visible in the fracture is extraneous fluorescence from the thin section mounting medium, thus in general, making identification of oil/bitumen stain difficult. 08-31-30-23W4, 1800 m. Scale bar = 40 μm.

d) Fluorescence photograph of bitumen (B) within an Ireton aquitard fracture network of the sample shown in Figure 5.7a (14-2-39-22W4, 5391 ft). The fracture network (Fr) is filled with non-fluorescent calcite (C). Oil entered along the fracture network after calcite cementation, but subsequently the calcite has diagenetically re-sealed the fracture (no porosity is visible along the fracture). The oil is now present as solid bitumen, as revealed by the rather irregular cracks seen in the centre of the "droplet" (unusual of liquid oil). Scale bar = 80 μm.

Figure 5.7: Recognition of hydrocarbon breaches in the Ireton aquitard.

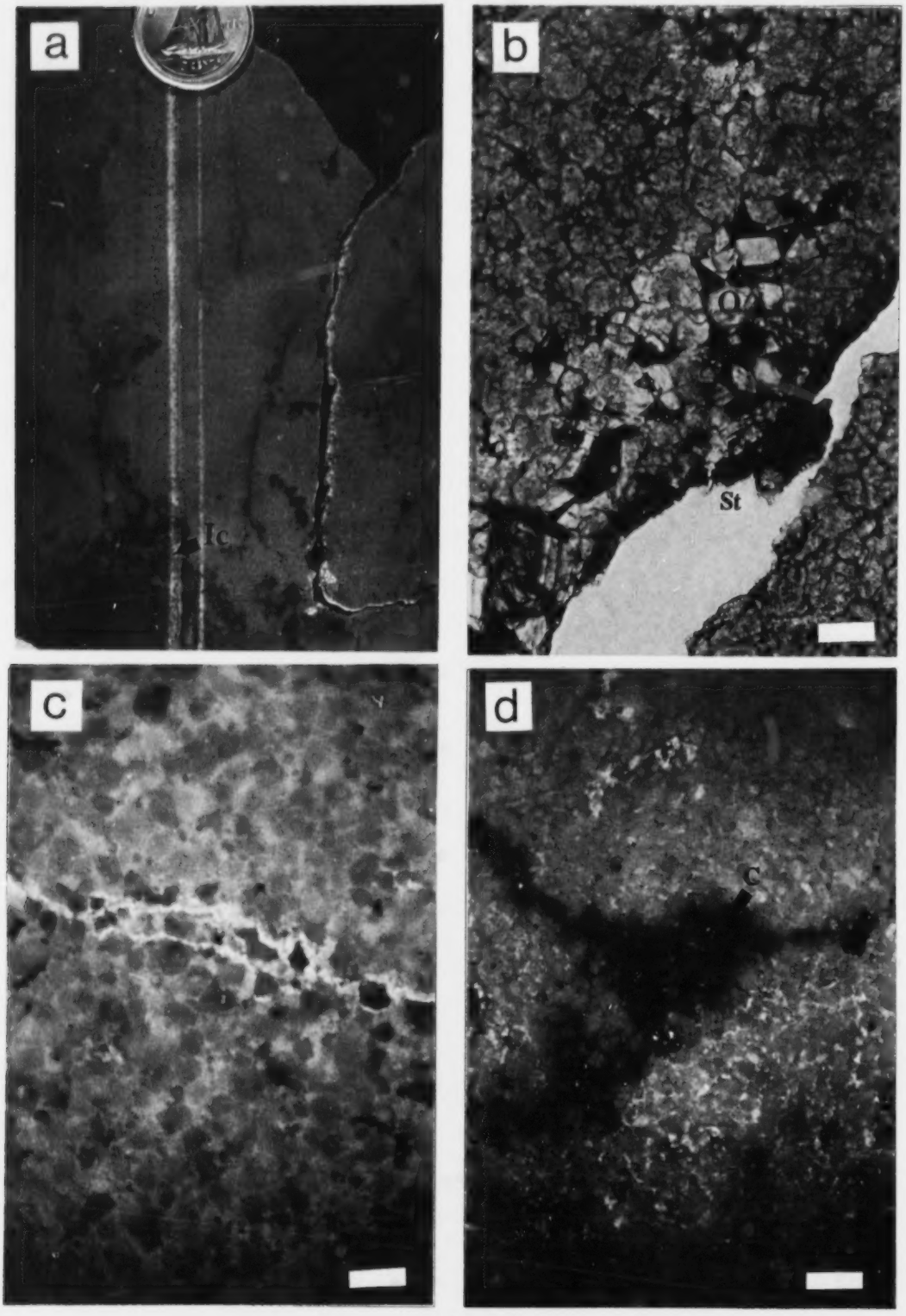

Location	Depth	Oil Y/N	Oil Stain in		
			Fracs	Ic	Mo
6-36-37-24W4	1835 m	Y	Y	Y	Y
8-31-38-23W4	1800 m	Y	Y	Y	N
2-15-38-24W4	6168 ft	Y	N	Y	N
14-2-39-22W4	5391 ft	Y	Y	Y	N
10-31-39-23W4	5991 ft	Y	Y	Y	N
16-2-40-24W4	1917.5 m	Y	Y	Y	N
16-2-40-24W4	1925.3 m	Y	Y	Y	N
12-10-43-23W4	1673.5 m	Y	N	Y	Y
16-16-37-25W4	6790 ft	N	N	N	N
16-16-37-25W4	6808 ft	N	N	N	N
6-31-38-22W4	5589 ft	N	N	N	N
6-22-38-24W4	6168 ft	N	N	N	N
6-22-38-24W4	6173 ft	N	N	N	N
16-26-39-24W4	1848.4 m	N	N	N	N
16-26-39-24W4	1856.5 m	N	N	N	N
2-35-39-24W4	1837 m	N	N	N	N
2-35-39-24W4	1842.9 m	Y	N	Y	N
10-22-39-26W4	2112 m	Y	N	Y	N
13-29-40-22W4	5506 ft	Y	Y	Y	N
2-10-40-24W4	6196 ft	N	N	N	N
5-33-40-24W4	1836 m	N	N	N	N
13-36-40-25W4	6236 ft	N	N	N	N
10-18-40-26W4	6842 ft	N	N	N	N
3-15-41-22W4	5634 ft	N	N	N	N
3-15-41-22W4	5758 ft	N	N	N	N
4-33-41-22W4	5726 ft	N	N	N	N
16-36-41-23W4	1726 m	N	N	N	N
6-25-41-25W4	6273 ft	N	N	N	N
6-25-41-25W4	6305 ft	Y	N	Y	N
2-12-42-23W4	5660 ft	N	N	N	N
12-3-43-23W4	5635 ft	N	Y	Y	N
11-9-44-24W4	5800 ft	N	N	N	N

Table 5.2: Thin section data on the presence or absence of oil/bitumen.

commonly associated with a pore system (Figure 5.7b). The use of fluorescence microscopy also, on occasion, provided a relatively effective method of identifying oil/bitumen in thin section, as oil/bitumen has the property to fluoresce light-blue/green/orange under blue-light excitation (450 nm; van Gijzel, 1981) (Figure 5.7c). However, oil/bitumen was mostly found to be non-fluorescent, or fluorescence was hindered by extraneous fluorescence (*e.g.*, from the fluorescence of the thin-section mounting medium (Figure 5.7c).

5.2.2. Rock-Eval Pyrolysis

The possibility that the Ireton aquitard in the Bashaw area was itself a source of oil was evaluated using Rock-Eval Pyrolysis. Samples of the organic-rich, banded, fine and coarse crystalline dolostones of the lower Nisku Formation (Figure 2.4b) were also analyzed to determine their source rock potential for the hydrocarbons trapped in the Camrose Member/Nisku Formation reservoirs. Twenty-four samples were analyzed providing data on the quantity and type of organic matter, and the level of organic maturity (see Appendix I for an explanation of the procedure and pyrolysis terminology). However, considerable culling of the data was required based on a set of empirical rules explained in Appendix I (Peters, 1986). Organic matter type and organic maturity parameters could only be determined on some samples with >0.5 wt.% total organic carbon (TOC) content, whereas all samples with <0.5 wt.% TOC were culled (Table 5.3). The pyrolysis parameters used were: maturity indicators, T_{max} (highest temperature required for the breakdown of kerogen in the rock sample) and Production Index (PI) (amount of kerogen converted to hydrocarbon, assuming no migrated oils are present); TOC content; and organic matter type indicators, Hydrogen Index (HI) and Oxygen Index (OI) (*i.e.*, kerogen types I, II, and III).

TOC analyses (accurate for all 24 samples; Table 5.3), indicate that the Ireton aquitard samples typically have a very low TOC content of <0.25 wt.%, lower than any recognized carbonate source rock, and are therefore considered unlikely to have generated migratable hydrocarbons (*cf.*, Gardner and Bray, 1984). The lower Nisku Formation samples, however, have TOC values up to 1.6 wt.% (Table 5.3), well above the norm for carbonate source rocks. World-wide values of TOC content for carbonate source rocks

LOCATION	DEPTH	FORMATION	Tmax	S1	S2	S3	PI	S2/S3	PC	TOC	HI	OI
> 0.5% TOC												
4-17-39-21W4	5520ft	I.Nisku	409.5	1.225	2.34	0.79	0.345	2.96	0.29	0.765	305.5	103
4-17-39-21W4	5523ft	I.Nisku	420	0.905	2.635	0.85	0.255	3.095	0.29	1.125	233.5	75
6-12-39-22W4	5427ft	I.Nisku	407	3.805	4.675	0.485	0.45	9.645	0.705	1.415	330	34
13-29-40-22W4	5474ft	I.Nisku	411	0.975	5.365	0.525	0.15	10.215	0.525	1.575	340.5	32.5
13-29-40-22W4	5478ft	I.Nisku	411	1.08	5.41	0.405	0.17	13.36	0.535	1.455	371.5	27.5
16-36-41-23W4	1722.7m	I.Nisku	429.5	1.08	5.235	0.685	0.17	7.64	0.52	1.47	356	46
< 0.5% TOC												
2-15-38-24W4	6134ft	I.Nisku	347.5	0.025	0.025	0.545	0.5	0.04	0	0	0	0
2-15-38-24W4	6168ft	Ireton aq.	435.5	0.07	0.035	0.32	0.7	0.105	0	0.025	150	1341.5
6-22-38-24W4	6173ft	Ireton aq.	412.5	0.18	0.115	0.615	0.635	0.185	0.02	0.056	205	1126.5
4-17-39-21W4	5530ft	I.Nisku	407	0.81	1.09	0.46	0.43	2.37	0.15	0.25	436	184
14-2-39-22W4	5391ft	Ireton aq.	389.5	0.075	0.075	0.14	0.505	0.545	0.01	0.03	250	466.5
6-12-39-22W4	5435ft	I.Nisku	411	0.445	1.2	0.47	0.27	2.55	0.135	0.41	292	114.5
16-26-39-24W4	1848.4m	Ireton aq.	515.5	0.23	0.29	0.405	0.45	0.715	0.04	0.13	223	311.5
16-26-39-24W4	1844m	Camrose	196.5	0.02	0.01	0.335	0.75	0.03	0	0.01	100	3350
16-2-40-24W4	1917.5m	Ireton aq.	410.5	0.16	0.13	0.235	0.59	0.54	0.02	0.13	97	180.5
5-33-40-24w4	1823m	I.Nisku	437	0.085	0.105	0.58	0.445	0.18	0.01	0.065	160.5	898.5
5-33-40-24W4	1836m	Ireton aq.	487	0.075	0.185	0.285	0.295	0.64	0.015	0.1	185	285
10-18-40-26W4	6827ft	I.Nisku	434.5	0.565	0.725	0.61	0.44	1.185	0.1	0.34	213	179
3-15-41-22W4	5542ft	u.Nisku	417.5	0.05	0.165	0.52	0.24	0.315	0.01	0.03	550	1733
3-15-41-22W4	5547ft	Ireton aq.	412	0.29	1.255	0.695	0.19	1.8	0.125	0.52	240.5	133.5
3-15-41-22W4	5758ft	Ireton aq.	411.5	0.16	0.45	0.21	0.265	2.14	0.05	0.145	310	145
16-36-41-23W4	1726m	Ireton aq.	417	0.14	0.39	0.435	0.275	0.89	0.04	0.15	257.5	290.5
6-25-41-25W4	6273ft	Ireton aq.	435	0.17	0.175	0.305	0.5	0.57	0.025	0.185	94	164.5
2-12-42-23W4	5660ft	Ireton aq.	353	0.075	0.055	0.395	0.6	0.135	0.005	0.065	82	611.5

Table 5.3: Mean results of the Rock Eval Pyrolysis data, with two to three analyses per sample. Data-set has been culled to just six samples that have >0.5% TOC content, some of which have usable maturity parameters -- shaded numbers (see Appendix I for discussion of culling procedure and Rock Eval parameters).

average at 0.6 wt.%, compared to shale source rocks at about 2 wt.% (Tissot and Welte, 1984). Unfortunately, oils may have migrated into the samples and raised some of the TOC values. However, thin section analysis revealed that most the lower Nisku Formation samples indeed have a relatively high kerogen content.

The Ireton aquitard could not be categorized in terms of organic matter type and organic maturity parameters because of its low TOC content. However, a number of the lower Nisku Formation samples could be evaluated. T_{max} maturity data of three unculled lower Nisku Formation samples (Table 5.3) indicate that, at temperatures of 411 to 429.5°C, these samples are beneath that of the oil generation window (435 - 470°C; Hunt, 1995). The unculled PI values, a rougher estimate of maturity, also indicate that the samples are of low maturity (<0.2) (Table 5.3; see Appendix I). The type of kerogen (I, II, or III) in the sample, however, also affects its maturity. A cross plot of HI versus OI of those unculled lower Nisku Formation samples (Figure 5.8) indicate that these samples contain kerogen types I or II. Kerogen types I and II are principally comprised of marine organic matter, are the most oil-prone kerogens, and require a slightly lower T_{max} to generate hydrocarbons, possibly suggesting that the lower Nisku Formation samples could be more borderline in maturity than T_{max} or PI values would otherwise indicate.

In summary, it appears that the Ireton aquitard was unlikely to have generated migratable hydrocarbons that could hinder the detection of Duvernay-sourced hydrocarbons that migrated through the Ireton aquitard. The lower Nisku Formation samples also probably did not produce hydrocarbons in areas overlying the Bashaw Reef Complex, although they do border the oil generation window. However, this facies may extend further into the "Moat" area to the east of the reef complex and perhaps off-platform toward the northwest (Figure 4.2) and may be buried to a temperature and depth capable of generating hydrocarbons. Oil generated within that area of the "Moat" could have subsequently migrated into the Camrose Member/Nisku Formation pools, if a migration pathway was available. A mixed-oil signature reported by T.Cadrin (pers. comm.) in the oils of the off-platform, D-2 Bashaw pools (Figure 4.2), may be an indication of such a process. Oil in the Nisku Formation in the Stettler and Drumheller areas (Figure 1.1) are also suspected to have been derived from evaporite-associated sediments in the Nisku Formation (Creaney *et al.*, 1994). Further work is required to evaluate the source rock

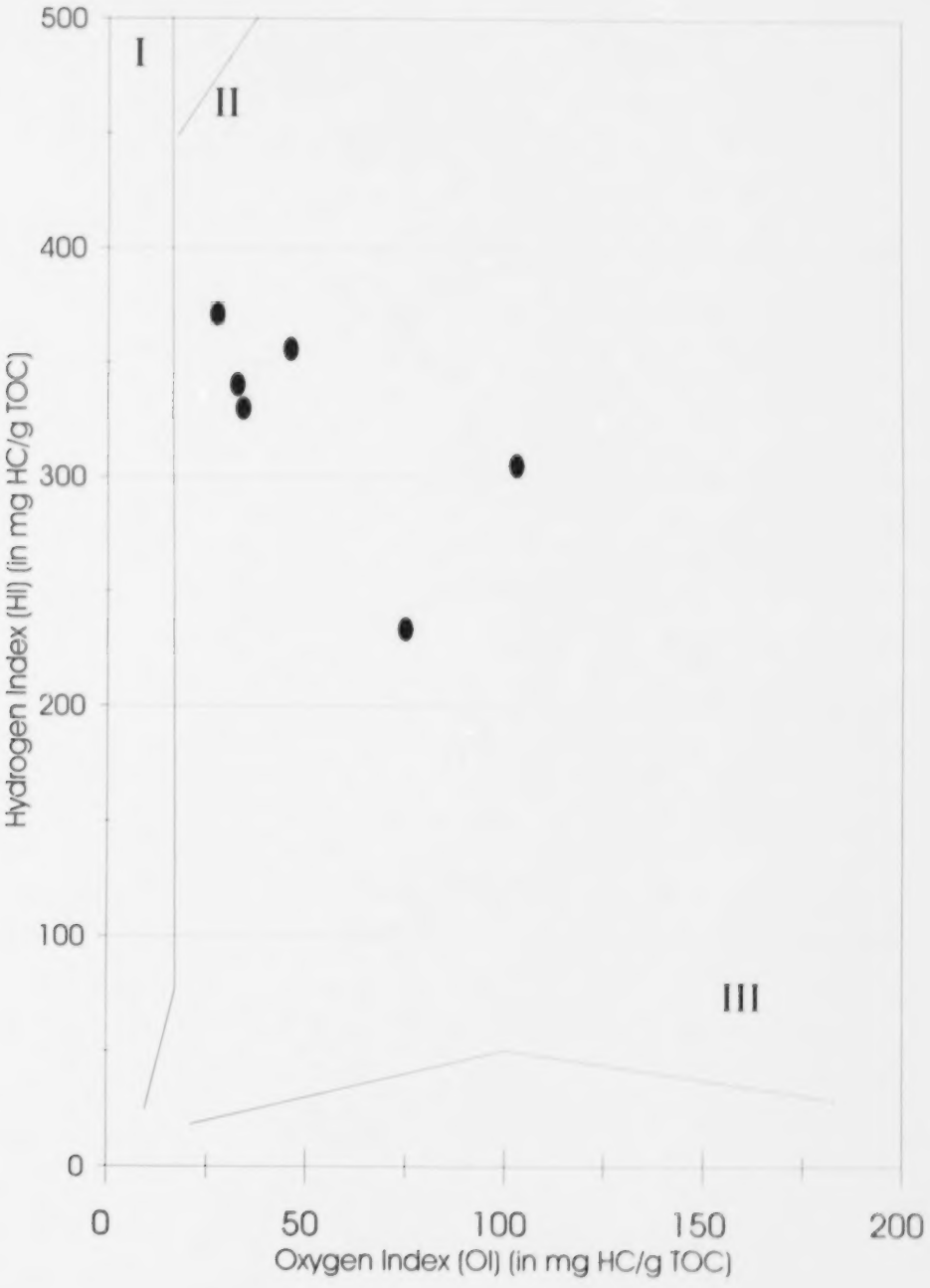

Figure 5.8: A pseudo-Van Krevelen diagram to determine the Kerogen type (I, II, or III) of the organic-rich Lower Nisku Fm. samples. Only samples with >0.5 wt.% TOC content were used (see Appendix I).

potential and extent of this lower Nisku Formation facies and its possible influence on hydrocarbon entrapment in the Bashaw area.

5.2.3. Mercury injection capillary pressure measurement (MICPM) data

Another method used in the investigation of Ireton aquitard breaches was that of MICPM. This procedure provided data on porosity, pore throat radii, pore volume accessible by mercury, and the approximate entry pressures required for mercury invasion. Initial mercury invasion was estimated from MICPM curves *(e.g.*, Figure 5.9; Appendix II) and was used as an approximation of the breaching potential of the plug. A discussion of the MICPM method is presented in Appendix I.

The MICPM data (Table 5.4) reveal a number of trends that are related to the depositional profile from platform to basinal facies. Porosities, in general, decrease toward the basin from a maximum of 4.2% in the platform facies (plug 2) to 1.2% in the basinal facies (plug 9). This corresponds with a decrease in carbonate content and a change in dolomite type from T3 to T2 (Figure 5.4). Pore throat radii also decrease down the depositional profile, with Plugs 1 and 3 of the platform facies having the highest pore throat radii at about 2 - 3 μm. The total percentage of pore volume invaded by mercury for each sample (Table 5.4) also indicates that a very low percentage of pore space was invaded by mercury in samples with initial entry pressures higher than 20,000 psi, as would be expected. However, below 20,000 psi there appears to be no trend.

Calculations of breaching potential.

Using the estimates of initial entry pressure for that of breaching pressure (Table 5.4), calculations can be made of the hydrocarbon column height sustainable by these samples. The values for the initial entry pressure, however, are likely to be the lowest estimate of the actual breaching pressure of the samples, but provide a useful starting point for interpretations (see Appendix I, for discussion). An equation to determine the maximum hydrocarbon column height sustainable down to the oil/water contact (h_o), when the hydrocarbon breaching pressure (displacement pressure of the aquitard (P_{dB})) is known, is (Eq.1; Smith, 1966):

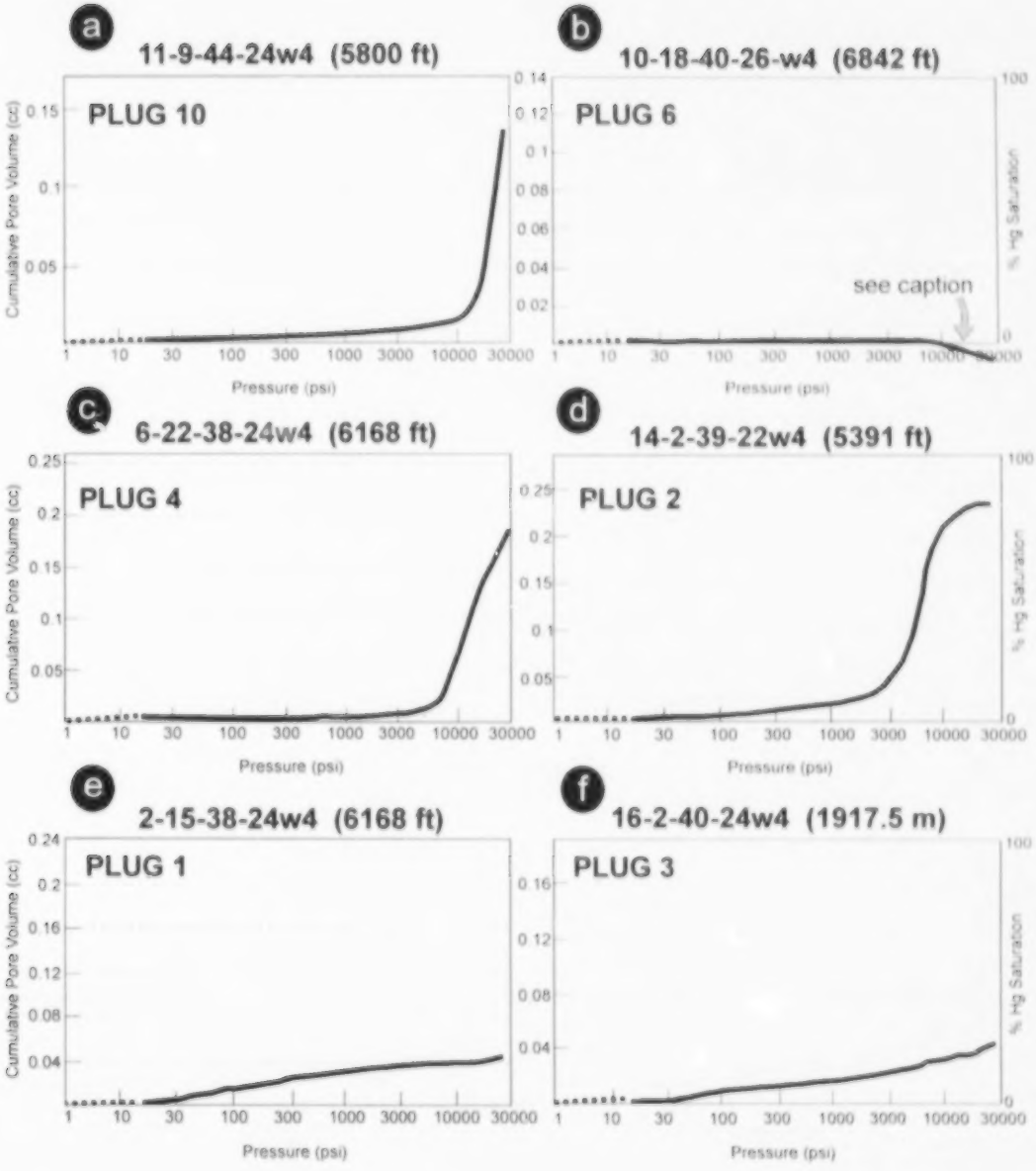

Figure 5.9: Examples of Ireton aquitard MICPM curves. (a) - (d) require very high entry pressures and act as effective "seals", whereas (e) and (f) are potentially leakage sites, with low initial entry pressures. The drop in the curve of (b) is a thermal effect of the mercury at high pressures causing the mercury to expand.

Plug #	Location	Depth	Aquitard Facies	Replacement Dolomite Type	Carbonate Content (%)	Migrated Oil?	MICPM DATA			
							Porosity (%)	% Pore Volume invaded by Hg	Pore Throat Radii (microns)	Initial Entry Pressure (psi)
1	2-15-38-24W4	6168ft	Platform	2 and 3	88	Y	3.2	16	upto .2	40 - 100
2	14-2-39-22W4	5391ft	Platform	3	93	Y	4.2	80	0.07 - 0.1	200 -1000
3	16-2-40-24W4	1918m	Upper slope	3	95	Y	3.0	21	upto .3	40 - 100
4	6-22-38-24W4	6168ft	Upper slope	3	76	N	3.6	68	0.007-0.03	7000
5	6-22-38-24W4	6172ft	Upper/Lower	2	5	N	2.8	38	upto .0.01	10000
6	10-18-40-26W4	6942ft	Upper slope	2	80	N	2.1	0	Tiny	>30000
7	5-33-40-24W4	1836m	Lower slope	2	63	N	1.7	0	Tiny	>30000
8	12-3-43-23W4	5635ft	Lower slope	2	52	N	2.3	5	0.004 - 0.006	20000
9	3-15-41-22W4	5758ft	Basin	2	36	N	1.2	-	Tiny	>30000
10	11-9-44-24W4	5800ft	Basin	2	58	N	2.7	81	upto .0.01	15000

Table 5.4: MICPM data combined with other relevant data.

$$h_o = \frac{P_{dB}}{(\rho_w - \rho_h)g} \qquad \text{- Eq. 1}$$

where ρ_w and ρ_h are the densities of the water (~1 gcm^{-3}), and the hydrocarbons in the reservoir (oil = ~0.7 gcm^{-3} and gas = ~0 gcm^{-3}), respectively, and g equals acceleration due to gravity. This equation can be converted to "field units" by introducing a constant, whereby:

$$h_o = \frac{P_{dB}}{(\rho_w - \rho_h)0.433} \qquad \text{- Eq. 2}$$

The constant 0.433 incorporates acceleration due to gravity, and provides the expression of breaching pressure in psi, densities in gcm^{-3}, and h_o in feet. However, before Equation 2 can be used, mercury entry pressures must be converted to a hydrocarbon breaching pressures (P_{dB}). Entry pressures are dependant on the surface tension of the invading medium with that of the pore medium being displaced, and the contact angle between the two fluids (wettability), according to Equation 3 (Purcell, 1949):

$$\frac{Pc_{Hg/a}}{Pc_{Hc/w}} = \frac{-(\delta_{Hg/a})(\cos\theta_{Hg/a})}{(\delta_{Hc/w})(\cos\theta_{Hc/w})} \qquad \text{- Eq. 3}$$

where: $\delta_{Hg/a}$ = 480 dynes cm^{-1}, surface tension of Hg/air

$\delta_{Hc/w}$ = ~32 (oil), ~70 dynes cm^{-1} (gas), surface tension of hydrocarbon/water

$\theta_{Hg/a}$ = 140°, contact angle of Hg/air

$\theta_{Hc/w}$ = 0°, contact angle of hydrocarbon with water

Application of Equation 3, for an average oil and gas, results in a value for $Pc_{Hg/a}$ $/Pc_{Hc/a}$ of 11.5 for oil and 5.25 for gas. Therefore, mercury entry pressure (as taken from MICPM curves) are simply divided by this gas or oil value to provide a value for P_{dB}.

The h_o value for each plug was calculated and a number of results shown in Table 5.5. Only Plugs 1, 2, and 3 had sufficiently low entry pressures to be considered breachable, the rest provide effective "seals". Plug 1 (2-15-38-24W4) is from the Haynes area, where no hydrocarbon production occurs from the Leduc Formation interval in this well. Estimates of h_o suggest that between 5.5 m of gas (40 psi Hg) to 20.4 m of oil (100 psi Hg) are sustainable by this plug. Thin sections reveal, however, that this well was breached by oil and, as no hydrocarbon column exists in the area of this well, may indicate that either the estimates of entry pressure are too high or that diagenetic resealing

PLUG	Hg Entry Pressure (psi)	Oil/Gas Entry Pressure (psi)	h_o (feet)	h_o (metres)	Pool Column Height (in metres)
1	40	3.5 (oil)	27	8	0 (Haynes)
	100	8.7 (oil)	67	20.4	
	40	7.6 (gas)	18	5.5	0 (Haynes)
	100	19 (gas)	44	13.4	
2	200	38 (gas)	88	27	41 (Nevis)
	1000	190 (gas)	439	134	
3	40	3.5 (oil)	27	8	27 (Clive)
	100	8.7 (oil)	67	20.4	
	40	7.6 (gas)	18	5.5	27 (Clive)
	100	19 (gas)	44	13.4	
4	7,000	608 (oil)	4680	1426	0 (Haynes)
	7,000	1333 (gas)	3079	938	0 (Haynes)

Table 5.5: Hydrocarbon column heights (h_o) required to breach Plugs 1 to 4. In some cases there are ranges given for the initial mercury entry pressure values of each plug (see Appendix I) — there is also the assumption that initial entry pressures can breach the plug). Most plugs are evaluated for both a 100% gas or 100% oil column, except for Plug 2 from the Nevis "Devonian" gas pool (Figure 4.1).

has occurred subsequent to breaching. It may also be a result of the fact that breaching calculations are based on a hydrostatic system and that a hydrodynamic system exists in this area (Paul, 1994; Rostron, 1995). Incorporating a hydrodynamic system into calculations would likely reduce the hydrocarbon column necessary to breach the Ireton aquitard and thus Plug 1 could indeed be breached at this initial entry pressure value.

Calculations of h_o for Plug 2 (well 14-2-39-22W4) indicate that this well may be breached, requiring a minimum of between 27 to 134 m of gas to breach the seal, where a 41 m gas column is present in the Nevis D-3 horizon today. From thin section analysis the plug indeed reveals evidence of breaching and has fractures that are oil/bitumen-lined. However, the fractures appear to have been diagenetically resealed and enclose the oil/bitumen (Figure 5.7d). Therefore, it seems more likely that higher entry pressures are required to breach the plug and that the plug presently acts as an effective "seal".

The h_o values estimated for Plug 3 (16-2-40-24W4; max. h_o = 20.4 m; Table 5.5) indicate that the present-day hydrocarbon column of 27 m exerts an even greater pressure than 100 psi (Hg equivalent). Yet, the Ireton aquitard of this area is still presently withholding hydrocarbons in the Clive D-3A pool, contrary to the interpretation of the breaching data. It is assumed, therefore, that breaching has occurred or is occurring over a prolonged period of time through a very low permeability cap-rock (of 9 m thickness). The low total percentage of pore volume invaded for this plug (~20%) may also be suggestive of a very tortuous permeability pathway.

5.2.4. Stable isotope analysis

In a recent case study by Huebscher and Machel (1995a), stable isotope signatures (oxygen and carbon) for dolostones of the Grosmont Formation and Leduc Formation reefs of the northern part of the Rimbey-Meadowbrook reef trend were used to indicate that cross formational fluid flow occurred from the Leduc Formation, across a shale break, and into the overlying Grosmont Formation. Above areas of thin shale, it was found that an alteration "halo" of isotopic signatures was present within the Grosmont. This case study therefore suggests the possibility that similar "haloes" of distinct isotopic signature may be preserved around the suspected breaching locales of the Ireton aquitard in the Bashaw area. The stable isotopic signatures of the replacement dolostones for the

study area (Chapter 3) imply that the dolomitizing fluids were reflux brines from the upper Nisku Formation/Wabamun Group that pervasively replaced the underlying lower Nisku, Ireton, and Leduc formations. A faint isotopic trend was observed in the $\delta^{13}C$ signatures of the replacement dolostones of increasingly positive $\delta^{13}C$ values from the Nisku Formation down into the Leduc Formation. This trend appears to be related to a decrease in alteration (by $\delta^{13}C$ depleted fluids) of the precursor limestone with depth during reflux (Figure 3.10). No trend was present in the $\delta^{18}O$ signatures over the relatively short core interval analyzed in this study.

In order to pin-point preferential reflux conduits (breaching locales) through the Ireton aquitard from the Nisku Formation down into the Leduc Formation, the $\delta^{13}C$ values have been plotted on a well by well basis in a cross section (Figure 5.10). Based on the proposed reflux dolomitization of the Bashaw area, it might be expected that a greater alteration of the dolostone $\delta^{13}C$ signatures of the Leduc Formation (towards the negative) would have occurred beneath suspected breaching locales, if the permeability was sufficiently enhanced in these areas. This diagram clearly demonstrates, however, that Ireton aquitard thickness over the reef complex did not impede reflux, as all the wells preserve a faint trend toward positive $\delta^{13}C$ values from the Nisku Formation into the Leduc Formation and were affected to a similar extent by the refluxing brines. One anomaly is that the Ireton aquitard $\delta^{13}C$ values of well 3-15-41-22W4 should, theoretically, have been the least altered from the Late Devonian $\delta^{13}C$ calcite signature of +2 to +3‰ due to the lower porosity of the basinal Ireton aquitard. Instead, the Ireton aquitard $\delta^{13}C$ values are more depleted (between 0 and -1‰) than most of the Leduc Formation dolostones of the other wells, but it may be that these values are simply a result of bacterial sulphate reduction during early (near surface) diagenesis, and unrelated to reflux dolomitization.

In conclusion, isotopic tracing was unable to pinpoint specific breaching locales within the Ireton aquitard. Instead, the Ireton aquitard drape appears to have been permeable across the whole reef complex during dolomitization. Therefore, the Ireton aquitard thickness of <25 m over the reef complex was more permeable to the Late Devonian reflux of dense hypersaline fluids, than to hydrocarbon migration today, and

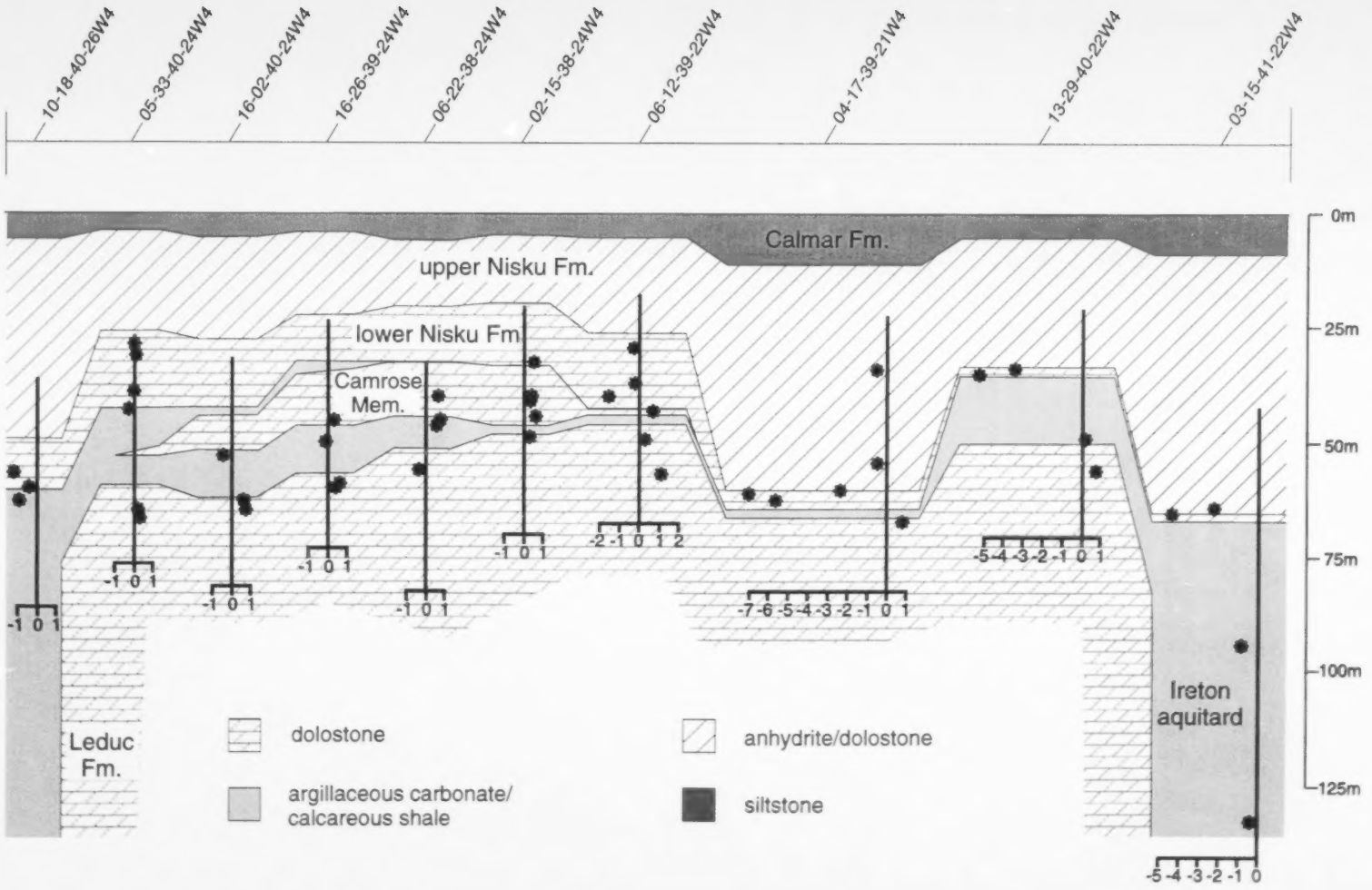

Figure 5.10: A cross section schematic of the $\delta^{13}C$ isotope values for the wells analyzed in the Bashaw area.

probably during oil migration in the Cretaceous/Tertiary.

5.2.5. Magnetic anomalies associated with hydrocarbon seepage

A further technique used to determine hydrocarbon breaching is that of analyzing the magnetic susceptibility in and around breaching locales. The migration of hydrocarbons has been found, in various case studies, to generate and destroy magnetic minerals, thus creating anomalous magnetic signatures, either positive or negative, to that of the background signature prior to hydrocarbon migration (*e.g.*, Machel and Burton, 1991; Machel, 1995). A preliminary analysis was therefore performed (by Dr. M.E. Evans, Department of Physics, University of Alberta) to see if hydrocarbon seepage through the Ireton aquitard resulted in any magnetic anomaly. Ten samples were analyzed for their magnetic susceptibility from suspected breaching and "sealing" areas of the Ireton aquitard (Appendix II). The general methodology behind this procedure is discussed in Collinson (1983).

The results of these preliminary test runs reveal no trend that could be related to oil seepage, although the results of such a small dataset are inconclusive. However, when magnetic susceptibility was plotted versus percentage carbonate content, a linear regression was observed with a 0.91 correlation coefficient (Figure 5.11). This may suggest that with an increase in terrigenous clastic content (lower carbonate content), there is an increase in the (detrital?) magnetic mineral content. If this correlation could be confirmed, magnetic susceptibility would provide a relatively rapid and cheap technique of obtaining estimates of clay/carbonate content of the aquitard.

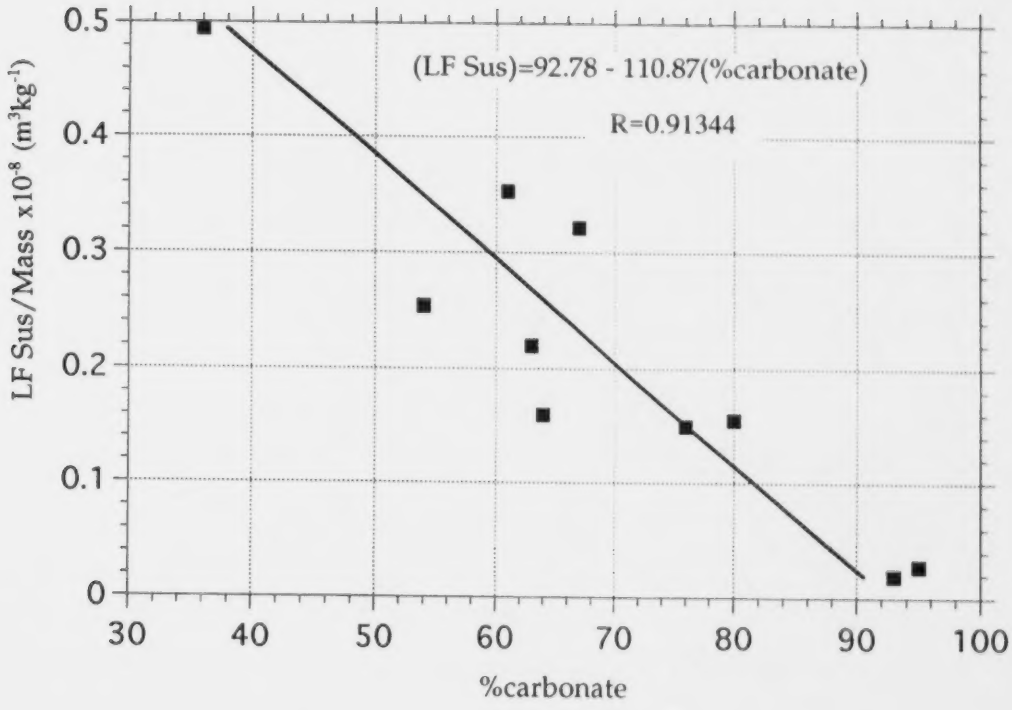

Figure 5.11: Correlation between low-frequency magnetic susceptibility and percentage carbonate content of the Ireton aquitard (see Appendix II for dataset). There is a 0.91 correlation coefficient in the line of best-fit.

CHAPTER 6

SYNTHESIS AND DISCUSSION

This chapter integrates the previous chapters into elucidating where suspected hydrocarbon breaching occurs across the Ireton aquitard, why it may occur, and how suspected breaching locales affect the present-day pool distribution. A discussion will also be presented on the migration and entrapment of hydrocarbons in(to) the study area. Lastly, there will be an assessment of the future hydrocarbon potential of the Bashaw area, as well as the application of this type of study to other parts of the Western Canada Sedimentary Basin (WCSB).

6.1 Determination of Ireton Aquitard Breaching Locales.

The determination of the Ireton aquitard breaches was based on the compiled data-set attained in this study (Table 6.1). Establishing whether and where the Ireton aquitard has been breached requires knowledge of: i) the presence or absence of oil/bitumen stain within the samples; ii) the hydrocarbon self-generation potential of the Ireton aquitard in that area (tested by Rock-Eval); iii) the position of each sample within the aquitard, *i.e.*, whether the sample was close to the upper contact of the aquitard and was within or above the suspected tightest facies within the aquitard (determined approximately from clay content or gamma-ray logs); iv) if a continuous fracture network exists or existed through the aquitard; and v) MICPM data of plug samples.

A flow chart in Figure 6.1 summarizes the general approach to identifying suspected breaching locales. It is worth noting that criteria (i) to (iv) provide enough information to determine breaching by oil. MICPM data, however, provides an additional quantitative assessment of the breaching potential and, furthermore, can indicate if areas with no visible hydrocarbon migration are capable of transmitting hydrocarbons.

6.2 Breaching Characteristics.

Characterization of the breaches in the Ireton aquitard is based on a comparison

	Location	Depth	Dolomite Type	Ireton aquitard Facies	Nisku/Leduc Production	Thickness of aquitard (m)	Position from top of aquitard (m)	% Carbonate of sample	Average % Carb.	Oil Y/N	Oil Stain in			TOC (%)	Initial Entry Pressure (psi)	Overall Leak/Seal
											Fracs	Ic	Mo			
LEAKY?	6-36-37-24W4	1835	T3	Upper Slope	Y/N	4	1.8	95	95	Y	Y	Y	Y			Leak
	16-16-37-25W4	6790	T3	Upper Slope	N/N	9	3	94	82	Y	Y	Y	N			Leak
	16-16-37-25W4	6808	T2	Lower Slope	N/N	9	8.5	78	82	Y	Y	Y	N			Leak
	8-31-38-23W4	1800	T3	Upper/Platform	Y/N	5	2.7	84	84	Y	Y	Y	N			Leak
	2-15-38-24W4	6168	T2/T3	Platform	Y/Y	1	0.3	88	88	Y	Y (c)	Y	N	0.03	30 - 100	Leak
	14-2-39-22W4	5391	T3	Platform	Y/Y	1	0.3	93	96	Y	Y (c)	Y	N	0.03	3000	Leak
	10-31-39-23W4	5991	T3	Platform	Y/N	3	1.8	95	95	Y	Y	Y	N			Leak
	16-2-40-24W4	1917.5	T3	Upper Slope	Y/Y	9	1.8	95	85	Y	Y	Y	N	0.13	30 - 100	Leak
	16-2-40-24W4	1925.3	T3	Upper Slope	Y/Y	9	7.6	77	85	Y	Y	Y	N			Leak
	12-10-43-23W4	1673.5	T3	Upper Slope	N/N	10	4.3	88	70	Y	N	Y	Y			Leak/Lat.?
SEALING?	6-31-38-22W4	5589	T3	Upper Slope	Y/Y	6	1.2	90	90	N	N	N	N			Seal
	6-22-38-24W4	6168	T3	Upper Slope	Y/Y	4	2.4	76	71	N	N	N	N		7000	Seal
	6-22-38-24W4	6173	T3	Upper Slope	Y/Y	4	4	70	71	N	N	N	N	0.05	~10000	Seal
	16-26-39-24W4	1848.4	T3	Upper Slope	Y/Y	10	1.8	64	78	N	N	N	N	0.13		Seal
	16-26-39-24W4	1856.5	T3	Upper Slope	Y/Y	10	9.1	82	78	N	N	N	N			Seal
	2-35-39-24W4	1837	T2	Lower Slope	Y/Y	9	3	53	67	N	N	N	N			Seal
	2-35-39-24W4	1842.9	T3	Upper Slope	Y/Y	9	8.8	95	67	Y	N	Y	N			Seal
	10-22-39-26W4	2112	T3	Upper Slope	Y/Y	46	45.4	59	59	Y	N	Y	N	0.25		Seal
	13-29-40-22W4	5506	T3	Lower Slope	N/Y	10	7.9	83	75	Y	Y	Y	N			Seal/Lat.?
	5-33-40-24W4	1836	T2	Lower Slope	Y/Y	17	1	63	63	N	N	N	N	0.1	>30000	Seal
	13-36-40-25W4	6236	T3	Lower Slope	N/N	18	0.3	80	N/A	N	N	N	N			Seal
	10-18-40-26W4	6842	T2	Upper Slope	N/N	167	1	80	N/A	N	N	N	N		>30000	Seal
	3-15-41-22W4	5634	T2	Basin	N/N	98	25.6	57	48	N	N	N	N			Seal
	3-15-41-22W4	5758	T2	Basin	N/N	98	63.4	36	48	N	N	N	N	0.15	>30000	Seal
	4-33-41-22W4	5726	T2	Lower Slope	N/Y	24	1.2	53	53	N	N	N	N			Seal
	16-36-41-23W4	1726	T2	Upper/Lower	N/Y	5	2.7	54	54	N	N	N	N	0.15		Seal
	6-25-41-25W4	6273	T3	Upper Slope	N/N	~120	10.7	73	76	N	N	N	N	0.19		Seal
	6-25-41-25W4	6305	T2/T3	Lower Slope	N/N	~120	20.4	79	76	Y	N	Y	N			Seal/Lat.?
	2-12-42-23W4	5660	T2	Lower Slope	Y/Y	9	1.2	70	66	N	N	N	N	0.07		Seal
	12-3-43-23W4	5635	T2	Lower Slope	Y/N	4	1.8	52	52	N	Y	Y	N		20000	Seal
	11-9-44-24W4	5800	T2	Basin	N/N	91+	1.2	58	63	N	N	N	N		15000	Seal

Table 6.1: A chart of leaky versus sealing Ireton aquitard cores, and the dataset that led to that interpretation. Lat.?= possible lateral migration, (c) = fairly continuous fracturing through the whole Ireton aquitard core.

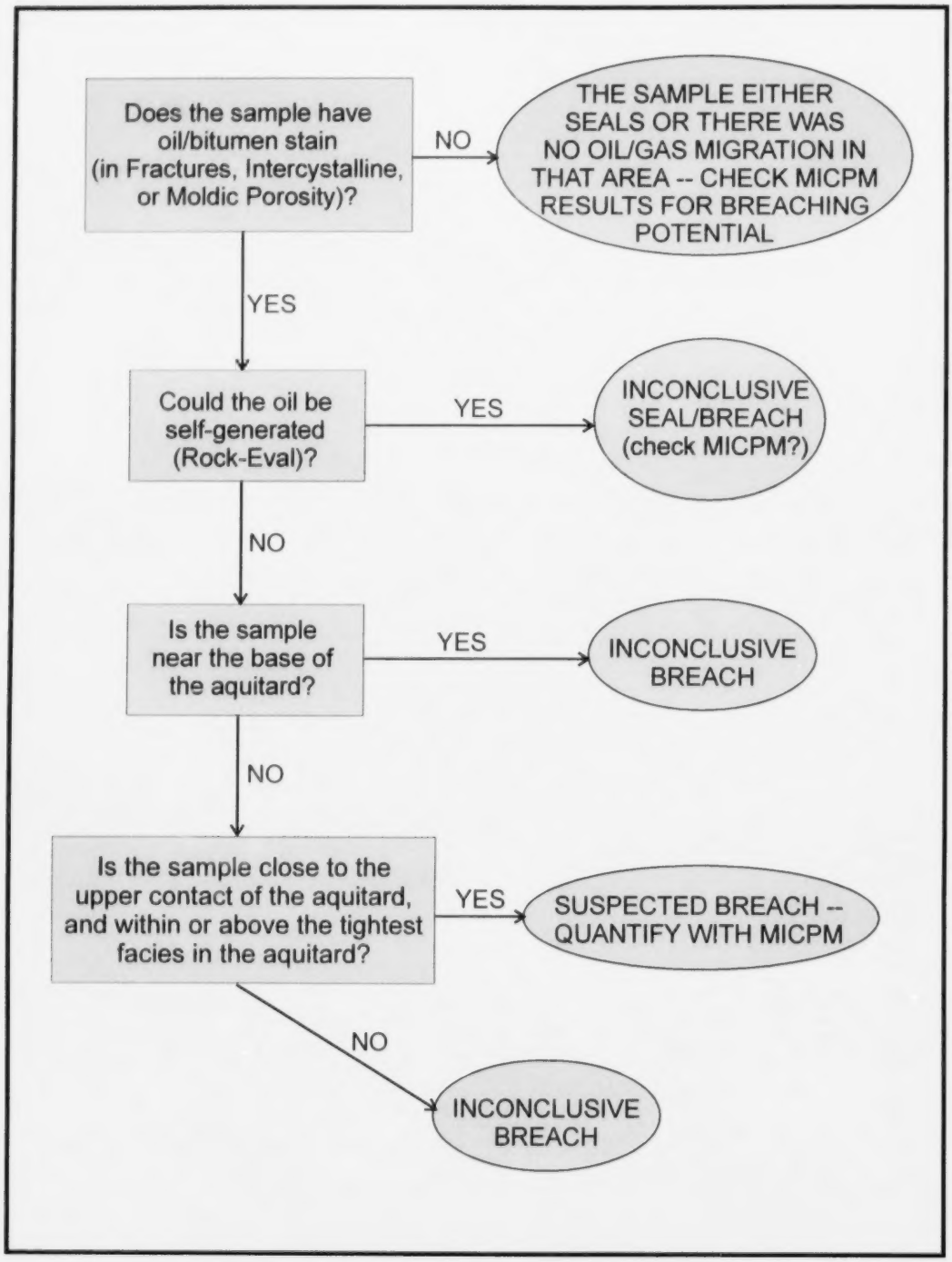
Does the sample have oil/bitumen stain (in Fractures, Intercystalline, or Moldic Porosity)?
NO
THE SAMPLE EITHER SEALS OR THERE WAS NO OIL/GAS MIGRATION IN THAT AREA -- CHECK MICPM RESULTS FOR BREACHING POTENTIAL
YES
Could the oil be self-generated (Rock-Eval)?
YES
INCONCLUSIVE SEAL/BREACH (check MICPM?)
NO
Is the sample near the base of the aquitard?
YES
INCONCLUSIVE BREACH
NO
Is the sample close to the upper contact of the aquitard, and within or above the tightest facies in the aquitard?
YES
SUSPECTED BREACH -- QUANTIFY WITH MICPM
NO
INCONCLUSIVE BREACH

Figure 6.1: A flow chart of the principal factors used in determining if an aquitard acts/acted as a seal and/or is suspected of breaching (see text for further discussion).

of the eight cores in the Bashaw area that are suspected of having been breached by hydrocarbons with those that are suspected "seals" (Table 6.1). Breaching almost invariably occurred where the thin Ireton aquitard cover is <~4 m. However, breaching has also occurred where the Ireton aquitard thickens to as much as 10 m. Hydrocarbon migration through the suspected breaches has typically occurred via intercrystalline pore networks, or in conjunction with fracture porosity. These pore networks correspond to platform/upper slope facies that consist of >80% carbonate and are dominated by the coarser T3 dolomite. This would suggest that during matrix replacement dolomitization the higher carbonate content facies of the platform/upper slope environment were comprised of a more coarsely crystalline limestone that offered fewer dolomite nucleation sites and greater pore-space for dolomite crystal growth (Gregg and Sibley, 1984; Sibley and Gregg, 1987). This enabled the development of a more coarsely crystalline dolomite with greater intercrystalline porosity (in the order of 2-4%) and permeability — such a coarse dolomite is unlikely of a precursor micrite matrix. The higher carbonate content may have also increased the likelihood of fracturing by lowering the ductility of the Ireton aquitard. Rarely does the Ireton aquitard have fractures in its thicker, more clay-rich intervals. Breaching locations are also commonly accompanied by a greater abundance of late diagenetic products within fractures and moldic porosity, such as late calcite and anhydrite.

Breaches can therefore be categorized in two ways: i) breaching of the Ireton aquitard where the Ireton aquitard is effectively missing (0-4 m thickness), through a discontinuous/patchy Ireton aquitard drape (always >80% carbonate content); and ii) breaching through an Ireton aquitard drape that is 4-10 m thick, but only where carbonate content averages >80%.

The location of the wells that have breached Ireton aquitard (Figure 6.2) demonstrate the strong influence of carbonate content on the integrity of the Ireton aquitard. Areas with no core data, but that have <~4 m of Ireton aquitard drape, are highlighted as probable breaching locales (Figure 6.2).

Generally, where the Ireton aquitard is >10 m thick, the aquitard has functioned as an effective seal since hydrocarbon entrapment. However, within the thicker Ireton aquitard intervals, vertical facies changes into more carbonate-rich facies may provide

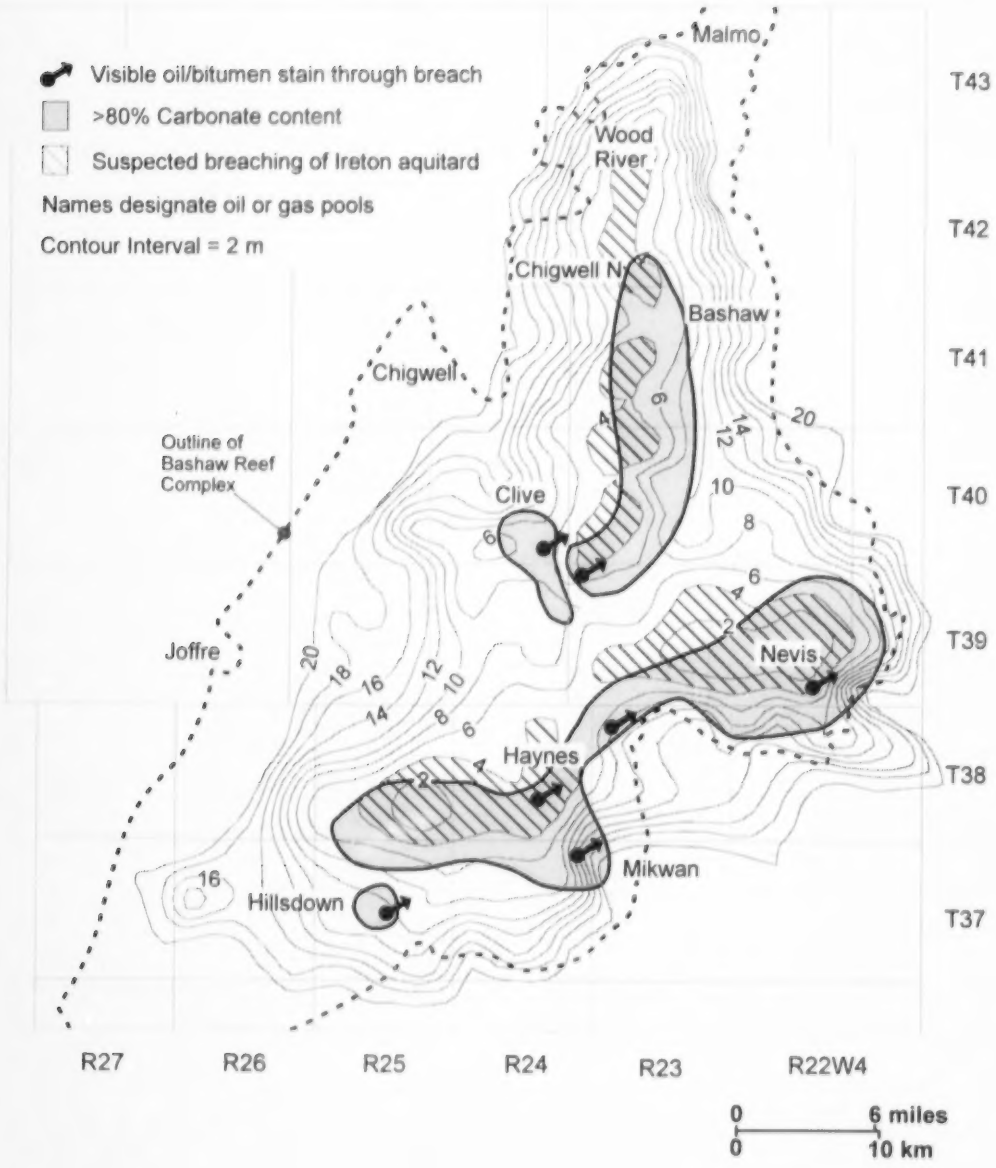

Figure 6.2: Isopach map of the Ireton aquitard (modified from Rostron, 1995). Arrows indicate where there is visible evidence of breaching within areas of Ireton aquitard with >80% carbonate content. Suspected breaching locales are indicated at <4 metres of Ireton aquitard.

possible lateral migration pathways. One possible example is in well 6-25-41-25W4 (6305 feet) where the Ireton aquitard thickness is 120 m. Oil appears to have migrated within a coarsely-crystalline burrowed horizon just 20 m below the uppermost Ireton aquitard contact. Ten metres further up the core (at 6273 feet) there is no oil staining, and it is concluded that no vertical breaching occurred. It is possible, therefore, that the oil-filled burrows were sourced laterally through more permeable Ireton aquitard facies or fractures, perhaps breaching the Ireton aquitard elsewhere. In most of the thicker Ireton aquitard intervals there are no hydrocarbons visible.

6.3 Control of Breaching Locales on Pool Distribution.

6.3.1. Leduc Formation (D-3) reservoirs

Hydrocarbon entrapment in the known Leduc Formation reservoirs principally occurs within the present-day structural highs of the reef complex that resulted from differential compaction and are covered by >~10 m of Ireton aquitard, with typically <80% carbonate content (compare Figures 2.1, 4.1, and 6.2). Exceptions to this include the Nevis "Devonian" pool and the Clive field.

In the Nevis "Devonian" pool (Figures 4.1 and 4.2) there is a nearly complete absence of Ireton aquitard, *i.e.*, direct breaching (Figure 6.2), whereby a common gas/water contact now exists between the Leduc Formation and Nisku Formation reservoirs. It would appear, therefore, that trapping of the Leduc Formation gas is not by the Ireton aquitard but instead by the upper Nisku Formation evaporites, and that the Ireton aquitard only provides a lateral updip aquitard in the Leduc Formation. However, MICPM data for an Ireton aquitard sample in well 14-2-39-22W4 (5391 feet; Plug 2; Table 5.5) indicate that in the area of that well the Ireton aquitard may indeed provide a partially effective seal today because, in thin section, the sample appears to have been diagenetically resealed after it was initially breached by hydrocarbons. Nevertheless, in other areas of Nevis the Ireton aquitard is virtually absent and the Leduc Formation is probably still in direct communication with the Camrose Member today.

In the Clive field area, the isopach map of the Ireton aquitard (Figure 6.2) indicates that the thickness of the aquitard is <10 m over many parts, which suggests potential breaching. These thicknesses, however, are explained by Rostron (1995) to be

an artefact of the contouring program he used, and that the Ireton aquitard thickness rarely thins to less than 10 m over the Clive area. Even so, some breaching has occurred or may still be occurring in the area of well 16-2-40-24W4. This was determined from MICPM data for this well (Plug 3; Table 5.5) which indicate that a greater hydrocarbon column exists in the pool today than can possibly be sustained by the Ireton aquitard.

The rate of hydrocarbon migration through many of the suspected breaches in the Ireton aquitard has led to the nearly complete absence of accumulation beneath the breaches, *e.g.*, beneath the thin Ireton aquitard in the central-northern part of the Bashaw Reef Complex, and in the Haynes area. However, it is apparent that in some areas breaching may be occurring over a much more extended period of geologic time, *e.g.*, the Ireton aquitard in the area of well 16-2-40-24W4.

6.3.2. Nisku Formation/Camrose Member (D-2) reservoirs

Entrapment in known D-2 pools is principally within drape structures located over the present-day topographic highs of the Leduc Formation (Figure 6.3). In addition, trapping also occurs due to anhydrite plugging within the lower Nisku Formation and Camrose Member platforms, and within "pinnacle" reefs just off the carbonate platform (*e.g.*, Wood River area; Figure 6.3). In the lower Nisku Formation and Camrose Member, the distribution of most of the pools can be explained with relation to suspected breaching locales of the Ireton aquitard (although some pools may have viable alternatives). Entrapment of hydrocarbons within the Nisku Formation/Camrose Member can therefore be categorized as follows:

1) pools that are located above areas where the Ireton aquitard is effectively missing (0-4 m thickness), *e.g.*, Haynes, Nevis "Devonian", and some of the Bashaw and Wood River D-2 pools;
2) pools that are located above breaches through an Ireton aquitard drape with >80% carbonate content and thickness of ≤10 m, *e.g.*, Mikwan, Hillsdown, (Clive), D-2 pools;
3) pools that are located updip from known breaches, *e.g.*, Clive (sourced from Haynes) and some of the more easterly Bashaw D-2 pools;
4) pools that may have been sourced from a Nisku Formation source-rock within the

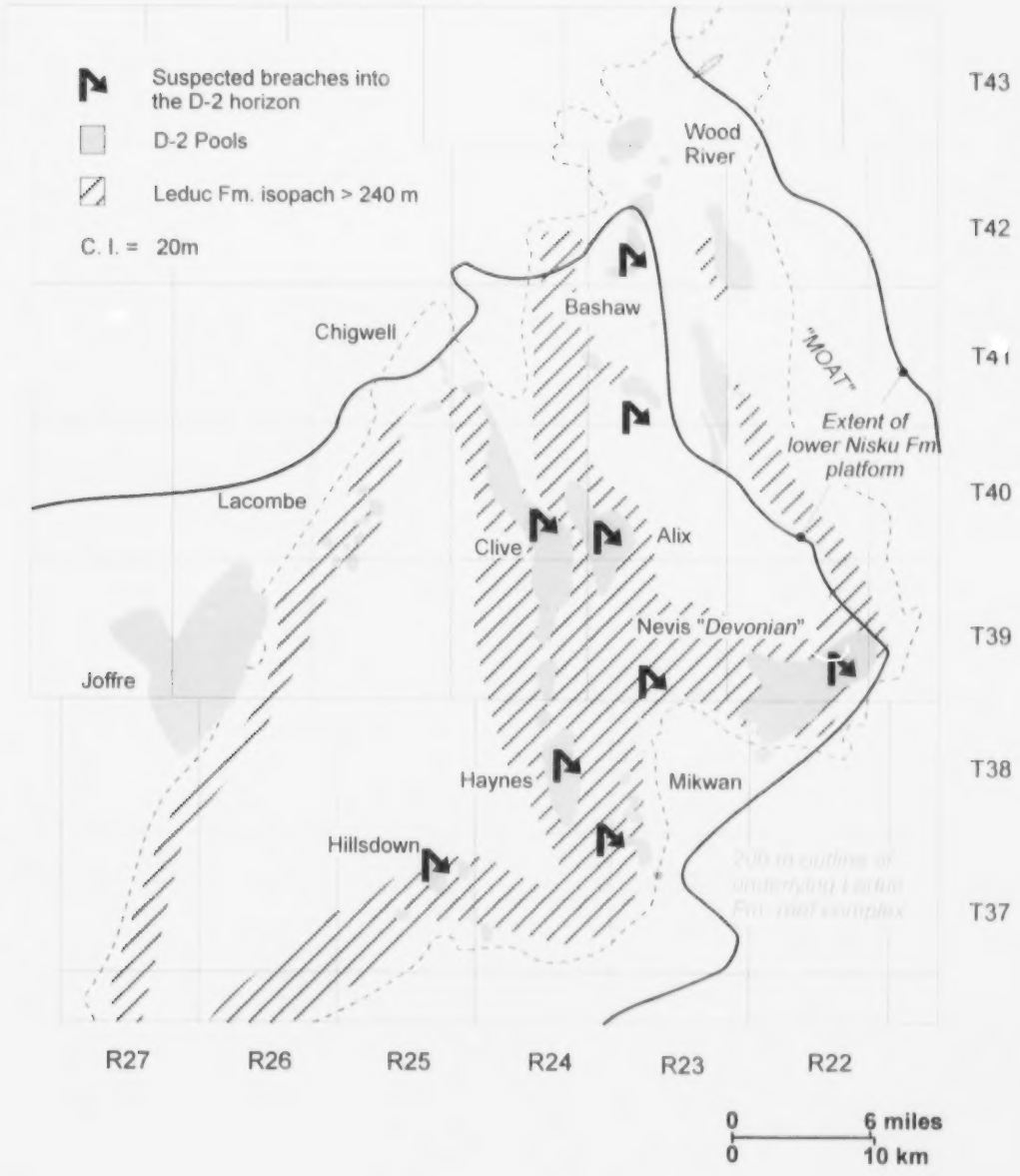

Figure 6.3: Distribution map of D-2 pools indicating their close spatial relationship with topographic highs of the Leduc Formation (>240 m) due to compactional drape. Also indicated are suspected breaching locales.

"Moat" area, *e.g.*, the off-platform Bashaw pools (D-2 A, G, and L), otherwise these Bashaw pools probably have a similar origin to (3);

5) Other possible origins:

   i) major fracturing or lateral migration through a very thick Ireton aquitard drape may account for the Joffre (D-2) pool. The Joffre (D-2) pool may also source the Lacombe and Chigwell pools. Also a possible lateral breach near 6-25-41-25W4 may source the Chigwell pools.

   ii) Long distance migration of hydrocarbons through the lower Nisku Formation platform from Ireton aquitard breaches outside of the area, *e.g.*, from Wimborne and Innisfail areas.

   iii) Hitherto unidentified breaches/faults within the study area, *e.g.*, H_2S may have been sourced through deep-reaching faults related to basement faulting (Edwards *et al.*, 1995).

6.4 Hydrocarbon Migration and Entrapment.

Migration into the reservoirs of the Bashaw area can be divided into two main phases, an initial predominantly oil phase, and then gas. It is uncertain, however, as to whether the gas phase could also be separated into an initial phase of "sweet" gas migration that is followed by a later phase of sour (H_2S) gas migration, or whether most of the gas in the area may have migrated during essentially one phase.

6.4.1. Oil migration

Oils in the Bashaw area are most likely a mixture of oils of various maturities that migrated along the Bashaw reef trend from the southwest. Similarities between the API gravities of oils in the Bashaw area to oils in the Wimborne and Innisfail areas farther to the southwest (~40 API) are suggestive of an allochthonous origin to the oils in the Bashaw area. In addition, Duvernay source-rocks around the Bashaw Reef Complex are of lower maturity (Stoakes and Creaney, 1985) and probably generate(d) oils of <40 API gravity.

Oils that migrated from the southwest would likely have migrated to the top of the reservoir interval along the Bashaw trend, and then gradually moved up-dip along the reef

trend and systematically filled traps to their spill points. In this manner, the oils would have entered the study area from the south. From the known reservoir distributions it seems likely that most of the oil migrated along the "raised rims" on the east and west sides of the Bashaw Reef Complex (Figure 6.4).

Oils that migrated along the eastern "raised rim" probably filled the Hillsdown and Mikwan D-3 pools first (also perhaps leaking into the D-2 pools), and subsequently migrated into the structural highs of Haynes/Clive and the Nevis high. From Haynes, oil would have migrated on toward the Clive D-3 pool, as well as breaching into the overlying Haynes D-2 pools (Figure 6.3). The Haynes D-2 pools probably then reached spill-point and provided lateral sourcing of oil to the Clive D-2 pools (the Clive D-2 pools may also be sourced to some extent by direct breaching from the Clive D-3 pool in the vicinity of the 16-2-40-24W4 well location (Figure 6.3)). Oils that migrated into the Nevis area would have filled the Nisku Formation reservoir directly (little/no Ireton aquitard), and back-filled into the Leduc Formation where spill point was probably achieved (closure within the Nisku Formation preventing spill-point being reached in the Nisku Formation). Oil that spilled-over from the Nevis Leduc Formation horizon (Figure 6.4) then likely migrated across the Bashaw reef area updip toward the northwest into the Alix, Bashaw, Wood River, and Malmo areas. These oils probably leaked straight up through an Ireton aquitard breach in the Alix area to the Alix D-2 pool (Figure 6.3), as well as probably migrating through the thin Ireton aquitard in the central-northern part of the Bashaw Reef Complex (Figure 6.2). This thin Ireton aquitard probably provided the sourcing to the D-2 pools in the Bashaw and Wood River areas (Figure 6.3).

Oil that migrated along the western "raised rim" likely filled the Penhold, Joffre, and Chigwell D-3 pools (Figure 6.4). It is possible that breaching may have occurred in the area of the Joffre D-3 pool to fill the relatively large reserves of the Joffre D-2 pool (as suggested in section 6.3.2.). This would then have also provided a source to the oils in the Lacombe and Chigwell D-2 fields. Otherwise, unknown breaches along the western "raised rim" or sources external to the area may provide viable migration alternatives (and could possibly alter the migration scenario for several of the other pools).

A suspected breach in the south-central portion of the reef complex (west of the Haynes area; Figure 6.2) appears not to have been breached by hydrocarbons as there is

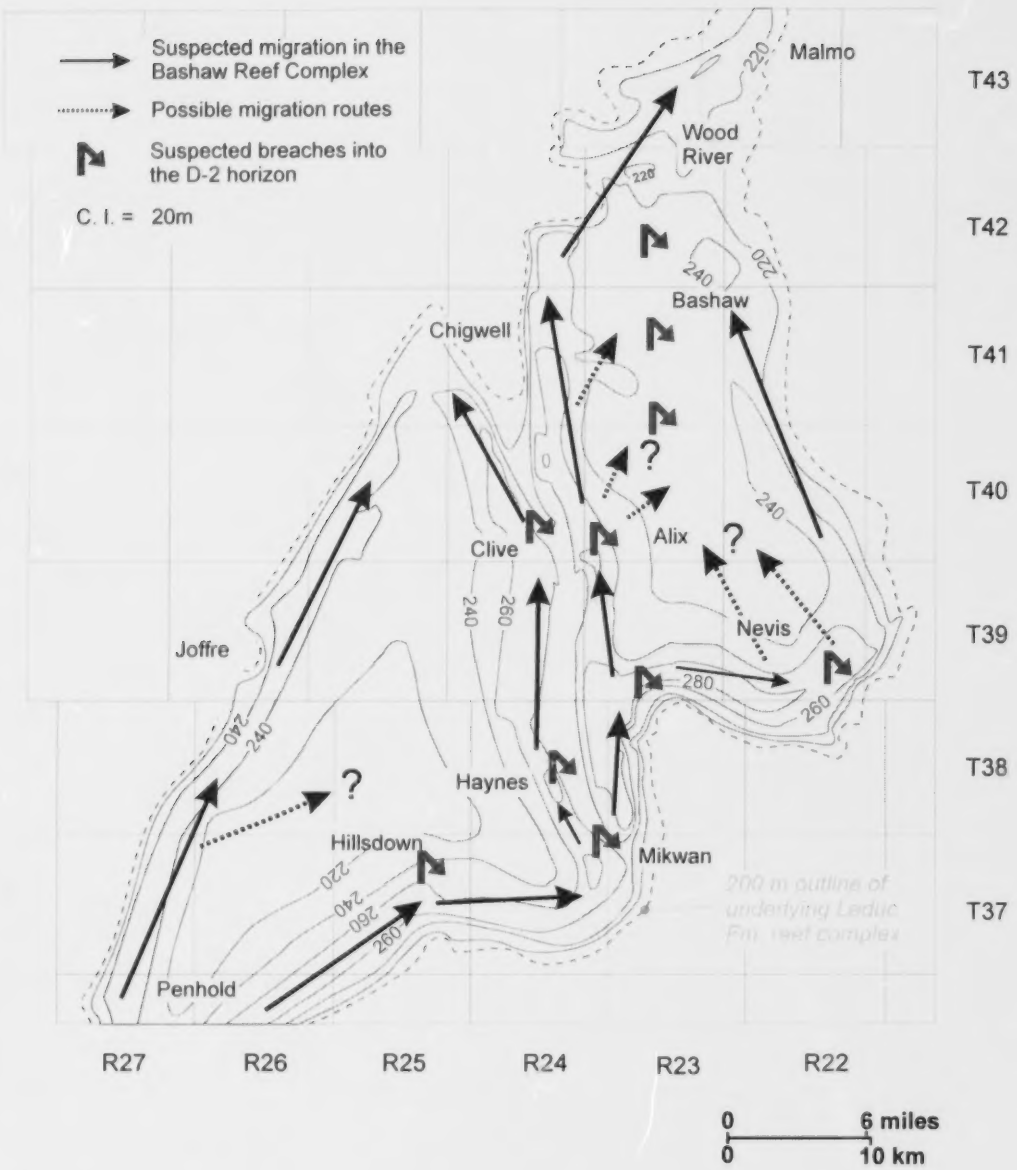

Figure 6.4: Isopach map of the Bashaw Reef Complex (modified from SCG, 1989) with suspected hydrocarbon migration pathways through the reef complex indicated by arrows. Hooked arrows indicate suspected breaching into the D-2 horizon (see text for further discussion).

no hydrocarbon entrapment in the D-2 horizon. It is possible, however, that no suitable traps are present in that area for migrated oils to accumulate. However, experimental data by Dembicki Jr. and Anderson (1989) suggest that secondary migration probably occurs along restricted pathways following the uppermost part of a reservoir interval, and therefore in this case, secondary migration is most likely to have been only along the eastern and western "raised rims".

6.4.2. Hydrocarbon gas migration

Hydrocarbon gas generation and migration was almost certainly allochthonous to the Bashaw area because the Duvernay source-rock is of insufficient maturity around the Bashaw Reef Complex (Stoakes and Creaney, 1985). However, because there is no data available that conclusively links the accumulated hydrocarbon gas to a Duvernay origin, two possible sources are hypothesized for the gas: 1) hydrocarbon gas was generated in the more deeply-buried Duvernay source-rocks to the southwest; or 2) gas was derived through deep-reaching faults within or downdip of the Bashaw area.

Based on present-day knowledge, it seems likely that much of the gas was generated from Duvernay source-rocks (as a "sweet" gas) in the southwest and migrated updip along similar flow-paths to that of the oils and postdated initial oil emplacement (determined from the fact that oil stain was present in the Nevis "Devonian" gas pool, and was most likely displaced by gas). However, one might expect that if indeed gas migrated from the southwest that the more southerly, downdip pools in the Bashaw area be filled by gas to a greater degree than the updip pools (Gussow's (1954) theory of differential entrapment). This is not the case, however, with the more southerly Bashaw Reef pools, *e.g.*, Mikwan and Hillsdown, having an oil "leg", whereas the updip Nevis "Devonian" pool, for example, is a non-associated gas pool. Therefore, assuming that there was updip migration of the gas from Duvernay source-rocks, this apparent "lack" of differential entrapment in southerly pools could be accounted for by either: a) there was greater permeability beneath the southerly pools to preferentially funnel the gas toward the Nevis area; or 2) possible oil/water washing at the base of these pools left an oil mat that deflected later gas migration.

The alternative to Duvernay-sourced hydrocarbon gas is that the gas may have

migrated up deep-reaching faults from within or downdip of the study area and into the Bashaw pools, or perhaps via a combination of both theories. The fault origin could also account for the present-day gas distribution. However, no reservoirs have been discovered in the units underlying the Upper Devonian to support a fault related origin.

6.4.3. H_2S gas migration

The H_2S present in the Bashaw area is also considered allochthonous in origin, and was most likely generated from thermochemical sulphate reduction (TSR). TSR typically requires higher temperatures than sweet normal gas generation, and would therefore postdate the majority of any "sweet" gas migration into the Bashaw area. H_2S gas, however, has "soured" most, if not all pools in the area, and therefore an initial phase of "sweet" hydrocarbon gas migration cannot be determined. H_2S gas could therefore have originated either from high maturity Duvernay source-rocks and postdated any "sweet" oil and gas migration into the Bashaw area, or migrated up deep-reaching faults, perhaps associated with "sweet" hydrocarbon gases. Again, as with the hydrocarbon gas, H_2S gas is unevenly distributed in the pools of the Bashaw area (Figures 4.1 and 4.2) and does not follow the differential entrapment theory of Gussow (1954) for updip migration of this gas.

6.5 Implications for Exploration.

Characterization of the aquitard properties of the Ireton aquitard in the Bashaw area, in addition to reservoir characterization and the analysis of migration pathways, is essential to the understanding of hydrocarbon entrapment in the D-2 and D-3 reservoirs, and for the prediction of future discoveries. This study reveals that new hydrocarbon discoveries may exist in the D-2 and D-3 horizons of the Bashaw area.

D-3 reservoirs are located in topographic highs that are typically draped by >~10 m of Ireton aquitard. Hydrocarbon migration is suspected to have occurred along these highs (Figure 6.4) — many have been drilled and found to contain commercial hydrocarbon accumulations. The western margin, however, has few D-3 pools (Figure 4.1). This reflects the updip orientation of the western margin and that, as a consequence, probably very little structural closure exists along this margin. However, small

hydrocarbon accumulations may be present in diagenetic or stratigraphic traps.

D-2 reservoirs are either located directly above or up-dip from suspected Ireton aquitard breaches, and mostly within drape structures over topographic highs of the Leduc Formation (Figure 6.3). Future exploration in the D-2 horizon should, therefore, be focused in areas toward the northeast end of the lower Nisku Formation platform, up-dip from the Haynes, Nevis, and Alix areas. The most prospective exploration areas are likely to be undiscovered "pinnacle" reefs in the Wood River area, or drape structures within the "Moat" area that lies directly above the eastern "raised" margin of the Bashaw Reef Complex (Figure 6.3). On the main carbonate platform, and directly above the thin Ireton aquitard in the central-northern portion of the Bashaw reef area (Figure 6.2), further accumulations may exist in diagenetically controlled traps. New discoveries may also exist in drape structures created over the western "raised" margin of the Bashaw Reef Complex (*e.g.*, Lacombe and Chigwell), however, hydrocarbon migration into the D-2 horizon in this area is less well understood.

This study also has significant implications to exploration strategies in other parts of the WCSB. The Ireton aquitard over the Bashaw Reef Complex clearly shows that there is significant lithologic heterogeneity within the Ireton aquitard. Similar occurrences exist in other parts of the WCSB. For example, in the Grosmont Formation (Figure 1.1) Huebscher and Machel (1995b) demonstrated that cross-formational hydrocarbon flow is possible where the Ireton aquitard marls are thin or patchy between the Grosmont and Nisku formations. A similar situation may also be present over the Cheddarville reef complex in the southern part of the Rimbey-Meadowbrook reef trend (Figure 1.1). Here, the Ireton aquitard thins to <5 m and based on hydrogeologic evidence may have provided the principal breach for hydrocarbon migration into the D-2 pools that are present further up-dip along the reef trend (Wilkinson, 1995). Above the Rimbey-Meadowbrook reef trend, where the aquitard is typically >35 m thick, there is no hydrogeologic evidence for breaching of the Ireton aquitard (Rostron, 1995).

In conclusion, identification of breaching locales can have a significant impact on the exploration strategy of a region. Indeed, accurate identification of the areal extent of the breaching locales may also focus exploration on a pool scale.

CHAPTER 7

CONCLUSIONS

1) The Ireton aquitard provides the principal control to cross-formational fluid flow in the area of the Bashaw Reef Complex, influencing hydrocarbon entrapment in the Leduc Formation (D-3) and Camrose Member/lower Nisku Formation (D-2) reservoirs. The Ireton aquitard over the reef complex contrasts from the basinal Ireton aquitard in that it has a much reduced clay content.

2) Duvernay-sourced hydrocarbons have migrated across the Ireton aquitard principally through an intercrystalline pore network of relatively coarse crystalline replacement dolomite, and in some cases fractures. Breaching has occurred in two principal ways:
   i) breaching where the Ireton aquitard is effectively absent (0-4 m thick); and
   ii) breaching through an Ireton aquitard drape that is 4-10 m thick, but only where the average carbonate content exceeds >80%.

3) Hydrocarbon breaching of the Ireton aquitard and entrapment in the Leduc Formation and Camrose Member/lower Nisku Formation has come about via a complex interplay of stratigraphic and diagenetic events. These can be summarized as follows:
   i) Carbonate accretion on the Bashaw Reef Complex at the end of sediment deposition of the Leduc Formation resulted in a morphology that was likely affected by reef backstepping related to relative rises in sea level.
   ii) Ireton aquitard sediment deposition occurred across the reef complex and was deposited as a <25 m thick drape, that thins over the paleotopographic highs to <1 m;
   iii) The Ireton aquitard developed distinctive facies related to the antecedent topography, with facies of higher carbonate content developed over paleo-topographic highs;
   iv) Replacement dolomitization likely occurred in the latest Devonian via the

process of reflux dolomitization, with hypersaline brines being sourced from the upper Nisku Formation and Wabamun Group evaporites. These dolomitizing brines pervasively replaced the precursor limestone within the area down to the lowermost Leduc Formation, and developed a more coarsely crystalline and porous dolomite in the Ireton aquitard sediments of higher carbonate content (~2-4%). Replacement dolomitization also generated excellent intercrystalline, moldic, and vuggy porosity in the reservoir units;

v) Increased differential compaction of the interior of the Bashaw Reef Complex, relative to the margins, resulted in the present-day "raised rim" morphology to the reef complex. This has typically resulted in a thicker Ireton aquitard drape being present over these "raised rims";

vi) Dolomite and anhydrite cementation reduced porosity throughout the area. These diagenetic products are present in the Ireton aquitard only where it was particularly thin. Various fracturing and dissolution episodes enhanced porosity; and finally,

vii) In the Late Cretaceous/early Tertiary, oil, hydrocarbon gas, and H_2S gas, from Duvernay source-rocks to the southwest of the study area or through deep reaching faults, migrated into the Bashaw Reef Complex and were trapped in the raised rims of the reef complex, typically where there was a >10 m Ireton aquitard drape. Where breaching of the Ireton aquitard occurred, entrapment in the Camrose Member/lower Nisku Formation reservoirs was either directly above or up-dip from the breaches in traps principally related to compactional drape over the Bashaw Reef Complex. Some pools in the area cannot be linked to breaches, either because there are undiscovered breaches, or there was a source to the hydrocarbons from outside the study area.

4) Breaching identification and characterization requires detailed sedimentologic, and diagenetic work on both a micro- and macro-scale. Hydrocarbon migration could not be determined by geochemical tracers of oxygen or carbon isotopes, or from magnetic anomaly mapping (although a more detailed study is required with respect to magnetic studies).

5) Characteristics of the Ireton aquitard breaches over the Bashaw Reef Complex may apply to other aquitards within the WCSB (*e.g.*, the Rimbey-Meadowbrook reef trend).

REFERENCES

Al-Bastaki, A., Humphrey, J.D., and Moore, C.H., 1995a, Sedimentology, diagenesis, and dolomitization of the Nisku Formation (Upper Devonian, Frasnian) at Joffre Field, Alberta, Canada (abs): 1995 Annual Convention of the AAPG, Houston, p. 1A.

Al-Bastaki, A., Humphrey, J.D., and Moore, C.H., 1995b, Origin and timing of dolomitization and anhydrite cementation of the Nisku Formation, Joffre Field, Alberta, (abs): 1995 Annual Meeting of the GSA, New Orleans, p. A171.

Alberta Society of Petroleum Geologists, 1960, Oil Fields of Alberta - a reference volume: Calgary, ASPG, 272 p.

Alberta Society of Petroleum Geologists, 1966, Oil Fields of Alberta (supplement): Calgary, ASPG, 136p.

Alberta Society of Petroleum Geologists, 1969, Gas Fields of Alberta: Calgary, ASPG, 407 p.

Amthor, J.E., Mountjoy, E.W., and Machel, H.G., 1993, Subsurface dolomites in Upper Devonian Leduc Formation buildups, central part of Rimbey-Meadowbrook reef trend, Alberta, Canada: Bulletin of Canadian Petroleum Geology, v.41, p. 164-185.

Andrichuk, J.M., 1958a, Stratigraphy and facies analysis of Upper Devonian reefs in Leduc, Stettler, and Redwater areas, Alberta: AAPG Bulletin, v.42, p. 1-93.

Andrichuk, J.M., 1958b, Cooking Lake and Duvernay (Late Devonian) sedimentation in Edmonton area of central Alberta, Canada: AAPG Bulletin, v.42, p. 2189-2222.

Andrichuk, J.M., 1961, Stratigraphic evidence for tectonic and current control of Upper Devonian reef sedimentation, Duhamel area, Alberta, Canada: AAPG Bulletin, v.45, p. 612-632.

Behrens, E.W. and Land, L.S., 1972, Subtidal Holocene dolomite, Baffin Bay, Texas: Journal of Sedimentary Petrology, v.42, p. 155-161.

Belyea, H.R., 1955, Cross-sections through the Devonian system of the Alberta Plains: Geological Survey of Canada, Paper 55-3, p. 1-29.

Belyea, H.R., 1958, Designation of type section Camrose Tongue, Upper Devonian, Alberta: Journal of Alberta Society of Petroleum Geologists, v.6, p. 105-110.

Blanchon, P., 1995, Controls on Modern Reef Development Around Grand Cayman: unpublished Ph.D. Thesis, University of Alberta, Canada, 200 p.

Boles, J.R. and Franks, S.G., 1979, Clay diagenesis in Wilcox sandstones of southwest Texas: implications of smectite diagenesis on sandstone cementation: Journal of Sedimentary Petrology, v.49, p. 55-70.

Brennan, P.F. and Warden, A.S., 1959, Wimborne oil and gas field, Alberta: Alberta Society of Petroleum Geologists, 9th Annual Field Conference, p. 139-144.

Campbell, F.A. and Oliver, T.A., 1968, Mineralogic and geochemical composition of Ireton and Duvernay Formations, central Alberta: Bulletin of Canadian Petroleum Geology, v.16, p. 40-63.

Carpenter, S.J. and Lohmann, K.C., 1989, $\delta^{18}O$ and $\delta^{13}C$ variations in Late Devonian cements from the Golden Spike and Nevis reefs, Alberta, Canada: Journal of Sedimentary Petrology, v.59, p. 792-814.

Carpenter, S.J., Lohmann, K.C., Holden, P., Walter, L.M., Huston, T.J., and Halliday, A.N., 1991, $\delta^{18}O$ values, $^{87}Sr/^{86}Sr$ and Sr/Mg ratios of Late Devonian marine calcite: implications for the composition of ancient seawater: Geochimica et Cosmochimica Acta, v.55, p. 1991-2010.

Collinson, D.W., 1983, Methods in Rock Magnetism and Palaeomagnetism: techniques and instrumentation: Chapman and Hall, London, 503 p.

Creaney, S. and Allen, J., 1990, Hydrocarbon generation and migration in the Western Canada Sedimentary Basin, *in* J. Brooks, ed., Classic Petroleum Provinces: Geological Society Special Publication No. 50, London, Geological Society, p. 189-202.

Creaney, S., Al'.n, J., Cole, K.S., Fowler, M.G., Brooks, P.W., Osadetz, K.G., Macqueen, R.W., Snowdon, L.R., and Riediger, C.L., 1994, Petroleum generation and migration in the Western Canadian Sedimentary Basin: *in*, G.D. Mossop and I. Shetsen (comps.), Chapter 31, Geological Atlas of the Western Canada Sedimentary Basin, Canadian Society of Petroleum Geologists and Alberta Research Council, Calgary, p. 455-468.

Cutler, W.G., 1983, Stratigraphy and sedimentology of the Upper Devonian Grosmont Formation, northern Alberta: Bulletin of Canadian Petroleum Geology, v.31, p. 282-325.

Degens, E.T. and Epstein, S., 1964, Oxygen and carbon isotope ratios in coexisting calcites and dolomites from Recent and ancient sediments: Geochimica et Cosmochimica Acta, v.528, p. 23-44.

Dembicki, Jr., H. and Anderson, M.J., 1989, Secondary migration of oil: experiments supporting efficient movement of separate, buoyant oil phase along limited conduits: AAPG, v.73, p. 1018-1021.

Deroo, G., Powell, T.G., Tissot, B., and McCrossan, R.G., 1977, The origin and migration of petroleum in the Western Canadian Sedimentary Basin, Alberta: a geochemical and thermal maturation study: Geological Survey of Canada Bulletin, 262, 136 p.

Dixon, R.J., Stoakes, F.A., and Campbell, C.V., 1991, Exploration for Nisku Formation isolate reefs of the Wood River area: a stratigraphic play-type in a structural world (abs): Bulletin of Canadian Petroleum Geology, v.39, p. 210.

Downey, M.W., 1984, Evaluating seals for hydrocarbon accumulations: AAPG Bulletin, v.68, p. 1752-1763.

Drivet, E., 1993, Diagenesis and reservoir characteristics of Upper Devonian Leduc dolostones, southern Rimbey-Meadowbrook reef trend, central Alberta, unpublished M.Sc. thesis, McGill University, 115p.

Edwards, D.J., Lyatsky, H.V., and Brown, R.J., 1995, Basement fault control on Phanerozoic stratigraphy in the Western Canada Sedimentary Province: integration of potential-field and lithostratigraphic data: Report of Transect Workshop (Lithoprobe - Alberta Basement Transects), April 10-11, 1995, Calgary, Alberta.

Energy Resources Conservation Board, 1979 - 1986 (Annual Reports), Reservoir Performance Charts Oil Pools: ERCB, Calgary.

Energy Resources Conservation Board, 1991, Alberta's reserves of crude oil, oil sands, gas, natural gas liquids, and sulphur. ERCB ST92-18 (1991), 31st Edition, Calgary.

Gardner, W.C. and Bray, E.E., 1984, Oils and source rocks of Niagaran Reefs (Silurian) in the Michigan Basin: *in* J.G. Palacas, ed., Petroleum Geochemistry and Source Rock Potential of Carbonate Rocks, AAPG Studies in Geology #18, p. 33-44.

Gilhooly, M.G., 1987, Sedimentology and geologic history of the Upper Devonian (Frasnian) Nisku and Ireton Formations, Bashaw area, Alberta: Unpublished M.Sc. thesis, University of Calgary, 203 p.

Geological Survey of Canada, 1988, Conventional oil resources of Western Canada (light and medium): GSC, Paper 87-26

Gregg, J.M. and Sibley, D.F., 1984, Epigenetic dolomitization and the origin of xenotopic dolomite texture: Journal of Sedimentary Petrology, v.54, p. 908-931.

Gussow, W.C., 1954, Differential entrapment of oil and gas: a fundamental principle: AAPG Bulletin, v.38, p. 816-853.

Haites, T.B., 1960, Transcurrent faults in western Canada: Journal of the Alberta Society of Petroleum Geologists, v.8, p. 33-78.

Hesse, R., 1990, Early diagenetic pore water/sediment interaction: modern off-shore basins, *in* I.A. McIlreath and D.W. Morrow, eds., Diagenesis, Geoscience Canada, Reprint Series No.4, p. 277-316.

Hitchon, B., 1984, Geothermal gradient, hydrodynamics, and hydrocarbon occurrences, Alberta, Canada: AAPG Bulletin, v.68, p. 713-743.

Hubbard, K.H., Randolph, B.B., and Gill, I.P., 1986, Styles of reef accretion along a steep, shelf-edge reef, St.Croix, U.S. Virgin Islands: Journal of Sedimentary Petrology, v.56, p. 848-861.

Huebscher, H. and Machel, H.G., 1995a, Cross-formational fluid flow in Devonian dolostones (abs): The 1st SEPM Congress on Sedimentary Geology, v.1, August 13-16, 1995, St. Pete Beach, Florida, 1 pp.

Huebscher, H., and Machel, H.G., 1995b, Seal quality related to facies distribution and diagenesis, an example from the Woodbend Group, north-central Alberta (abs): 1995 CSPG Annual Conference (Program and Abstracts), Calgary, 2 pp.

Hunt, J.M., 1995, Petroleum Geochemistry and Geology (2nd Edition): W.H. Freeman and Company, New York, 743 p.

Imperial Oil Ltd., Geological Staff, 1950, Devonian nomenclature in the Edmonton area, Alberta, Canada: AAPG Bulletin, v.34, p. 1807-1825.

James, N.P., Ginsburg, R.N., Marszalek, D.S., and Choquette, P.W., 1976, Facies and fabric specificity of early subsea cements in shallow Belize (British Honduras) reefs: Journal of Sedimentary Petrology, v.46, p. 523-544.

Kaufman, J., 1994, Numerical models of fluid flow in carbonate platforms: implications for dolomitization: Journal of Sedimentary Research, v.64, p. 128-139.

Kaufman, J., Hanson, G.N., and Meyers, W.J., 1991, Dolomitization of the Swan Hills Formation, Rosevear Field, Alberta, Canada: Sedimentology, v.38, p. 41-66.

Klovan, J.E., 1964, Facies analysis of the Redwater reef complex, Alberta, Canada: Bulletin of Canadian Petroleum Geology, v.12, p. 1-100.

Krouse, H.R., Viau, C.A., Eliuk, L.S., Veda, A., and Halas, S., 1988, Chemical and isotopic evidence of thermochemical sulphate reduction by light hydrocarbon gases in deep carbonate reservoirs: Nature, v.333, p. 415-419.

Lahann, R.W., 1980, Smectite diagenesis and sandstone cement: the effect of reaction temperature: Journal of Sedimentary Petrology, v.50, p. 755-760.

Lazar, B. and Erez, J., 1992, Carbon geochemistry of marine-derived brines: I. ^{13}C depletions due to intense photosynthesis: Geochimica et Cosmochimica Acta, v.56, p. 335-345.

Lloyd, R.M., 1964, Variations in the oxygen and carbon isotopic ratios of Florida Bay mollusks and their environmental significance: Journal of Geology, v.72, p. 84-111.

Machel, H.G., 1987, Saddle dolomite as a by-product of chemical compaction and thermochemical sulphate reduction: Geology, v.15, p. 936-940.

Machel, H.G., 1995, Magnetic mineral assemblages and magnetic contrasts in diagenetic environments - with implications for studies of paleomagnetism, hydrocarbon migration and exploration: *in* P. Turner and A. Turner, eds., Palaeomagnetic Applications in Hydrocarbon Exploration and Production, Geological Society Special Publication No. 98, p. 9-29.

Machel, H.G. and Mountjoy, E.W., 1986, Chemistry and environments of dolomitization — a reappraisal: Earth-Science Reviews, v.23, p. 175-222.

Machel, H.G. and Anderson, J.H., 1989, Pervasive subsurface dolomitization of the Nisku Formation in central Alberta: Journal of Sedimentary Petrology, v.59, p. 891-911.

Machel, H.G. and Burton, E.A, 1991, Causes and spatial distribution of anomalous magnetization in hydrocarbon seepage environments: AAPG Bulletin, v.75, p. 1864-1876.

Machel, H.G. and Hunter, I.G., 1994, Facies models for Middle Devonian shallow-marine carbonates, with comparison to modern reefs: a guide for facies analysis: Facies, v.30, p. 155-176.

Machel, H.G., Krouse, H.R., and Sassen, R., 1995, Products and distinguishing criteria of bacterial and thermochemical sulfate reduction: Applied Geochemistry, v.10, p. 373-389.

Maiklem, W.R., Bebout, D.G., and Glaister, R.P., 1969, Classification of anhydrite - a practical approach: Bulletin of Canadian Petroleum Geology, v.17, p. 194-233.

Marshall, J.D., 1992, Climatic and oceanographic isotopic signals from the carbonate rock record and their preservation: Geology Magazine, v.129, 143-160.

McCrossan, R.G., 1961, Resistivity mapping and petrophysical study of Upper Devonian inter-reef calcareous shales of central Alberta, Canada: AAPG Bulletin, v.45, p. 441-470.

McGillivray, J.G., and Mountjoy, E.W., 1975, Facies and related reservoir characteristics Golden Spike reef complex, Alberta: Bulletin of Canadian Petroleum Geology, v.23, p. 753-809.

McHargue, T.R. and Price, R.C., 1982, Dolomite from clay in argillaceous or shale-associated marine carbonates: Journal of Sedimentary Petrology, v.52, p. 873-886.

McKenzie, J.M., 1981, Holocene dolomitization of calcium carbonate sediments from the coastal sabkhas of Abu Dhabi, U.A.E.: a stable isotope study: Journal of Geology, v.20, p. 185-189.

Meyers, W.J. and Hill, B.E., 1983, Quantitative studies of compaction in Mississippian skeletal limestones, New Mexico: Journal of Sedimentary Petrology, v.53, p. 231-242.

Mossop, G.D., 1972, Origin of the peripheral rim, Redwater reef, Alberta: Bulletin of Canadian Petroleum Geology, v.20, p. 238-280.

Mossop, G.D. and Shetsen, I., (comps.), 1994, Geological Atlas of the Western Canada Sedimentary Basin: Canadian Society of Petroleum Geologists and Alberta Research Council, Calgary, 509 p.

O'Connor, M.J. and Gretener, P.E., 1974, Differential compaction within the Woodbend Group of central Alberta: Bulletin of Canadian Petroleum Geology, v.22, p. 269-304.

Oliver, T.A. and Cowper, N.W., 1963, Depositional environments of the Ireton Formation, central Alberta: Bulletin of Canadian Petroleum Geology, v.11, p. 183-202.

Oliver, T.A. and Cowper, N.W., 1983, Wabamun salt removal and shale compaction effects, Rumsey area, Alberta: Bulletin of Canadian Petroleum Geology, v.31, p. 161-168.

Packard, J.J., 1992, Early formed reservoir dolomites of the Mississippian Upper Debolt Formation, *in* Canadian Society of Petroleum Geologists and Faculty of Extension of the University of Alberta, Dolomite - from process and models to porosity and reservoirs: 1992 National Conference of Earth Science, Sept 13-18, Banff, Alberta.

Patterson, W.P. and Walter, L.M., 1994, Depletion of ^{13}C in seawater $\sum CO_2$ on modern carbonate platforms: significance for the carbon isotope record of carbonates: Geology, v.22, p. 885-888.

Peters, K.E., 1986, Guidelines for evaluating petroleum source rock using programmed pyrolysis: AAPG Bulletin, v. 70, p. 318-329.

Pe..., D., 1994, Hydrogeology of the Devonian Rimbey-Meadowbrook reef trend of central Alberta: unpublished M.Sc. Thesis, University of Alberta, Canada, 152 p.

Purcell, W.R., 1949, Capillary pressures - their measurement using mercury and the calculation of permeability therefrom: Transactions of the American Institute of Mining and Metallurgical Engineers (Petroleum Transactions, AIME), v.186, p. 39-48.

Rittenhouse, G., 1972, Stratigraphic trap classification, *in* R.E. King, ed, Stratigraphic oil and gas fields - classification, exploration methods and case histories: AAPG Memoirs No.16, p. 14-28.

Rostron, B.J., 1995, Cross-formational fluid flow in Upper Devonian to Lower Cretaceous strata, west-central Alberta, Canada: unpublished Ph.D. Thesis, University of Alberta, Canada, 195 p.

Schlager, W., 1989, Drowning unconformities on carbonate platforms, *in* P.D. Crevello, J.J. Wilson, J.F. Sarg, and J.F. Read, eds, Controls on carbonate platform and basin development: Society of Economic Paleontologists and Mineralogists, Special Publication, v.44, p. 15-25.

Shinn, E.A. and Robbin, D.M., 1983, Mechanical and chemical compaction in fine grained shallow-water limestones: Journal of Sedimentary Petrology, v.53, 595-618.

Sibley, D.F. and Gregg, J.M., 1987, Classification of dolomite rock textures: Journal of Sedimentary Petrology, v.57, p. 967-975.

Smith, D.A., 1966, Theoretical considerations of sealing and non-sealing faults: AAPG Bulletin, v.50, p. 363-374.

Stoakes, F.A., 1980, Nature and growth of shale basin fill and its effect on reef growth and termination: Upper Devonian Duvernay and Ireton Formations of Alberta, Canada: Bulletin of Canadian Petroleum Geology, v. 28, p. 345-410.

Stoakes Campbell Geoconsulting Ltd., 1989, Hydrocarbon potential of the Nisku Formation and Camrose Member of central Alberta, Calgary, SCG Ltd., 5 volumes (Private Consulting Report).

Stoakes, F.A. and Creaney, S., 1985, Sedimentology of a carbonate source rock: the Duvernay Formation of Alberta, Canada: Society of Economic Paleontologists and Mineralogists, Core Workshop Proceedings, No. 7, Golden, Colorado, August, 1985.

Tan, W. and Mountjoy, E.W., 1995 The origin and timing of the Nisku sucrosic dolomite reservoirs in the Enchant area, southeastern Alberta (abs): 1st Joint Symposium of the CSPG and Canadian Well Logging Society (program and abstracts), May 28-31, Calgary, Alberta, Canada.

Tissot, B.P. and Welte, D.H., 1984, Petroleum Formation and Occurrence (second edition): Springer-Verlag, Berlin, 699 p.

Tucker, M.E. and Wright, V.P., 1990, Carbonate Sedimentology: Blackwell Scientific Publications, Oxford, 482 p.

van Gijzel, P., 1981, Application of geomicrophotometry of kerogen, solid hydrocarbons and crude oils to petroleum exploration: *in* J. Brooks, ed., Organic Maturation Studies and Fossil Fuel Exploration, Academic Press, London, p. 351-377.

Walls, R.A. and Burrowes, G., 1985, The role of cementation in the diagenetic history of Devonian reefs, western Canada, *in* N. Schneidermann and P.M. Harris, eds, Carbonate cements: Society of Economic Paleontologists and Mineralogists, Special Publication No.36, p. 185-220.

Wardlaw, N.C. and Taylor, R.P., 1976, Mercury capillary pressure curves and the interpretation of pore structure and capillary behaviour in reservoir rocks: Bulletin of Canadian Petroleum Geology, v. 24, p. 225-262.

Wendte, J.C. and Stoakes, F.A., 1982, Evolution and corresponding porosity distribution of the Judy Creek reef complex, Upper Devonian, central Alberta, *in* W.G. Cutler, ed., Canada's giant hydrocarbon reserves: Canadian Society of Petroleum Geologists, CSPG-AAPG Core Conference, Calgary, Alberta, p. 63-81.

Wendte, J.C., Stoakes, F.A., and Campbell, C.V., 1992, Devonian-Early Mississippian carbonates of the Western Canada Sedimentary Basin: a sequence stratigraphic framework: Society for Sedimentary Geology (SEPM), Short Course No.28, Calgary, Alberta, 255 p.

White, R.J. and Charles, W.W., 1958, The Innisfail oil field - a case history: Alberta Society of Petroleum Geologists, 8th Annual Field Conference, p. 129-148.

Whittaker, S.G. and Mountjoy, E.W., in press, Diagenesis of an Upper Devonian carbonate-evaporite sequence: Birdbear Formation, southern interior plains: Journal of Sedimentary Geology.

Wilkinson, P.K., 1995, Is fluid flow in Paleozoic formations of west central Alberta affected by the Rocky mountain thrust belt? unpublished M.Sc. Thesis, University of Alberta, Canada, 102 p.

APPENDIX I

METHODOLOGY

A variety of techniques were employed to determine breaching of the Ireton aquitard over the Bashaw Reef Complex. These techniques were chosen on the basis of availability, cost, and time.

Initial evaluation involved the analysis of 45 cores from the Bashaw area (Table 1.1). These were logged and sampled at the ERCB Core Research Centre, Calgary in the summer of 1994 with approximately 150 core samples taken for analysis. Samples were selected for petrographic, petrophysical, mineralogical, geochemical, and magnetic investigation.

Seventy seven (77) thin sections were made for standard light microscopy, and blue-light epifluorescence (450 nm) and cathodoluminescence microscopy (15v, 0.5A). All thin sections were half stained with alizarin-red and potassium ferricyanide.

Isotope Analysis: Forty-nine (49) samples were analyzed for stable carbon and oxygen isotopes using the techniques of Degens and Epstein (1964). Results were reported according to the Pee Dee Belemnite (PDB) standard. All values have a reproducibility of ±0.3‰. Sample powders were obtained using a modified dental drill. Dolomite samples were digested in phosphoric acid for five days, whereas calcite samples were digested for only 12 hours. One sample was tested to assess whether phosphoric-acid was also digesting organic matter and therefore altering the isotope ratios. The most organic-rich sample (well 4-17-39-22W4, 5523ft) was treated with bleach and chloroform to remove any organic residue, and analyzed. The results were compared to an untreated analysis from the same bulk sample and were found to be comparable (with a difference of +0.3‰ PDB for $\delta^{18}O$ and +0.1‰ for $\delta^{13}C$) and within reproducible error, therefore the isotope ratios were assumed to be the sole product of carbonate digestion. All other samples were run untreated.

Carbonate Content: The total carbonate content of 51 Ireton aquitard samples were determined by acid leaching of powdered samples. The following procedure was used: a measured quantity (~1 gram) of powdered sample was added to a pre-weighed teflon vial that had been oven-dried (105°C) and cooled in a desiccator. One (1) ml of millipore water was added to the powder to make a "slurry" so that when an initial portion of a 5 ml aliquot of 1N HCl was added, there was a more controlled reaction (*i.e.*, no sample loss due to "spitting"). The reaction was then allowed to react to completion (~12 hours), at room temperature with periodic agitation . After the reaction was complete, the sample was centrifuged and the supernatant HCl solution removed by careful pipetting. A further 5 ml, of this time 2N HCl, was added to the residue and again allowed to react to completion. The sample was centrifuged again and the procedure repeated until there was no further reaction upon the addition of the 2N HCl. The stronger acid was chosen to ensure that all carbonate reacted fully. Leaching of ions from the clay within the sample is possible but considered a negligible effect relative to the weight of the carbonate. After the removal of the last acid wash, the sample residue was dried in an oven overnight at 105°C and allowed to cool in a desiccator. The vial and residue were then weighed and percentage carbonate dissolved calculated. Analytical error is probably within ±1%.

Rock-Eval Pyrolysis: This geochemical technique was performed by the Institute of Sedimentary and Petroleum Geology (ISPG), using standard procedures, on 24 Ireton aquitard and organic-rich lower Nisku Formation samples. This technique involves passing a stream of helium through 100 mg of pulverized rock sample, heated to 300°C. The temperature is then increased at a fixed rate of about 25°C/min and the vapours analyzed with a flame ionization detector (FID). The FID then records the data with respect to three peaks S_1, S_2 and S_3. An S_1 peak is recorded for any free hydrocarbons distilled from the sample at ~300°C (either migrated or *in situ* generated hydrocarbon). Between 300 and 390°C any CO_2 that is released is detected and recorded as an S_3 peak, whereas hydrocarbon generated by the cracking of kerogen at 350 to 550°C are recorded as an S_2 peak. All values are recorded in mg HC/g rock.

The S_1, S_2 and S_3 peaks can then be used to determine the organic matter type and

maturity, and Total Organic Carbon (TOC) content of the samples. The Rock-Eval Pyrolysis parameters derived from these peaks and used in this study are:

1) TOC content — determined by summing the carbon in the pyrolyzate (S_1, S_2 and S_3) with that obtained by oxidizing the residual organic matter at 600°C.
2) T_{max} — a measure of thermal maturity that corresponds to the Rock-Eval Pyrolysis oven temperature (in °C) at maximum S_2 generation.
3) Production Index (PI) $[S_1/(S_1+S_2)]$ — a measure of organic matter maturity based on the amount of kerogen converted to hydrocarbon (valid only when there is no contamination by migrated hydrocarbon). Values climbing from 0.1 to 0.4 indicate the beginning to the end of the oil-generation window (Hunt, 1995).
4) Hydrogen Index (HI) [(S_2/TOC) x100 (in mg HC/g TOC)] — a measure of the amount of Hydrogen in the kerogen and thus indicates the potential of the rock to generate hydrocarbon as well as indicating the type of kerogen in combination with the Oxygen Index.
5) Oxygen Index (OI) [(S_3/TOC) x100 (in mg CO_2/g TOC)] — a measure of the amount of Oxygen in the kerogen and is used to indicate the type of kerogen in a pseudo-Van Krevelen plot with the HI.

Culling of these data was required before meaningful interpretations could be made. In this study, culling of the data was based on a set of empirical rules determined by Peters (1986). However, only two criteria were used in this study of hydrocarbon generation potential. These are:

1) Where TOC values are ≤~0.5 wt.%, all other parameters are dismissed because the low TOC content increases T_{max} and OI values, reduces HI and S_2, and therefore affects the PI.
2) Where T_{max} values are <435°C and PI values exceed 0.2, T_{max} and PI values are dismissed as this indicates that there is low maturity and high maturity, respectively, and that contamination by migrated hydrocarbons has occurred.

Mercury injection capillary pressure measurements (MICPM): Ten samples of Ireton aquitard were run on a Micromeritic Pore-Sizer 9300 (max. 30,000 psi) at the Petroleum

Recovery Institute, Calgary, using standard procedure. These samples were selected on the basis of Ireton aquitard thickness, facies type, and evidence of oil staining in an attempt to represent the aquitard on and off the reef complex. A major limitation of the MICPM procedure, however, is the inability to determine a direction of breaching (*i.e.*,vertical or horizontal) because mercury invasion occurs on all sides of the plug.

Corrections to the initial MICPM curve data (Figure 5.9; Appendix II) were made because mercury invasion was found to occur at anomalously low pressures of 0 - 15 psi. This early invasion was clearly erroneous for some of the "tighter" samples, but was consistently seen in all samples and therefore deemed an artifact of the MICPM procedure. The most likely explanation for this phenomenon is that the uncoated plugs used in the analysis had surface properties (*e.g.*, surface-enlarged throats or procedurally-induced fractures) that allowed for this early mercury invasion (J.Shaw, PRI, pers. comm.). The affects of early mercury invasion may have been reduced if the plugs were coated with epoxy resin, whereby only one surface is exposed to mercury invasion (Wardlaw and Taylor, 1976). The mercury injection data up to 15 psi has subsequently been removed from the curves presented in Figure 5.9 (the dashed lines in Figure 5.9 indicate the corrected portion of the curve; the rest of the data-set is in Appendix II). Estimates of the initial entry pressures are now considered to be fairly accurate for plugs with high entry pressure (>5,000 psi, Plugs 4 - 10, Table 5.4). However, when mercury invasion of a plug occurred in the low pressure range (<100 psi), there was some difficulty in determining when mercury invasion of the surface of the plug becomes that of the real pore network. Therefore, in the cases of Plugs 1 and 3, a range of 40 - 100 psi was given as an estimate of initial entry pressure (Table 5.4 and Figure 5.9e, f). An initial range of entry pressure was given for Plug 2 (200 - 1000 psi), as its initial entry pressure was also difficult to determine from the injection curve (Figure 5.9d).

These initial entry pressure values were used as an estimate of the pressures required to breach the samples. These values, however, are likely to be the lowest estimated pressures for breaching, and are dependant on the pore system characteristics of each plug. Indeed, breaching may not occur at all. Unfortunately, without unidirectional invasion of a plug, breaching can only be assumed to occur at pressures ≥ the initial entry pressure of the plug. The initial entry pressure, therefore, was used as the starting point

with which to quantify breaching potential.

All graphs and diagrams were generated in QUATTRO® PRO for WINDOWS or CORELDRAW®. Well logs were digitized using programs developed by The Logic Group (LOGDIGI®, LOGPRINT®).

APPENDIX II

ADDITIONAL DATA

Magnetic Susceptibility data-set.

- Lf.Susc. is low frequency susceptibility.

Location	Depth	Breach (B) or Seal (S)	Lf.Susc $x10^{-5}$ (SI)	Mass (kg)	Lf/Mass $x10^{-8}$ (m^3kg^{-1})	% Carb
3-15-41-22W4	5758 ft	S	5.0	0.0101	0.5	36
5-33-40-24w4	1836 m	S	2.25	0.0103	0.22	63
14-2-39-22W4	5391 ft	B	0.2	0.0104	0.02	93
16-36-41-23W4	1726 m	S	2.6	0.0103	0.25	54
6-22-38-24w4	6168 ft	S	2.7	0.0181	0.15	76
16-26-39-24w4	1848.4 m	S	3.05	0.0191	0.16	64
2-12-42-23W4	5663 ft	S	6.4	0.0181	0.35	61
6-36-37-24w4	1835 m	B	0.55	0.0199	0.03	95
11-9-44-24w4	5829 ft	S	6.8	0.0211	0.32	67
10-18-40-26w4	6842 ft	S	3.6	0.0232	0.16	80

MICPM Curves.

- remaining three MICPM curves are shown over-leaf.

U. of A. Plug, 12-3-43-23W4, 5635'

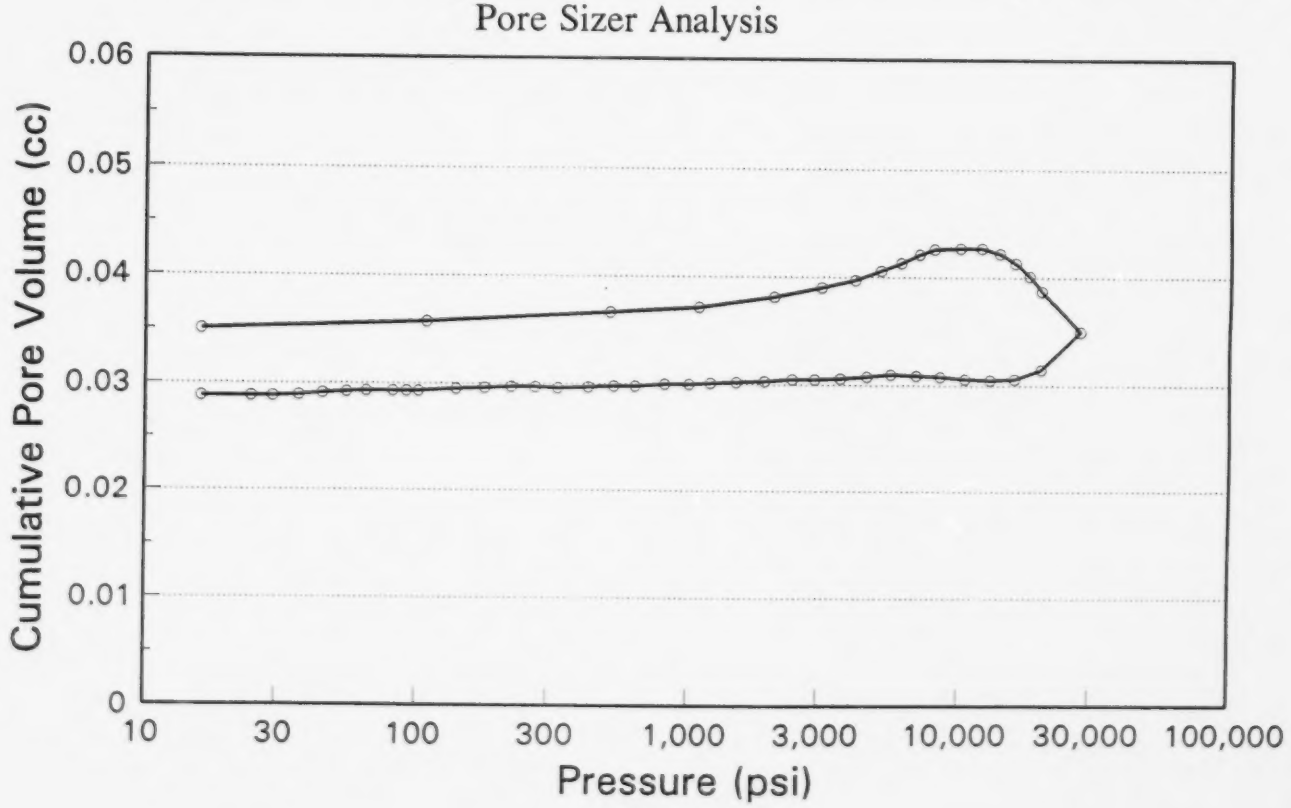

U. of A. Plug, 5-33-40-24W4, 1836m

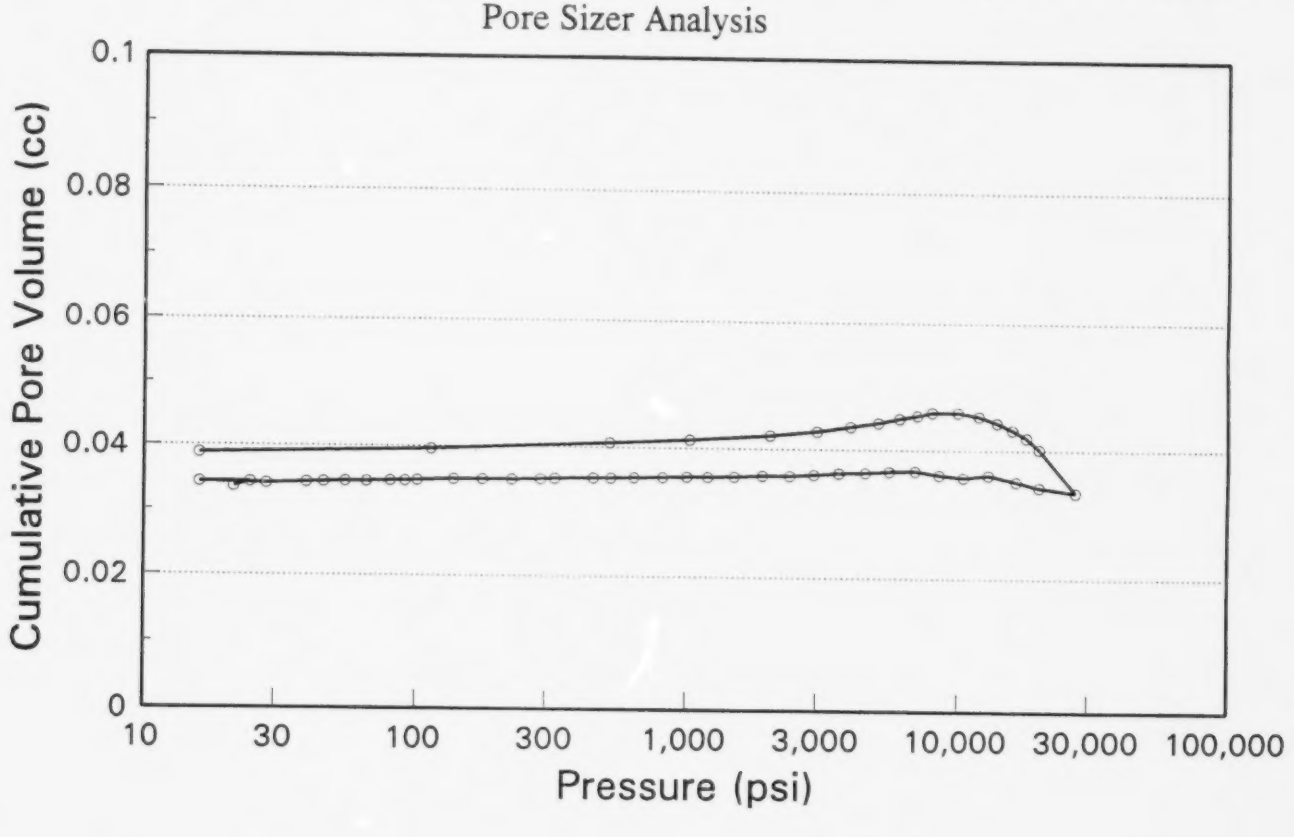
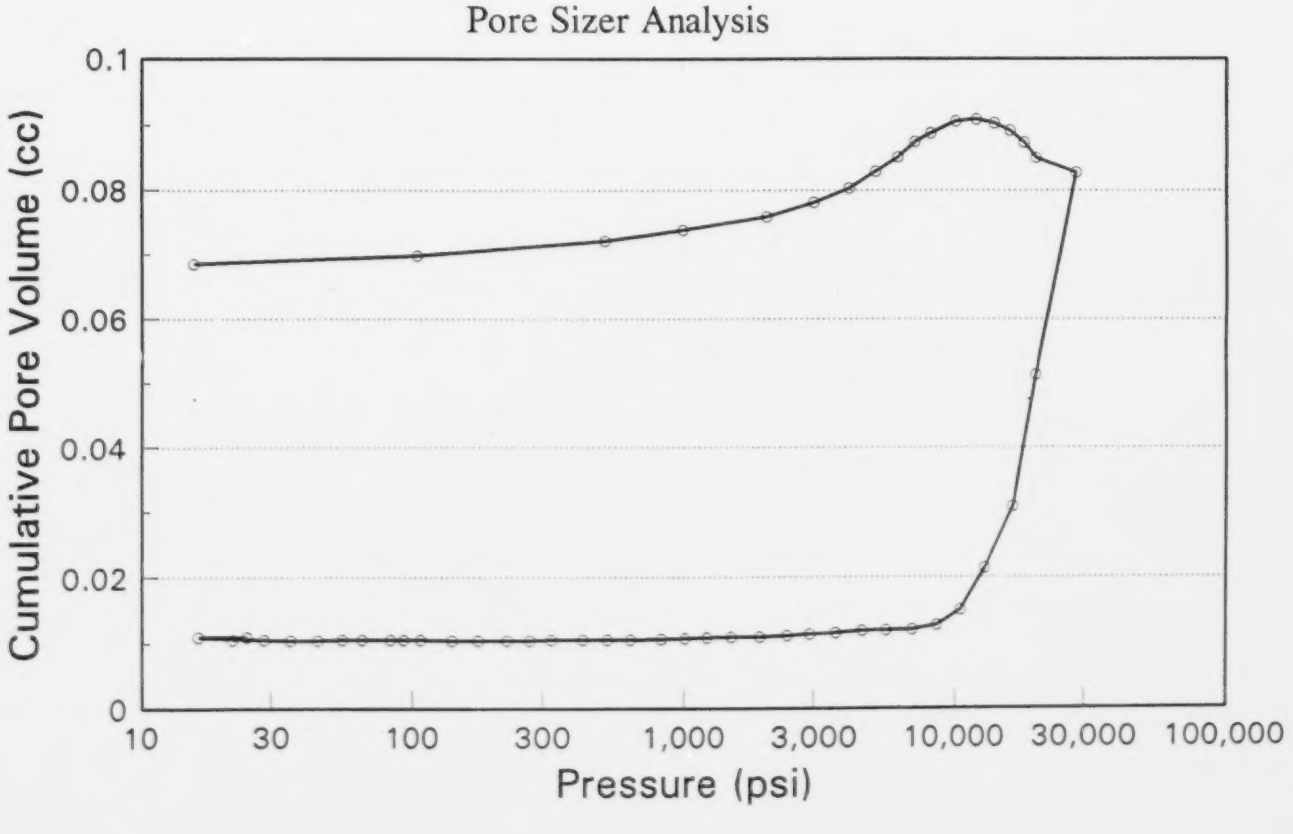
U. of A. Plug, 6-22-38-24W4, 6172'